To the Graduate Council:

I am submitting herewith a thesis written by Eugene Carlton Rankey entitled "Carbonate Platform Response to Tectonism and Eustasy: The Middle Cambrian Carbonates of the Lower and Middle Conasauga Group, East Tennessee." I have examined the final copy of this thesis for form and content and recommend that it be accepted in partial fulfillment of the requirements for the degree of Master of Science, with a major in Geology.

Kenneth R. Walker, Major Professor

We have read this thesis
and recommend its acceptance:

Accepted for the Council:

Associate Vice Chancellor
and Dean of The Graduate School

STATEMENT OF PERMISSION TO USE

In presenting this thesis in partial fulfillment of the requirements for a Master's degree at the University of Tennessee, Knoxville, I agree that the library shall make it available to borrowers under rules of the library. Brief quotations from this thesis are allowable without special permission, provided that accurate acknowledgement of the source is made.

Permission for extensive quotation from or reproduction of this thesis may be granted by my major professor, or in his absence, by the Head of Interlibrary Services, when, in the opinion of either, the proposed use of the material is for scholarly purposes. Any copying or use of the material in this thesis for financial gain shall not be allower without my written permission.

Signature Eugene C. Rawley

Date July 30, 1993

CARBONATE PLATFORM RESPONSE TO TECTONISM AND EUSTASY: THE MIDDLE CAMBRIAN CARBONATES OF THE LOWER AND MIDDLE CONASAUGA GROUP, EAST TENNESSEE

A Thesis

Presented for the

Master of Science

Degree

The University of Tennessee, Knoxville

Eugene Carlton Rankey

August 1993

ACKNOWLEDGMENTS

Although this thesis represents my work, many people have contributed to my education during its completion. I wish to thank Dr. Kenneth R. Walker, my advisor, for his continual input and support and for inviting me to come to Tennessee during the summer of 1991. His suggestions helped to make this a more complete thesis. I am also indebted to my committee members, Dr. Robert D. Hatcher, Jr., and Dr. Stephen Driese, for their contributions and comments. From all of these professors I have learned a great deal, in both classroom and field settings.

Completion of this project would have been much more difficult without the input of my fellow "bankers." I wish to thank Dr. Krishnan Srinivasan for setting the framework for study on the Maryville, and for his continual enthusiasm for, and input to, this project. Kenneth Tobin is also thanked for helping me run stable isotopes, for his guidance in carbonate and siliciclastic sedimentology labs, and for his support during my tenure here. I also wish to thank Boslikja Glumac, Andy Stephaniak, Dr. D. Mark Steinhauff for their input.

I also wish to thank Amy Halleran, Dr. Claudia Mora, and Dr. Stephen Goldberg for their aid on several isotope samples. The secretaries (Denise, Jayne, Melody, and Cindy) here at UT are also thanked for guiding me through the maze of a big school.

I appreciate the patience of my fiancee, Ms. Kelly Groves. Her patience and kindness through this time did not go unnoticed. Only three (four?) more years to go, Kelly!

Thanks to Mike and Kim Caudill for their friendship.

My sincere thanks go to my parents for all of their support and encouragement, patience and prayers. Your guidance and love is most appreciated. I only hope that one day I can emulate your example.

I wish to thank my former professors at Augustana, Dr. Richard Anderson, Dr. William Hammer, Dr. David Schroeder, and Dr. Harold Sundelius, for installing in me an undying love of, and appreciation for, geology. Past colleagues Matthew Schramm and Camie Jensen are also thanked.

Special thanks go to Dan Drommerhausen for giving me someplace to go on "those" weekends. "*Family Tradition*" forever!

Finally, especially, thanks to God.

ABSTRACT

The Middle Cambrian Craig Limestone Member (Rogersville Shale) and Maryville Limestone are part of the thick Cambro-Ordovician pericratonic sedimentary package exposed in the Valley and Ridge province in East Tennessee. Exposures in the Dumplin Valley fault zone provide further details concerning the origin and development of these limestone formations.

Description of five sections, analysis of 125 thin sections and 98 slabs, and regional reconnaisance in the Dumplin Valley area reveal that the Craig Limestone Member represents "premature" demise of a carbonate shelf in that it did not develop as fully as the Maryville shelf and had no rimmed edge or widespread peritidal environments. Instead, the underlying lower Rogersville Shale represents basinal and slope deposits, and the Craig represents deposition on a gentle ramp with deposits analogous to the mid-ramp and aggrading ramp packages of the Maryville. No shoal, lagoon, or peritidal deposits were observed.

In contrast, the Maryville Limestone consists of six genetic packages, each 10s of meters thick: 1) the slope package (debris flows and turbidites deposited below storm wave base); 2) the mid-ramp (burrow mottled mudstone with very thin packstone to grainstone lenses or layers deposited below storm wave base) / aggrading ramp package (subequal amounts of mottled mudstone and packstone/grainstone representing increased wave activity); 3) the shoal package (ooid grainstones representing migrating ooid shoals); 4) the lagoon package (mudstone and packstone/grainstone deposited in protected settings behind ooid shoals); 5) the peritidal package ("cyclic" shoaling-upward sediments deposited in settings associated with tidal flats and islands); and 6) the backstepping platform/shelf package (a variety of lithologies deposited in response to relative sea-level rise).

Through its evolution, the Maryville environmental regime developed from a ramp to a rimmed platform with *Renalcis/Girvanella* bioherms at the platform edge and platform-interior peritidal environments. 10s-of-meters-scale stratigraphic packages were controlled by sedimentary aggradation and progradation. Controls on subtidal meter-scale interbeds of mud-dominated lithologies and grain-dominated lithologies appear to have been processes such as wave sweeping and storm activity; no evidence for regular, shallowing-upward cycles is evident. Deposition of peritidal shallowing-upward parasequences was probably controlled by a combination of autocyclic mechanisms, irregular (jerky?) tectonism, and eustatic sea-level fluctuations.

A petrographic study of the Maryville revealed four "diagenetic patterns" (DP): 1) DP 1 (marine fibrous and bladed cements and burial calcites and dolomites, all non-ferroan); 2) DP 2 (extensively dolomitized sediments); 3) DP 3 (dissolution, vadose silt, equant calcite, depleted oxygen isotope ratios of -9 o/oo); 4) DP 4 (marine fibrous and bladed calcite, burial ferroan and non-ferroan calcites and dolomites). DP 1 is present in the subtidal sediments of the slope through lagoon packages. DP 2 is related to early? dolomitization of peritidal sediments. DP 3 is developed at the top of the Maryville in shelf-edge and lagoon areas, and at the top of and within the peritidal package in platform-interior areas. This facies is related to platform exposure. DP 4 is present in the backstepping shelf/platform package and shows no evidence for subaerial exposure.

The results of this study suggest that the Maryville platform and the Craig Limestone Member (Rogersville Shale) ramp are capped by surfaces of subaerial exposure. Subaerial exposure and meteoric diagenesis are manifest by fabric-selective and non-fabric selective dissolution, depleted oxygen isotope ratios, and erosionally truncated equant cements. In more off-platform areas, the exposure surface is also a drowning surface overlain by shale, whereas in platform interior locations, a deepening-upward trend is present within the carbonates. Framboidal pyrite, manganese- and phosphate-coated

grains, and deeper-water shales reflect relative deepening following platform exposure. Exposure provided a shutdown of carbonate production. Once re-flooded, the very slow sedimentation rates coupled with *episodic pulses of subsidence* resulted in an apparently "instantaneous" drowning of the platform, and the deeper-water lithologies directly overlying shallower-water lithologies.

The episodic pulses of tectonism documented herein and Middle Cambrian tectonism across much of the Iapetan "passive" margin suggest that the southern Appalachian continental margin was not completely stabilized until the Late Cambrian. The passive margin evolved in three stages: rift stage (characterized by active rifting and thick rift basin sediments; Ocoee Supergroup, parts of Chilhowee Group), immature passive margin (effects of thermal and episodic non-thermal subsidence combined; Conasauga Group), and mature passive margin (subsiding by thermal subsidence alone; Knox Group).

TABLE OF CONTENTS

CHAPTER PAGE

1. INTRODUCTION 1

Previous Investigations 3
Tectonic Setting 8
Stratigraphy 9
Conasauga Group 9
Rogersville Shale 10
Maryville Limestone 11

2. SEQUENCE STRATIGRAPHY AND SEDIMENTARY PACKAGING OF THE CRAIG LIMESTONE MEMBER, ROGERSVILLE SHALE (MIDDLE CAMBRIAN), EAST TENNESSEE 13

Introduction 13
Lithofacies and their genesis 13
Environmental synthesis 19
Conclusions 21

3. STACKING PATTERNS IN THE MARYVILLE LIMESTONE (MIDDLE CAMBRIAN), SOUTHERN APPALACHIANS 22

Abstract 22
Introduction 22
Stratigraphic Packaging in the Maryville 23
Slope Package 23
Mid-Ramp/Aggrading Ramp Package 26
Shoal Package 32
Lagoon Package 33
Peritidal Package 33
Backstepping Platform/Shelf Package 37
Model for Evolution of Maryville Shelf 37
Conclusions 42

4. CAN EUSTATIC, TECTONIC, AND AUTOCYCLIC PROCESSES BE RESOLVED FROM THE STRATIGRAPHIC RECORD IN PERITIDAL CYCLES, MARYVILLE LIMESTONE (MIDDLE CAMBRIAN), SOUTHERN APPALACHIANS? 43

Abstract 43
Introduction 44

Statement of Problem 44
Geologic Setting 44
Lithofacies and Stratigraphic Packaging in the Peritidal Parts of the Maryville 45
Cycle Models and Maryville Stacking Patterns 50
Milankovich Eustatic Sea-level Fluctuations 53
Tectonism 57
Autocyclic Processes 61
Summary and Conclusions 63

5. EPISODIC TECTONISM ON CAMBRIAN "PASSIVE" MARGIN, SOUTHERN APPALACHIANS: IMPLICATIONS FOR PASSIVE MARGIN DEVELOPMENT AND SEQUENCE ANALYSIS 65

Abstract 65
Introduction 66
Late Proterozoic-Early Cambrian Continental Breakup and Cambrian Tectonism 67
Development of Sequence Boundaries in the Conasauga Basin 71
Lower Rogersville-Craig Cycle Top 72
Upper Rogersville-Maryville Cycle Top 76
Model for Origin of the Limestone/Shale Transition 76
Grand Cycle Correlations 77
Exposure, Eustasy, Tectonics, and Sequence Boundaries 79
Model for the Development of the Cambrian Passive Margin 84
Comparison with Mesozoic/Cenozoic Passive Margins 85
Discussion 86
Conclusions 91

6. DIAGENETIC PATTERNS AND THEIR RELATION TO STRATIGRAPHIC PACKAGING, MARYVILLE LIMESTONE (MIDDLE CAMBRIAN), EAST TENNESSEE 92

Abstract 92
Introduction 92
Diagenetic Patterns 93
Diagenetic features - DP 1 93
Vertical distribution of cement and porosity types - DP 1 98
Diagenetic features - DP 2 (peritidal) 100
Vertical distribution of cement and porosity types - DP 2 104
Diagenetic features - DP 3 105

Vertical and lateral distribution of cement and porosity types - DP 3.... 107
Diagenetic features - DP 4..... 107
Vertical distribution of cement and porosity types - DP 4..... 109
Sequence stratigraphic control on diagenetic features..... 109
Conclusions..... 112

7. SUMMARY AND CONCLUSIONS..... 113

REFERENCES..... 116

APPENDICES..... 139

A. Measured Section Descriptions..... 140
B. Peritidal "Cycle" Data..... 187
C. Peritidal Lithologic Transition Data..... 188
D. Carbon, Oxygen, and Strontium Isotope Data..... 189

VITA..... 191

LIST OF FIGURES

1.1 Location map 2
1.2 Middle Cambrian paleogeography 5
1.3 Conasauga Group stratigraphic model 7

2.1 Photomicrographs of representative lithologies - Craig Limestone 15

3.1 Stratigraphic section of Maryville Limestone at DSR section 25
3.2 Photomicrographs of representative lithologies, subtidal sediments 29
3.3 Detailed stratigraphic comparison of DSR sections on-ramp and off-ramp 30
3.4 Photomicrographs of representative lithologies, peritidal package 36
3.5 Model for development of Maryville shelf 39

4.1 Regional exposures and distribution of the peritidal package, Maryville Limestone, Dumplin Valley TN 47
4.2 Characteristics of peritidal "cycles" 49
4.3 Detailed comparison of peritidal cycles, IS and SR sections 52
4.4 Cross-plot of distance from base of cycle to sequence boundary versus cycle thickness 56
4.5 Diagram showing regional cycle characteristics 60

5.1 Location map showing features associated with late Proterozoic-Early Cambrian continental breakup and later Appalachian-Ouachita orogenesis 70
5.2 Photomicrographs showing petrographic features related to meteoric diagenesis and later drowning 74
5.3 Cross-plot of carbon and oxygen isotope ratios of equant to drusy calcites in dissolution voids, Craig and Maryville 75
5.4 Interbasinal "correlations" of Middle Cambrian grand cycles and strata 78
5.5 Schematic diagram showing influence of exposure, "lag time," and tectonic subsidence on Tennessee grand cycle termination 83
5.6 Tectono-stratigraphic evolution, Conasauga basin, east Tennessee 90

6.1 Paragenetic sequence, Maryville Limestone, Dumplin Valley, Tennessee 94
6.2 Photomicrographs of diagenetic features, DP 1 97
6.3 Photomicrographs of diagenetic features, DP 1, 2, and 3 102

CHAPTER 1

Introduction

The Conasauga Group (Middle and Upper Cambrian) consists of six formations of alternating shale and limestone. Similar third-order (1-10 Ma) cyclic alternations of shale-dominated formations and carbonate-dominated formations have been recognized in many Cambrian passive-margin sequences, including those in the Canadian Rocky Mountains (Aitken, 1966), the Great Basin (Palmer and Halley, 1979; Mount and Rowland, 1981), the northern Appalachians (Chow and James, 1987; James and others, 1989), and the southern Appalachians (Palmer, 1971; Koerschner and Read, 1989; Srinivasan and Walker, 1993) Aitken (1966, 1981) called these repetitions "grand cycles," consisting of a lower shale half-cycle (with or without carbonate beds) gradationally overlain by a carbonate half-cycle. Most grand cycles represent a general shoaling-upward trend from deeper-water shale to shallow-water limestone (see Chow and James, 1987, however). At a given location, cycles may not culminate in peritidal deposits, because at the time of cycle termination, the full range of environments (deeper-water to peritidal) on the shelf would be effected by platform demise, as shown herein. Grand cycles were originally loosely defined as "300 to 2,000 feet of strata" spanning "two or more fossil zones" (Aitken, 1966), although these distinctions are guides rather than rules. As in the southern Appalachians, carbonate units of many other areas represent *cratonward* platform progradation across intrashelf basins (Aitken, 1981).

The primary goal of the present study was to interpret the genesis of stratigraphic packaging within the limestone part of one of these grand cycles, the Maryville Limestone, in several closely-spaced stratigraphic sections near Deep Springs, Tennessee in the Dumplin Valley fault zone (Figure 1.1). Secondary goals included documenting and

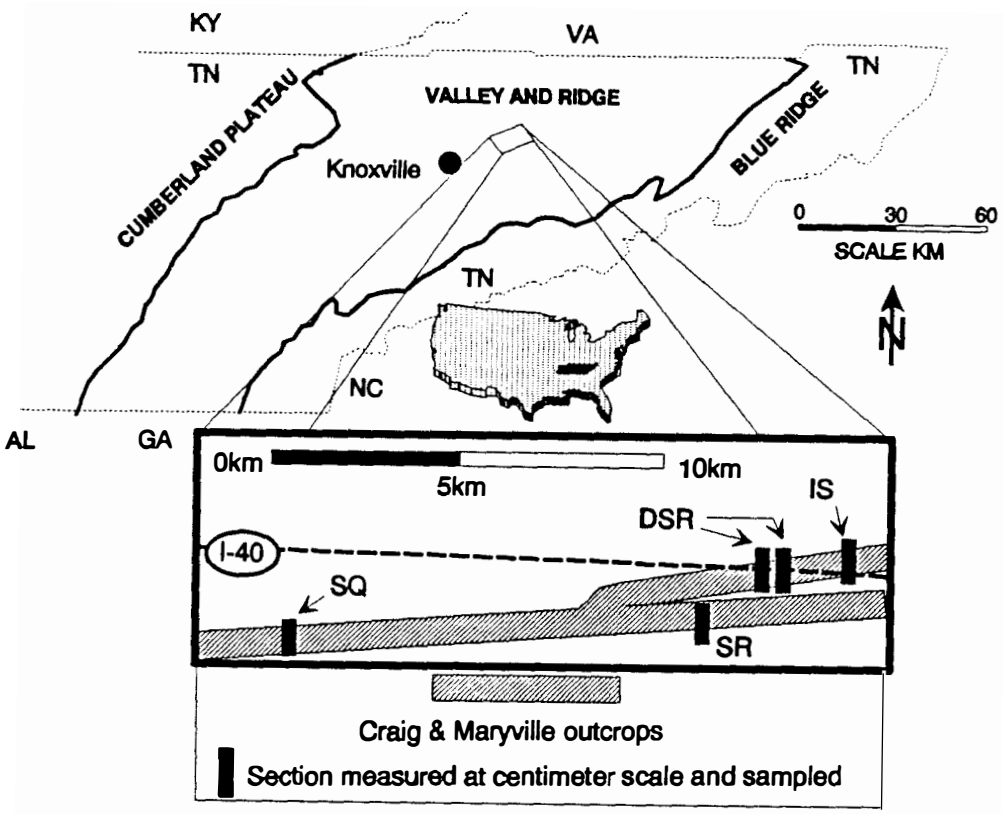


Figure 1.1 Location map. Schematic map of study area, Dumplin Valley fault zone, east Tennessee. Section names: JCQ = Jefferson City Quarry; IS = Interstate 40 section; DSR = Deep Springs Road and I-40 interchange (2 sections, on-ramp and off-ramp); SR = Sockless Road; CMR = Cook Mill Road; MH = Mutton Hollow; H = Hodge; SQ = Sevierville Recycling Center; KO = Kodak; see Figure 4.2 for more extensive information on regional distribution of peritidal package. Area mapped in detail by Hatcher (1965), Bridge and Hatcher (1973), and Hatcher and Bridge (1973).

interpreting the stratigraphic packaging in the Craig Limestone Member (Rogersville Shale) and providing a preliminary interpretation of the diagenetic history of the Maryville in that area. This thesis contributes to two on-going research projects of the UT Carbonate Research Group: 1) development of a carbonate sequence stratigraphic model of the Cambrian succession; and 2) analysis of how stratigraphic packaging influences/controls diagenetic patterns.

The most significant findings of this study include: 1) formation-scale sequencing of the Conasauga Group reflects the waning stages of the rift-drift transition in the southern Appalachians; 2) intra-formation decameter stacking patterns represent sedimentary aggradation and progradation, irregular eustatic sea-level fluctuations, thermal subsidence, and episodic pulses of non-thermal subsidence; and 3) meter-scale stacking patterns reflect primarily a combination of autocyclic processes, irregular minor eustatic fluctuations, and irregular subsidence.

PREVIOUS INVESTIGATIONS

Safford (1856, 1869) was the first to describe the alternating limestones and shales of the Conasauga Group, which he designated as the Knox Shale. Later workers provided more localized descriptions of the Conasauga Group. These include Hall and Amick (1934), who described the sequence near Thorn Hill, Tennessee, and Rodgers and Kent (1948), who studied a section at Lee Valley, in Hawkins County, Tennessee. In Virgina, Butts (1940) qualitatively described Cambrian units and provided faunal lists for the Rutledge, Rogersville, and Maryville units. Woodward (1949) provided faunal lists from the Rutledge, Rogersville, and Nolichucky units in Tennessee.

Before 1953, geologists studying the Conasauga Group noted the intercalation of limestone and shale and, based solely on lithologic data, inferred a southeasterly source for

the shales (Moore, 1949). After the publication of Rodgers' (1953) map and description of East Tennessee geology, a westerly, cratonic source for the Conasauga Shales was recognized (see also Sloss, 1963; Harris, 1964; Palmer, 1971).

Geologic mapping within the study area includes the work of Hatcher (1965), Hatcher and Bridge (1973), and Bridge and Hatcher (1973). These studies also documented the presence of a northwest-thinning dolostone unit within the Maryville, informally called the Dumplin Valley Dolomite member, near the top of the Maryville. This unit is discussed in detail in chapter 4.

Within the past 15 years, geologists have recognized a more complex environmental setting for the Conasauga Group. In southwestern Virginia, Markello and Read (1981, 1982) interpreted lateral facies changes within the Conasauga to represent a shallow intrashelf basin, bounded to the east by a shallow carbonate ramp. Read (pers. comm., 1992) proposed that initial development of the basin was synchronous with development of the Rome trough. Erwin (1981) studied the Maryville and upper Honaker in Virginia and Tennessee. He described the dolomite/limestone interfingering and modified the Markello and Read (1981) model.

In Virginia, ramp and platform sediments contain peritidal sediments. Koerschner and Read (1989) and Osleger and Read (1991) have postulated that sedimentation patterns of the Conasauga Group within the ramp and platform parts of the depocenter were driven by Milankovitch-forced sea-level oscillations. They inferred that deposition of the Maryville Limestone (as well as the other limestone units) was controlled primarily by the long-range 1-5 Ma cycle, with effects of the 19-23 ka, 41 ka, 95-123 ka, and 413 ka cycles superimposed ("composite eustasy," Goldhammer and others, 1990).

In East Tennessee, the Conasauga Group represents the interplay between the carbonate platform to the east and the adjacent shale basin to the west (Figure 1.2). Carbonate units such as the Maryville represent times when the platform prograded over

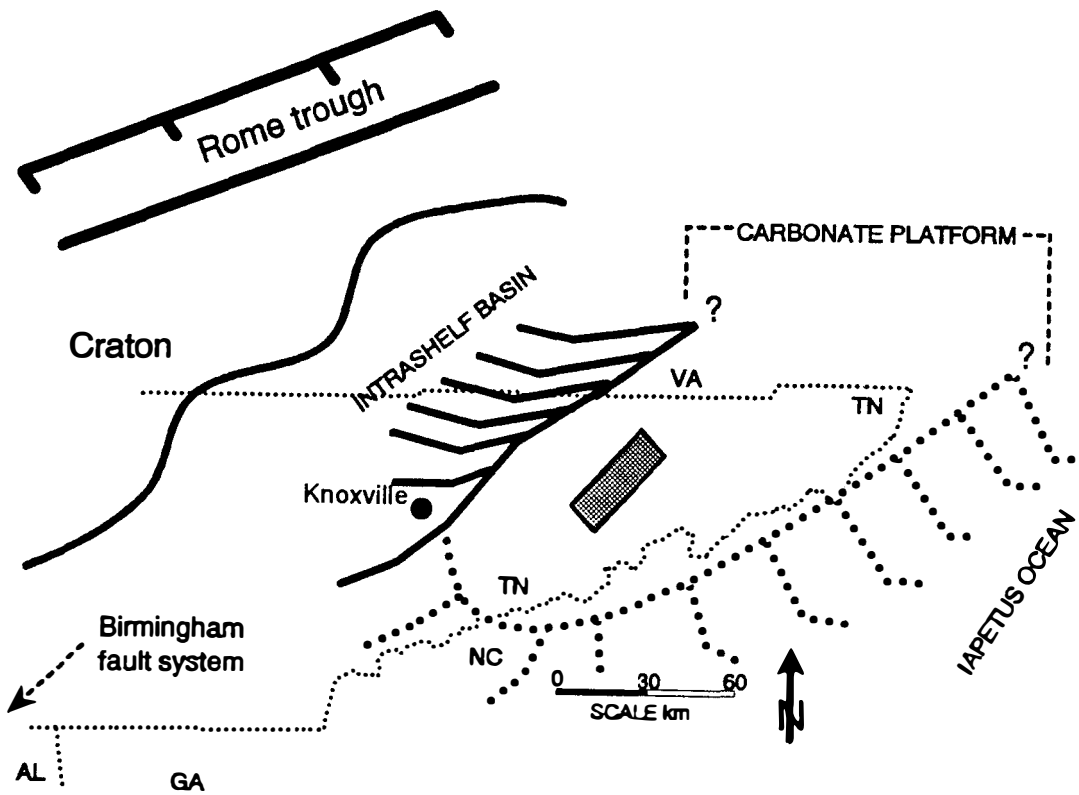


Figure 1.2 Middle Cambrian paleogeography. Map shows major Middle Cambrian structural and sedimentary features. Study area indicated by stippled rectangle. Modified from Srinivasan and Walker, 1993.

previously basinal (shale) areas (Figure 1.3). Srinivasan and Walker (1993) suggested that varying siliclastic input and consequent changes in carbonate sediment production controlled depositional patterns of the basin, adjacent ramp, and platform, similar to that proposed in Walker and others' (1983) "carbonate suppression model." Recent work by Srinivasan (1993) has shown mostly autocyclic controls on depositional patterns within the Maryville Limestone. His results showed that the lower part of the Maryville Limestone represents deep ramp deposition and the upper part represents gradual shallowing and slope steepening, resulting in deeper water in basinal areas, the development of a flat-topped platform, and shallow-water algal buildups and ooid banks in the platform edge environments. In contrast to Read's dominantly eustatic controls, this model (Walker and others, 1990; Srinivasan and Walker, 1993; Rankey and others, 1992) suggests that progradation of the platform over previously basinal areas was a major control on facies patterns, along with variations in sedimentation rate, subsidence, and absolute sea level change.

Three students have analyzed the Maryville Limestone at the University of Tennessee within the past eight years. Simmons (1984) described the stratigraphy and interpreted the depositional setting of the Maryville Limestone near Thorn Hill, Tennessee. Kozar (1986) did the same for the area near Oak Ridge, Tennessee. Srinivasan (1993) interpreted depositional history, sequence stratigraphy, and diagenetic patterns for the Maryville Limestone exposed within the Copper Creek fault block (in an area lying between the study areas of Simmons and Kozar). The rocks studied in greatest detail were located approximately 80 km across strike palinspastically (Hatcher, 1989) from those studied by Srinivasan and Walker (1993) and Srinivasan (1993). The present study includes some of the southeasternmost exposures of Maryville Limestone in Tennessee.

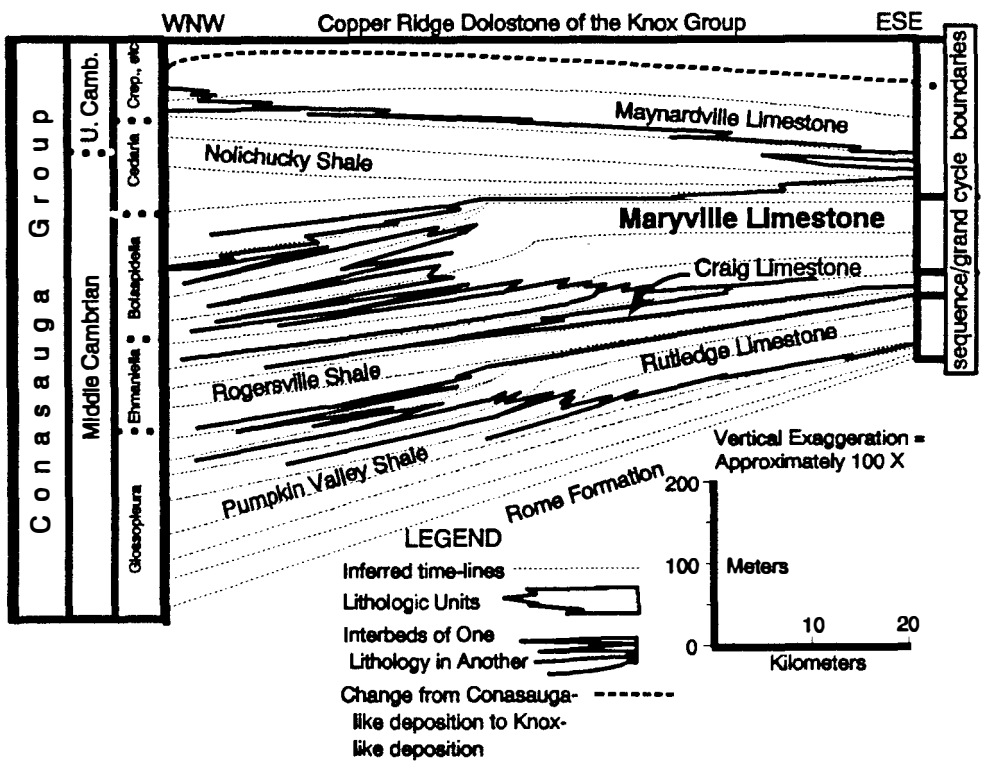


Figure 1.3 Conasauga Group stratigraphic model. Sequence boundaries are exposure/flooding surfaces, as shown. Biostratigraphy (trilobite zones) based on Rasetti (1965), Palmer (1981), Derby (1965); zones higher than *Cedaria* are not shown. Middle - Upper Cambrian boundary is within Cedaria zone (Robison, 1984). Modified from Walker and others (1990) and Srinivasan and Walker (1993).

TECTONIC SETTING

Following the Middle Proterozoic Grenville orogeny, extension resulted in rifting of southeastern Laurentia between 690-570 Ma (Bond and others, 1984; Odom and Fulgar, 1984). In most areas, the Grenvillian basement is block faulted, and sedimentation patterns and facies reflect the rift environment (Hatcher, 1989). In craton-marginal areas, widespread grabens and thick sedimentary sequence indicate the development of a lower-plate passive margin, which consists of faulted upper crust overlying deep crystalline rocks and an attenuated lithosphere (Lister and others, 1991).

The first post-rift unit in the southern Appalachians is the Chilhowee Group, a series of sandstones and shales that mature upwards (Simpson and Eriksson, 1989; Hatcher, 1989; Walker,1990; Thomas, 1991). The first carbonate unit in the post-rift sequence is the Shady Dolomite, which reflected an open, oxygenated Iapetus Ocean. The Rome Formation immediately underlies the limestones and shales of the Conasauga Group. The Rome consists of shales and sandstones, and served as a major detatchment for later thrusting. Like the shales of the Conasauga, it too grades eastward into a carbonate bank (Watauga phase of Rogers, 1953), part of which was temporally equivalent to the Shady Dolomite (McReynolds,1988; McReynolds and Driese, in press).

By Middle Cambrian time, the carbonate bank flanking the eastern edge of Laurentia was well established. To the east, an abrupt shelf break bounded the bank, seaward of which fine clastics, volcanics and minor carbonates were deposited (Read, 1989). The bank is represented by the Middle to Late Cambrian carbonate units (the Honaker Dolomite, Conasauga Group limestones, and Elbrook Dolomite). To the west, a shallower intrashelf shale basin developed and remained active until the Late Cambrian.

The origin of this basin is complex. The great thickness of lower-to-upper Cambrian units in both basinal and non-basinal areas reflects passive margin post-rift

thermal subsidence and infilling of accommodation space (Bond and others, 1984, Thomas, 1991). Although this subsidence is a dominant control on sediment accumulation, it is also probable that synsedimentary faulting and/or accentuated subsidence related to regional extension, sediment loading, or sporadic release of stresses associated with thermal subsidence created extra accommodation space for these sediments, as shown herein

. STRATIGRAPHY

Conasauga Group

The Conasauga Group, originally named for exposures along the Conasauga River in Whitfield and Murray Counties, Georgia, consists of silty claystone with numerous small lenses of thinly bedded limestone in the type area (Hayes, 1891). Campbell (1894) and Keith (1895) documented facies relations and the transition from the Conasauga "Shale" to the Conasauga "Group."

Rodgers (1953) classified the Conasauga into a northwestern phase of shale, a central phase of shale and limestone, and a southeastern phase of dolomite with some limestone and shale. The type locality is within the northwestern phase of Rodgers (1953), and consists of over 600 m of shales with minor limestone lenses. The central phase consists of six alternating shale and limestone formations (in ascending order): the Pumpkin Valley Shale, the Rutledge Limestone, the Rogersville Shale, the Maryville Limestone, the Nolichucky Shale, and the Maynardville Limestone. The southeastern phase is defined as the area where the Rogersville Shale pinches out and the Rutledge and Maryville combine to form part of the Honaker Dolomite. In these areas, the Pumpkin Valley (?), Nolichucky, and Maynardville are still present.

The present study is located within Rodgers (1953) central phase of the Conasauga, very near the southeasternmost exposures of these units in Tennessee. The

thin Rogersville Shale and the abundant dolomite in the Maryville indicate that this area is proximal to Rodgers (1953) southeastern phase, however.

Rogersville Shale

Although Campbell (1894) named the Rogersville Shale for exposures near Rogersville in Hawkins County, Tennessee, Keith (1895) was the first to describe it in the type area. No complete type section has been defined. In the study area, the Rogersville consists of three members defined by Rodgers and Kent (1948): a lower shale member, the Craig Limestone Member, and an upper shale member, not recognized by Hatcher (1965). At the type section at the Craig quarry at Rutledge, Tennessee, Bridge (1956) measured 26.2 m of Craig, overlain by 5.2 m of shale.

Where thickest, the Rogersville approaches 80 m (Bridge, 1956; Bridge and Hatcher, 1973). The upper shale member pinches out to the southeast and northeast and the Craig and the Maryville merge and become indistinguishable (Hatcher, 1965; Erwin, 1981). Further northeast, the shales of the Rogersville pinch out into the Honaker Dolomite.

Within the study area, all three members of the Rogersville Shale are present. The lower shale member was not measured for the present study because of poor exposures, but geologic mapping by Bridge and Hatcher (1973) indicates that it may be up to 50 m thick in this area. The uppermost one m of the lower member was observed, ensuring that the base of the Craig is indeed known. The Craig Limestone Member is 26.4 m thick in the study area, and consists predominantly of burrow-mottled mudstone/wackestone. The upper shale member is only 0.6 to 0.75 m thick in the study area, where it consists of medium to dark gray to green clay shale with scattered carbonate nodules. All contacts are sharp. No dolostone is present at the top of the Craig, but has been documented elsewhere by VanArsdall (1974) and Erwin (1981).

Maryville Limestone

The rocks of the Maryville Limestone were first observed by Safford (1869), and included in his Knox Shale. Keith (1895) delineated the Maryville "Formation" to describe the thick, massive, blue limestone exposed near Maryville, Tennessee, but chose no type section. Bridge (1956) stated that the type section is located in exposures northwest of Maryville, Tennessee, but structural complexities may result in repeated sections, and hence greater apparent thicknesses in the area (Cattermole, 1962). Although the lower contact of the Maryville is sharp, the upper contact is less distinct because the shales of the overlying Nolichucky are intimately interlayered with limestone beds. Earlier geologists, including Rodgers and Kent (1948), Rodgers (1953), Derby (1965) and Erwin (1981), encountered difficulty in delineating an upper bound to the Maryville because of this interstratification. Srinivasan (1993) documented an exposure/drowning surface at the top of the Maryville and interpreted this limestone-to-shale transition to represent a sequence boundary. I followed the interpretation of Rodgers and Kent (1948) and Simmons (1984), which designates the the lowermost shale as the Maryville/Nolichucky lithologic contact. In the Dumplin Valley area, the sequence boundary documented by Srinivasan (1993) is *within* the Maryville (see Chapter 3 for a complete discussion).

Hall and Amick (1934) measured the Maryville Limestone at Thorn Hill to be 165 m thick. Rodgers and Kent (1948) measured 272 m at Lee Valley, Tennessee, but note that true thickness is probably closer to 181 m due to faulting. Simmons (1984) documented 169 m along U.S. 25 near Thorn Hill, Tennessee. In the study area, Bridge and Hatcher (1973) observed between 230 and 280 m of Maryville Limestone, but these measurements clearly include the Craig Limestone Member as part of the Maryville because of the very thin (and probably unrecognizable in most exposures) upper Rogersville Shale. At the Deep Springs section measured for this study, the Maryville is

211.6 m thick, but some of the upper part may be duplicated. In general, like the other Conasauga limestones, the Maryville becomes thicker to the southeast at the expense of adjacent shale units. Where no shale occurs above and below the Maryville, Honaker Dolomite is used for time-equivalent rocks.

CHAPTER 2

Sequence straigraphy and sedimentary packaging of the Craig Limestone Member, Rogersville Shale (Middle Cambrian), east Tennessee

INTRODUCTION

This chapter represents a preliminary interpretation of the origin and evolution of the Craig Limestone Member (Rogersville Shale). It is based on detailed observations of two outcrops, and general knowledge of the regional character of the Craig. It is not as compete as obseravtions and interpretations for the Maryville (next chapter).

LITHOFACIES AND THEIR GENESIS

The Craig Limestone, as observed in the field, consists of five lithologies: burrow-mottled mudstone, peloid-ooid-oncoid-fossil packstone to grainstone, ooid grainstone, oncoid-*Renalcis* packstone, and oncoid-fossil grainstone. These lithologies, their petrographic characteristsics,and their depositional environments are described below. All of these lithologies represent subtidal, open-marine deposition, as Srinivasan and Walker (1993) suggested for similar lithologies in the Maryville Limestone.

Burrow-mottled mudstone comprises over 95% of the basal 22 m of the Craig, and occurs, but is less dominant, in the next 3.2 m. In the field, these units are 0.4 to 13 m thick and are thin to massively bedded. They typically have a gradational base with the underlying packstones or grainstones and are dark gray. The burrows are commonly dolomitized (Figure 2.1A), giving this unit its distinctive mottled appearance in the field

Figure 2.1 Photomicrographs of representative lithologies - Craig Limestone. All samples are from DSR section, on-ramp. Long axis on all photomicrographs is 4.5 mm.

A) Burrowed mudstone/wackestone. Larger burrow (elongate across axis of photo) dolomitized, other burrow (ovoid) filled with internal sediment (S) and clear equant non-ferroan calcite. Note concave-up trilobite fragment, indicating slow deposition. From sample 7.5.

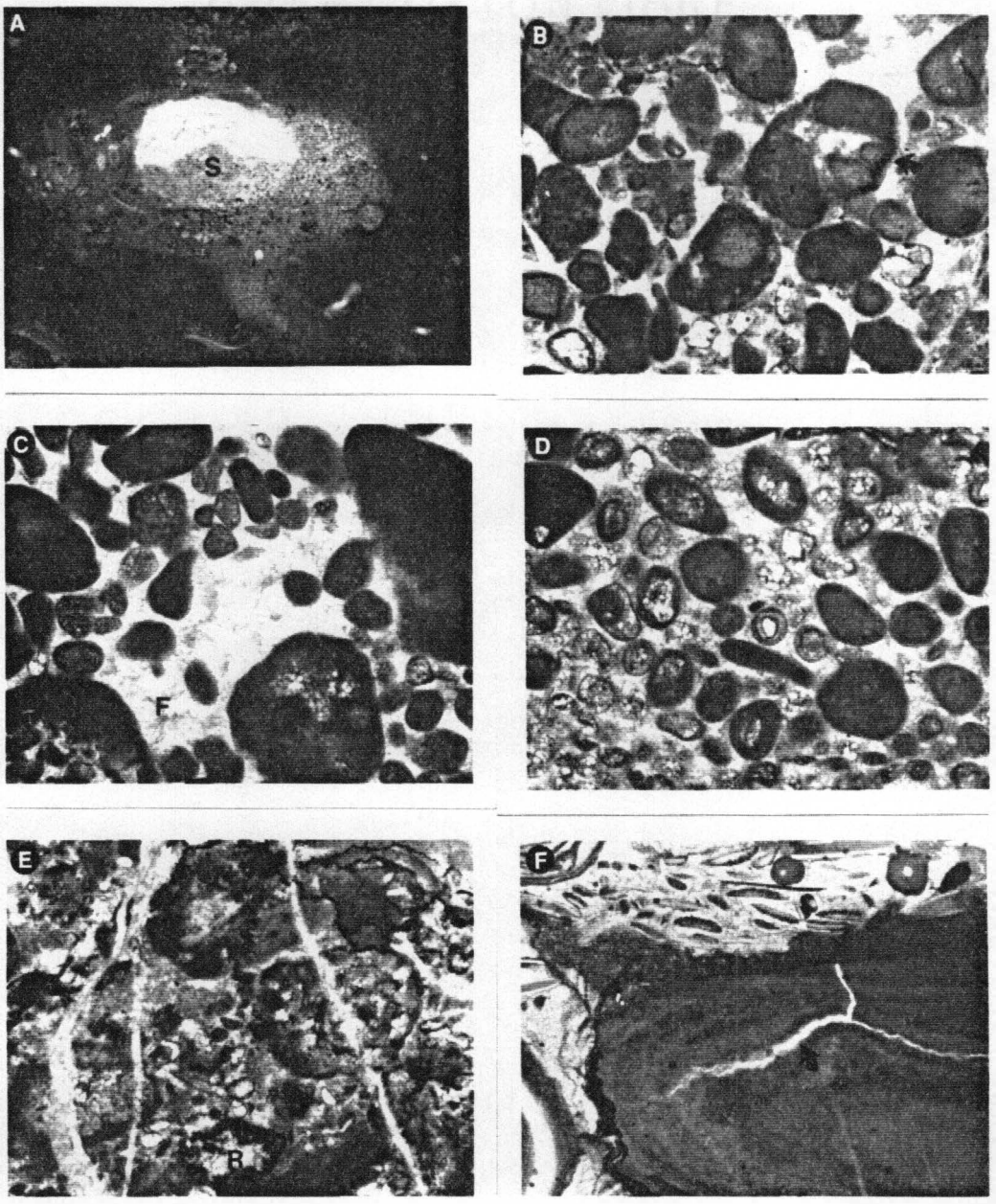
B) Peloids and composite grains in grainstone. Note truncated grains (arrow) and cements within composite grains, indicating early lithification. From sample 5.5.

C) Peloids and composite grains. Note extensive fibrous cement (F). From sample 7.5.

D) Ooid-peloid-composite grain grainstone. Note the "mixed" constiuents, suggesting that this does not represent the shoal facies. Many allochems are dissolved and partly replaced by fine-grained dolomite. From sample 25.8.

E) Oncoid-*Renalcis* packstone. Note the broken *Renalcis* (R) clasts. Echinoderms also present in thin section. From sample 25.4.

F) Oncoid-fossil packstone-grainstone. Fossils are echinoderms and trilobites. Note darkened, mineralized rims on some grains and the healed fracture in the oncoid (arrows). From sample 26.4.


A
S
B
C
F
D
E
R
F

(ii2-ii4 of Droser and Bottjer, 1986). Petrographic analysis reveals that this lithology actually consists of burrowed mudstone, wackestone, and packstone with varying admixtures of composite grains, peloids, trilobites and echinoderms, with ooids and *Girvanella* oncoids becoming more important constituents upwards in the section. A small amount of quartz silt is also commonly present. This lithology also contains numerous non-cyclic peloid-fossil-composite grain-oncoid grainstone lenses that are laterally discontinuous over 0.1 - 10 m. These lenses are always less than 0.05 m thick and typically have an abrupt, scalloped base and a gradational top. Locally, vertical escape burrows are present in the underlying mudstones. The lenses often pinch out laterally and at times contain cross-laminae. In thin section, they may also exhibit small-scale fining-upward and/or muddying upward sequences.

This lithofacies is interpreted to represent subtidal open-marine deposition, below normal wave base but above storm wave base. Srinivasan (1993) estimated deposition in water shallower than 30 m within the inner shelf. The times of mud deposition represent intervals of calm, relatively slow deposition, indicated by the abundance of burrows, the dominance of composite grains, and the presence of hydrodynamically unstable (concave up) trilobites (see Figure 2.1A). At times, deposition was very slow, as shown by the presence of glauconite. In contrast to these intervals of slow deposition, the thin grainstone lenses represent times when the wave base reached the sediment-water interface, probably during storms. Their abrupt, scalloped bases, lateral discontinuity, shelter voids, mud-poor matrix, and rare cross-lamination suggest such a higher energy environment, while their gradational upper contact with overlying mudstones represent waning energy conditions (Kreisa, 1981). A downslope flow interpretation is not likely because of the inferred shallow slopes present on the platform. In general, however, these thin grainstone lithologies are but minor high-energy interludes punctuating a predominantly lower energy environment.

Peloid-ooid-oncoid-fossil-composite grain packstone to grainstone lithologies within the Craig are typically thinly bedded and range from 0.05 to 0.5 m thick. These units are laterally persistent. They typically have an abrupt, scalloped to undulatory to planar base and are medium to dark gray. Thin-section analysis reveal peloids, composite grains, trilobites, echinoderms, ooids, *Girvanella* oncoids, and *Renalcis* clasts present in varying amounts (Figure 2.1B). In general, however, ooids and *Girvanella* oncoids increase in abundance upwards. Ooids are tangential to superficial and commonly are dissolved and collapsed. Composite grains almost always have a micritic rim and are comprised of cemented peloids and/or ooids, which may or may not be truncated by the micritic rim (Figures 2.1B and 2.1C). Cements are most commonly fibrous to bladed. Some contain evidence for two or more episodes of micritization.

These packstones and grainstones represent shallow subtidal open marine deposition associated with periodic storms, an origin similar to that suggested for deposition of grainstone lenses in the burrowed mudstone lithofacies. The scalloped bases, grainy mud-poor lithologies, truncated grains, and diverse composition within and between beds suggest resedimentation by storms rather than *in situ* production of these allochems.

Ooid-peloid grainstone occurs as a 0.2 - 0.25 m thick bed near the top of the Craig Limestone. This lithology is not extensively developed in the Craig, and no cross bedding or ripples were observed. It has an abrupt, irregular base and contains numerous thin (<2 cm) mudstone lenses. In thin section, many ooids are collapsed; those that are not are tangential to (less commonly) radial. Superficial ooids, peloids, fossils, and composite grains made of ooids and/or peloids are also present (Figure 2.1D).

This lithofacies represents sediments deposited downramp from an ooid shoal, similar to those documented in the Bahamas (Ball, 1967; Hine, 1977). The lack of observed cross bedding, the thin bedding, and the mudstone lenses all suggest that this

was not the high-energy shoal itself, but the dominance of ooids and intraclasts composed of cemented ooids suggest a proximal up-ramp source area for these allochems.

Oncoid-Renalcis packstone is present only in the uppermost 2 m of the Craig. In the field, it appears as oncoidal packstone to wackestone because of the micritic microscopic nature of *Renalcis*. Petrographically, it consists of *Girvanella* oncoids, much less common *Renalcis* clasts, and rare echinoderms (Figure 2.1E). It also contains numerous mudstone lenses, some of which are burrowed. The burrows are filled with blocky to fibrous cements.

This lithology represents downramp sediments derived from shallower, shelf-edge areas. The poorly sorted nature of these sediments, their mud-rich matrix, and the broken and abraded nature of allochems suggest transport, probably by storms.

Oncoid-fossil grainstone is present as a 0.2 m thick bed at the top of the Craig Limestone and rare 1 cm thick interbeds in the basal 3 cm of the Rogersville shale. This unit has a planar base and consists of a basal peloid-oncoid grainstone that rapidly grades up into oncoid-fossil grainstone. At the limestone-shale interface, many of these oncoids are not truncated, and where the shale is removed by weathering, they appear as an "oncoidal pavement." Thin-section analysis reveal that this unit is comprised of *Girvanella* oncoids, trilobites, and less common echinoderm grains, *Renalcis* clasts, and rare phosphatic brachiopods (Figure 2.1F). It contains abundant framboidal pyrite and phosphate and manganese encrustations. It is cemented by blocky to bladed to fibrous calcite. In the thin packstone to grainstone layers present within the shale, the fibrous cements are ferroan (as indicated by staining).

This unit was deposited as grainflow(s) into deeper water perhaps triggered by storms, as suggested by the encrustations, pyrite, thin interbeds in the overlying shale, and grainy nature. Long intervals of time are represented by the various truncation surfaces, some of which truncate pyrite.

ENVIRONMENTAL SYNTHESIS

The Craig Limestone Member is underlain and overlain tongues of the Rogersville Shale, both of which represent deeper-water deposition (Walker and others, 1990). Before it pinches out to the west and southwest, the Craig Limestone most commonly consists of deeper-water slope-basin lithologies, similar to those documented by Srinivasan and Walker (1993) for the Maryville Limestone. Like many other documented carbonate sequences (James, 1984; Hardie, 1986), the Craig Limestone in platformward areas (such as that documented here) represents a generally shallowing-upwards trend, although it is not as fully developed as other Middle Cambrian cycles (such as the Maryville; see Chapter 3).

The basal Craig and the underlying lower Rogersville Shale represent deposition on a ramp setting developed during the shale part of grand cycle development. Debris flow and turbidite beds (not observed at DSR because most of the shale areas are covered, but present elsewhere) are present within the shale. The contact of the Craig with the lower Rogersville Shale is abrupt, and no slope lithologies such as intraclast packstones or grainstones are present in the basal Craig. Rather, mudstones with framboidal pyrite and glauconite dominate the basal few meters. Because of the lack of any evidence for a change in sedimentation rate, the transition from shale to limestone in this cycle seems be a result of the termination of siliciclastic input. This change could be the result of several possible causes. First, the source area could become more distal because of continental transgression. Second, clastic input could become diminished because of climatic fluctuations (Cowan and James, 1990). The upper parts of the lower Rogersville Shale and the basal Craig represent deposition in an outer ramp setting, characterized by rare storm reworking and generally slow deposition.

Above this basal outer ramp interval, mid-ramp sediments dominate for most of the

rest of the Craig. A general proximal-distal trend with respect to shallower platform areas is present from the base of this interval to the top. The bottom two-thirds of the Craig represents more distal mid-ramp environments, with relatively rare storm reworking (i.e. grainstone layers). The grains in these layers are most commonly composite grains, which suggest slow deposition and cementation (Fluegel, 1982). The upper one-third contains evidence of much more frequent storm activity typical of proximal mid-ramp settings. In these layers, ooids and oncoids typical of inner ramp shoals predominate, suggesting that these environments were closer during this interval. This trend is similar to that in the mid-ramp and aggrading ramp packages of the Maryville (Chapter 2).

Only in the upper 4 m of the Craig does storm reworking and transport become dominant. In this interval, ooids, *Girvanella* oncoids, and *Renalcis* clasts dominate, suggesting that these allochem-producing environments were still closer.

Approximately 0.4 m from the top of the Craig, a 0.2 m thick mudstone-wackestone bed contains common outcrop-scale dissolution voids filled with blocky calcite, the result of subaerial exposure and meteoric diagenesis (see detailed description in Chapter 5). Above this interval are truncation surfaces that cut both the blocky calcite and framboidal pyrite, and are overlain by allochthonous packstones to grainstones. Thin interbeds of this lithology are present in the basal parts of the overlying shales suggesting that platformward source areas were still producing carbonate sediment even while these basinward areas were being inundated by siliciclastics, and that an environmental crisis (temperature or salinity variations) or siliciclastic "poisoning" of carbonate-producing environments was not the cause of platform demise. Chapter 5 discusses the probable tectonic control of platform termination.

CONCLUSIONS

In general, the Craig Limestone contains stacking patterns similar to the lower quarter of the Maryville Limestone. The underlying lower Rogersville Shale represents basinal and slope deposition, as does the basal part of the Craig. The Craig then contains a shoaling-upward trend, from mid-ramp to aggrading ramp packages and contains evidence that shoal deposits (ooid shoals and bioherms) were relatively close to the study area when the platform was terminated by meteoric exposure and subsequent drowning. The Craig represents the "premature" death of a platform, in that it does not develop as fully as the Maryville platform (documented in Chapter 3). The cause of platform demise was the same for both platforms, however.

CHAPTER 3

Stacking patterns in the Maryville Limestone (Middle Cambrian), southern Appalachians

ABSTRACT

The Maryville Limestone (Middle Cambrian) of the southern Appalachians is divided into six distinct stratigraphic packages (slope, mid-ramp, aggrading ramp, shoal, lagoonal, and peritidal, and backstepping platform/shelf). The slope through peritidal packages are interpreted to reflect reestablishment of carbonate sedimentation after a drowning interval. This reestablishment of the platform was followed by sedimentary aggradation and platform progradation, yielding a shallowing-upward trend. At the top of the peritidal package, an exposure surface (also present elsewhere on the platform) represents a sequence boundary. Above this exposure surface, a significant change in platform dynamics, interpreted to be due to non-thermal subsidence and decreased sedimentation rate, is manifest as a deepening-upward trend (backstepping platform/shelf package).

INTRODUCTION

Stratigraphic packaging can reveal important details concerning the genesis of sedimentary sequences. The purpose of this chapter is four-fold: 1) to document the sedimentary packages present in the limestone part of the Maryville Limestone; 2) to refine and expand the model for Middle Cambrian carbonate shelf development

(Srinivasan and Walker, 1993); 3) to consider various controls on the development of the sequence; and 4) to distinguish the varying effects of tectonism in different parts of the platform facies array. The results of the data in this chapter suggest that sedimentary aggradation and progradation were dominant controls on internal stratigraphic packaging of the Maryville platform, but that episodic tectonism, coupled with platform exposure, were responsible for platform termination.

STRATIGRAPHIC PACKAGING IN THE MARYVILLE

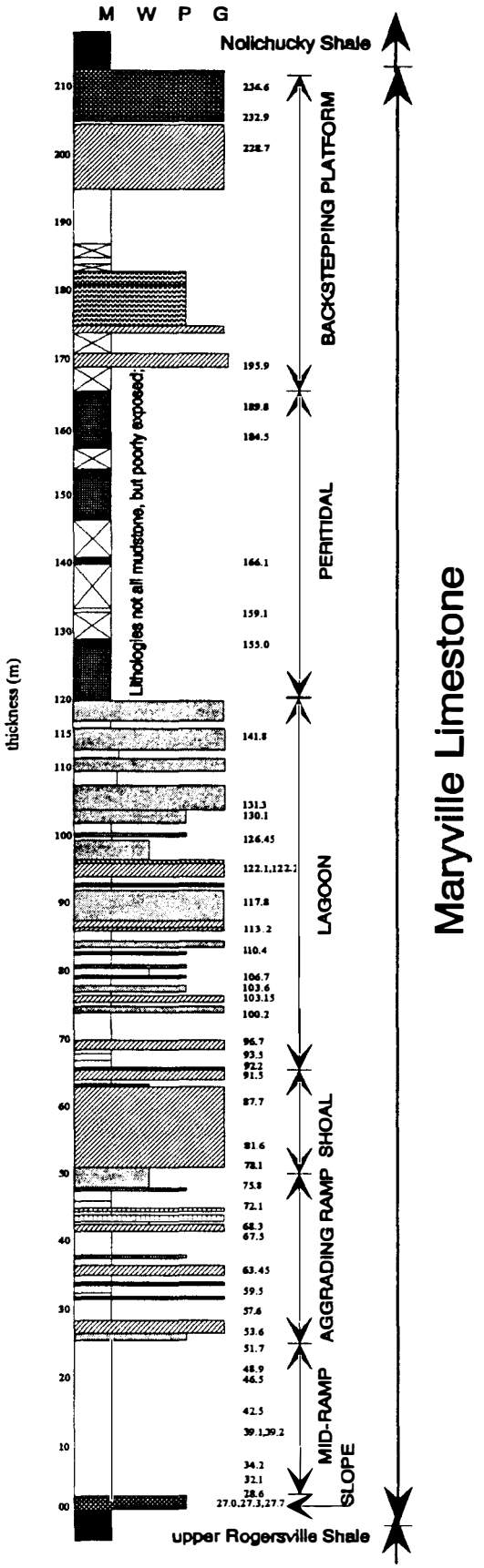
In this paper, the term *stratigraphic packages* refers to a group of genetically related lithologies, all "linked" in the sense that they all formed in a similar setting (i.e. slope or peritidal), but were deposited under slightly different environmental conditions. The purpose of this part of the thesis is to document the various genetic packages and their components.

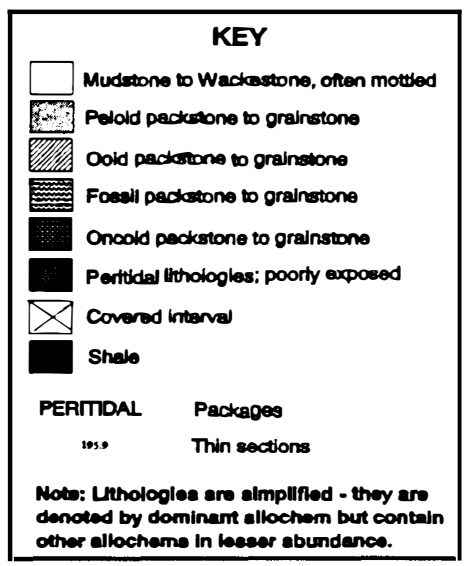
The Maryville consists of six stratigraphic packages (Figure 3.1): slope, mid-ramp/aggrading ramp, shoal, lagoon, peritidal, and backstepping platform/shelf. Each package consists of several lithologies.

Slope Package

The slope package is sharply underlain by the upper Rogersville Shale. This shale is clay-rich, dark gray to black to dark green, contains paper-thin laminations, and occurs with interbeds of iron, phosphate, and manganese-coated allochthonous intraclasts, fossils, and oncoids. No evidence for wave or storm activity is present in these shales. The basal 25 m of the Maryville also contains no evidence for the influence of normal- or storm-wave base, suggesting that deeper water was still present during deposition of the shale and the beginning of carbonate (Maryville) deposition. Bond and others (1989) estimated

FIGURE 3.1 - Stratigraphic section of Maryville Limestone at DSR section. Measured section at I-40 and Deep Springs Road on-ramp (DSR-1 section). The peritidal package is poorly exposed at this location. Small numbers to the right of the column represent samples from which thin sections were prepared. For a detailed lithologic description, see Appendix A of this thesis.


M W P G
Nolichucky Shale
upper Rogersville Shale
Maryville Limestone
thickness (m)
Lithologies not all mudstone, but poorly exposed
BACKSTEPPING PLATFORM
PERITIDAL
LAGOON
SHOAL
AGGRADING RAMP
MID-RAMP
SLOPE
234.6
232.9
228.7
195.9
189.8
184.5
166.1
159.1
155.0
141.8
131.3
130.1
126.45
122.1,122.2
117.8
113.2
110.4
106.7
103.6
103.15
100.2
96.7
93.5
92.2
91.5
87.7
81.6
78.1
75.8
72.1
68.3
67.5
63.45
59.5
57.6
53.6
51.7
48.9
46.5
42.5
39.1,39.2
34.2
32.1
28.6
27.0,27.3,27.7


KEY
Mudstone to Wackestone, often mottled
Peloid packstone to grainstone
Ooid packstone to grainstone
Fossil packstone to grainstone
Oncoid packstone to grainstone
Peritidal lithologies; poorly exposed
Covered interval
Shale
PERITIDAL Packages
195.9 Thin sections
Note: Lithologies are simplified - they are denoted by dominant allochem but contain other allochems in lesser abundance.

30-50 m water depth during deposition of similar Cambrian sediments in the Canadian Cordillera. Similar shales are dominant to the west in the intrashelf Conasauga basin. Thus, the shales are interpreted to represent basinal deposits that onlapped the underlying Craig platform following its drowning.

The slope package is less than 3 m thick in the Dumplin Valley area (Figure 3.1), but thickens to the southwest and northwest (Srinivasan and Walker, 1993). It is comprised of intraclast packstone, nodular mudstone, trilobite packstone, and oncoid/ooid packstone (summarized in Table 3.1) and contains numerous hardgrounds and abundant phosphate and manganese coated grains (Figure 3.2A). These sediments represent distal storm deposits and/or pelagic carbonate mud deposits deposited below storm wave base. The westerly thickening of this package reflects the westerly siliciclastic source (Rodgers, 1953) as well as the deeper water in those areas during carbonate deposition and the longer time before *in situ* carbonate production began. For a more complete discussion of this package, see Simmons (1984), Kozar (1986) or Srinivasan and Walker (1993).

Mid-Ramp/Aggrading Ramp Package

At the Deep Springs Road section, mid-ramp deposits of the Maryville are 21.8 m thick (Figure 3.1); constituent lithologies are given in Table 3.1 and illustrated in Figure 3.2B. The dominant lithology in the mid-ramp deposits is burrow-mottled mudstone-wackestone. Packstones to grainstones (Figure 3.2B) in this package are all less than 0.2 m thick - most are less than 0.1 m (Figure 3.3), and many are discontinuous across the outcrop.

The mid-ramp sediments of the Maryville were deposited below normal wave base, but above storm wave base. The thin packstones and grainstones represent times of lowered wave base caused by higher energy storms or irregular relative sea-level falls. The mid-ramp package was subdivided from the overlying aggrading ramp package on the

TABLE 3.1- LITHOLOGIC DESCRIPTION OF MARYVILLE COMPONENTS

Lithology	Thickness	Base	Constituent Particles	Sedimentary Structures	Other
Slope Package					
Packstone	< 0.5 m	abrupt, irregular	Major- intraclasts, trilobite fragments, oncoids Minor- peloids, ooids, glauconite	hardgrounds, imbrication	allochems commonly have micritized rim fibrous cement
Nodular Mudstone	< 0.5 m	abrupt, irregular	micrite, rare trilobites, glauconite	hardgrounds and truncation surfaces (Fig. 3.2A)	
Mid-Ramp Package					
Mottled Mud-Wackestone	up to 21 m	gradational	Major - micrite Minor - trilobites, composite grains, peloids	abundant burrows (ii2-ii4 of Droser and Bottjer, 1986) convex-up fossils hardgrounds in lower 7 m	
Packstone-Grainstone	< 0.15 m	abrupt, scalloped, up to 2 cm relief (Fig. 3.2B)	Major - peloids, ooids, small intraclasts (commonly identical to underlying lith.) Minor - echinoderms, trilobites, oncoids, ostracods	fining-upwards cross-laminations	laterally discontinuous, often form lenses allochems commonly found in burrows in underlying mudstones
Aggrading Ramp Package					
Mottled Mud-Wackestone	up to 5 m	abrupt to gradational	Major - micrite Minor - trilobites, composite grains, peloids, ostracods	abundant burrows (Fig. 3.2C) convex-up fossils	
Packstone-Grainstone	up to 1.9 m	abrupt, irregular	Major - ooids, peloids, composite grains, small intraclasts Minor - oncoids, trilobites, echinoderms, ostracods	grade upwards to mud-wackestone cross-laminations intraclasts common near base of unit; made of micrite, similar to underlying unit	laterally continuous across outcrop, but often discontinuous across 0.3 km; may thicken and thin across outcrop
Shoal Package					
Grainstone	up to 10 m (massive)	abrupt, irregular	Major - ooids (Fig. 3.2D) Minor - echinoderms, trilobites, peloids, ostracods, intraclasts (most commonly oolitic w/ fibrous cement)	cross-laminated	ooids relatively small (up to .2mm), radial to tangential; up to 5 laminae; nuclei composed of echinoderms, peloids, trilobites early fibrous cement
Mudstone to Wackestone	< 0.5 m	abrupt to gradational	micrite with rare ooids, echinoderms	occasionally burrowed	
Lagoon Package					
Mottled Mud-Wackestone	up to 4 m,	gradational to abrupt	micrite, with minor fossils, peloids, ooids	burrows	contains thin (< 1 cm) fossil and peloid lenses
Packstone	up to 1.2 m	gradational to abrupt, irregular	Major - peloids, ooids Minor - trilobites, echinoderms, small intraclasts near base	cross-laminations	peloids very fine grained (Fig. 3.2e) often completely dolomitized ooids identical to those in shelf-edge
Peritidal Package – see Table 3.3					
Backstepping Shelf-Platform Package					
Packstone to Grainstone	up to 5 m	abrupt to gradational	Major - ooids, oncoids, trilobites Minor - echinoderms, peloids, intraclasts	cross-laminations imbricated intraclasts hardgrounds (Fig. 3.2F)	
Mud- Wacke- to Packstone	up to 4 m	gradational to abrupt	Major - micrite Minor - peloids, ooids, quartz silt, glauconite	fine laminations burrows (ii2-ii4)	

Figure 3.2 - Photomicrographs of a representative lithologies, subtidal sediments. Stratigraphic up is towards the top of the page. Long axis of all photos is 4.5 mm.

A. Slope package. Mineralized hardground/truncation surface. Note truncated intraclast (I) and hardground (arrows). From DSR-1 section, 0.2 m above base of Maryville.

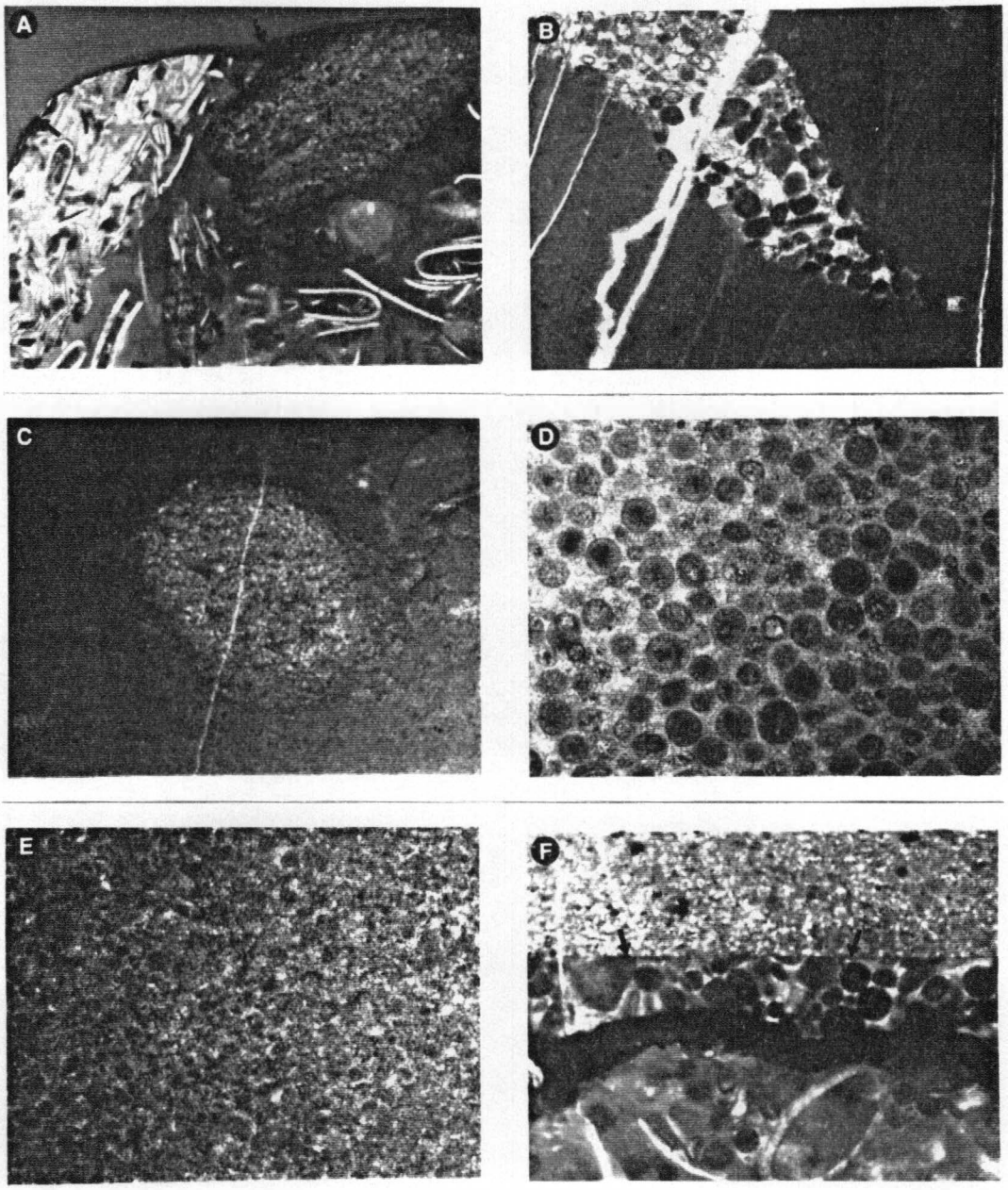
B. Mid-ramp package. Scalloped base of packstone/grainstone lens. These lenses contain variable amounts of peloids, ooids, trilobites, echinoderms, ostracods, and less commonly oncoids. From DSR-1 section, 13 m above base of Maryville.

C. Aggrading Ramp package. Dolomitized burrow in mudstone/wackestone. From DSR-1 section, 32 m above base of Maryville.

D. Shoal package. Ooid grainstone. Some ooids completely replaced with fine grained dolomite. From 61 m above base of Maryville, DSR-1 section.

E. Lagoon package. Peloid packstone/grainstone. Note very fine-grained peloids, completely dolomitized. From 8 m below peritidal package, SR section.

F. Backstepping platform/shelf package. Truncation surface (arrows) cuts ooid/peloid/fossil grainstone. Overlain by quartz silty peloid packstone. IS section, 48.0 m from base.


A
B
C
D
E
F

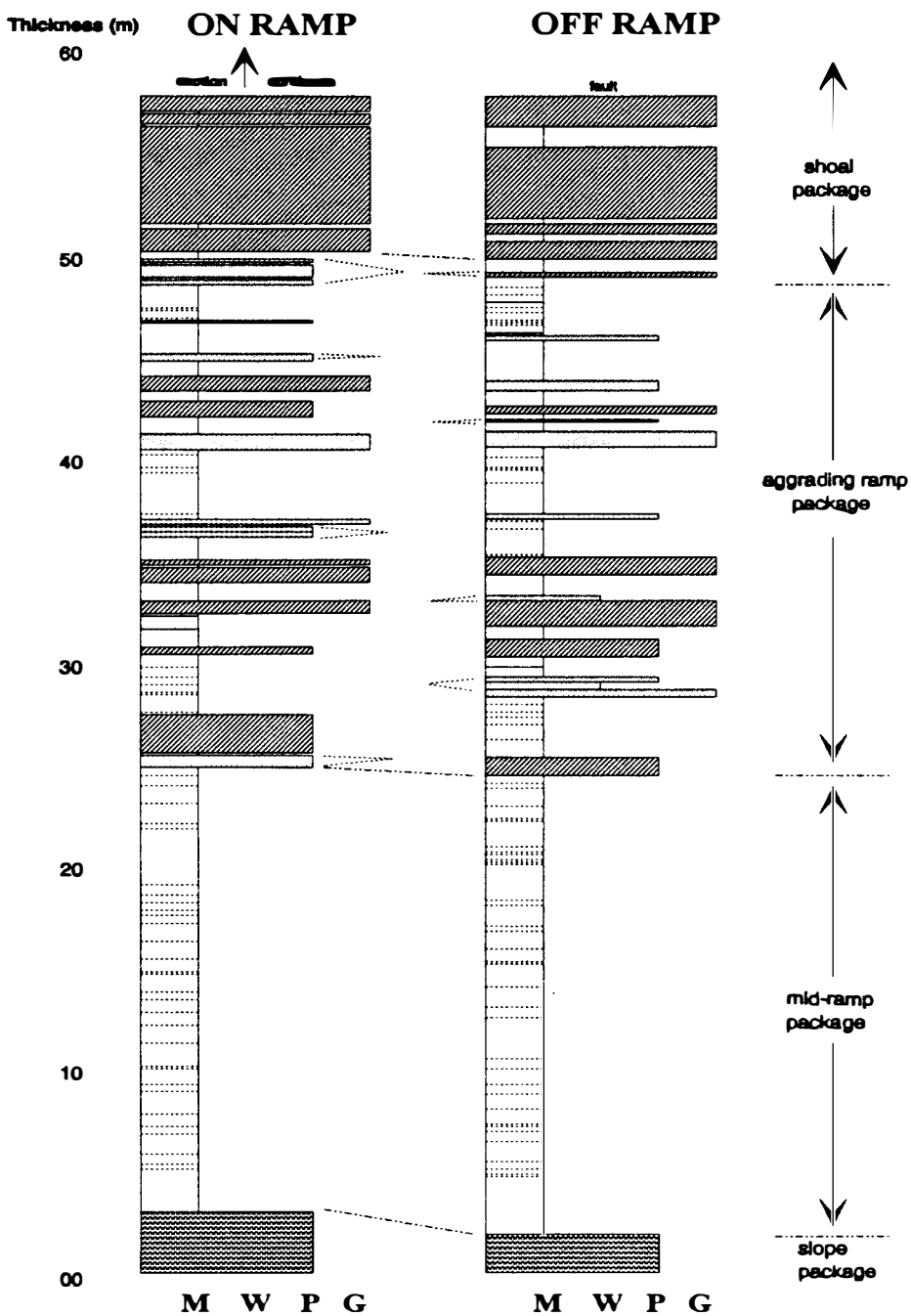


Figure 3.3 - Detailed stratigraphic comparison of DSR section off-ramp and on-ramp. Sections located less than 400 m apart. Thin dashed lines in mid-ramp package represent packstone-grainstone layers less than 0.05 m thick. Note the lack of correlation of these layers and that one-third of the grainy layers in the aggrading ramp package are likewise not continuous across this distance. See figure 3.1 for lithologic legend.

Table 3.2 Abundances (by stratigraphic thickness) of lithologies in packages

		← wacke-, pack-, and grainstones, by most abundant and second most abundant allochem →								
Package	mud	pel-oo	oold	oo-pel	oo-fos	pel-fos	foss.	onc-etc.	Qsil	pel-int
Mid Ramp	94	—6 total—								
Aggr. Ramp	60	5	21	1	1	6	<1	-	-	-
Shoal	8	-	89	3	-	-	-	-	-	-
Lagoon	43	10	24	5	<1	2	<1	-	-	15
Backstepping	32	-	12	<1	11	-	13	26	2	3

	x-alg	oold	oo-pel	pel-oo	IC	pel	pel-IC	mud	exp	IC-pel
Peritidal (IS)	29	4	3	3	4	16	19	15	4	3
Peritidal (SR)	33	3	11	9	1	21	6	14	2	<1

Table 3.2 Lithologic abundances (by thickness) normalized to 100 % per package. Note the abundance of mudstone in mid-ramp package, the paucity of mudstone in the shoal package, and the distinct backstepping platform/shelf lithologies. The differences in SR and IS peritidal packages are discussed in Chapter 4. Abundances based on field measurements supplemented by slabs and thin sections. Abbreviations: mud = mudstone; pel = peloid; oo = ooid; fos = fossil; onc = oncoid; Qsil = quartz silt; int = intraclast; x-alg = cryptalgal laminite; exp = exposure-altered interval; IS = Interstate 40 section, SR = Sockless Road section.

basis of thickness of component packstone and grainstone units. As Table 3.2 shows, the mid-ramp package is dominated by mudstone; the aggrading ramp strata have subequal amounts of mudstone and grainy lithologies. The contact between these packages is gradational.

Table 3.1 summarizes the lithologies of the Maryville aggrading ramp package. The package is 26 m thick, and Figure 3.2C is a photomicrograph of a representative lithology from this package. Figure 3.3 indicates that the grainy layers of this package are non-cyclic and that many are discontinuous across the 300 m between sections. The alternating muddy and grainy layers are probably the result of in influence of major storm events. The upward increase in the abundance of grainy layers from mid-ramp to aggrading ramp (Figure 3.3) probably indicates a general shoaling-upwards trend into a zone of more frequent wave reworking.

Shoal Package

Table 3.1 summarizes the lithologies of the shoal package, and Figure 3.2D is a photomicrograph of a representative lithology. At the Deep Springs Road section, this package is 16 m thick (Figure 3.1) and is comprised primarily of ooid grainstones with rare interfingering thin mudstone lenses (Table 3.1). No peritidal facies or exposure surfaces are present.

The thick ooid grainstones (Figures 3.1, 3.2D) are interpreted to represent migration of ooid shoals through the area, probably infilling available accommodation space. These deposits formed in areas persistently agitated by wave action, similar to ooid shoals documented in the Holocene by Hine (1977) and Harris (1979) and in the Cambrian by Markello and Read (1981, 1982) and Erwin (1981). Ooid shoals gave way to algal bioherms during later stages of platform development at the shelf-edge (Srinivasan and Walker, 1993), but bioherms were not observed in the Dumplin Valley area. The thin

mudstone lenses present in this package probably represent ephemeral protected environments leeward of shoals.

Lagoon Package

The lagoon package (Tables 3.1, 3.2; Figure 3.2E) is present between the shoal package and the peritidal package. At the Deep Springs Road section, it is 50 m thick (Figure 3.1). The sediments of the lagoon package are interpreted to represent deposition in protected settings bankward of the shelf-edge ooid shoals. The mudstones, which are commonly burrowed, and the fine-grained peloidal packstones to grainstones (Figure 3.2E) were deposited in environments similar to those documented in the modern Bahamas by Purdy (1963) for "pellet-mud" and "mud" facies. The ooid-peloid packstones were probably formed by sporadic bankward storm or tidal deposits or washovers, similar to those documented by Purdy (1963) in the lagoonal facies of the modern Bahamas, and by Beach and Ginsburg (1980) in the Plio-Pleistocene of the Bahamas.

Peritidal Package

The peritidal package ranges in thickness from zero to 58 m in the Dumplin Valley area. The lithologies of the peritidal package are summarized in Table 3.3 and representative photomicrographs are shown in Figures 3.4A-F. The sediments contain features similar to peritidal deposits of both the Persian Gulf, Bahamas, and Florida Bay (see references in Table 3.3). These lithologies were formed on an arid tidal flat, in environments such as intertidal-supratidal marshes, levees, and beach ridges, as well as subtidal channels, deltas, and lagoons (Table 3.3). Only two intervals contain features possibly associated with prolonged exposure. The lower (Figure 3.4D; observed only at the SR section) may correspond to the lower exposure surface that Srinivasan and Walker (1993) observed at Woods Gap, TN. The uppermost strata of the peritidal package also

TABLE 3.3 - LITHOLOGIC DESCRIPTIONS OF PERITIDAL PACKAGE

Lithology	Thickness	Base	Constituent Particles	Sedimentary Structures	Other	Interpreted Environment	References
Cryptalgal laminite	up to 4 m, most < 2 m	gradational to abrupt	small peloids, micrite	fine laminations, mostly planar, some undulose; fining upwards "anti-gravity" features mudcracks irregular and laminar fenestrae	many completely dolomitized thin (cms) packstone layers early cementation, as shown by truncated cements and laminite intraclasts (Fig. 3.4A)	intratidal-supratidal marsh intratidal-supratidal levees	Aitken, 1967; Black 1933 Ginsburg and Hardie, 1975 Kendall and Skipworth, 1968 Laporte, 1971; Logan, 1961 Logan and others, 1974 Shinn, 1968, 1973, 1983, 1986
Fenestral Mud- to Packstone	up to 2 m	gradational	peloids, small intraclasts, ooids	laminar to irregular fenestrae (Fig. 3.4B)	fenestrae filled with coarse blocky dolomite to calcite early cementation	supratidal marsh	Fischer, 1964; Grover and Read, 1978 Logan, 1974 Shinn, 1968, 1983, 1986
Ooid Packstone-Grainstone	<2 m	abrupt, irregular, erosional?	Major - ooids (Fig. 3.4A,F) Minor - peloids, small intraclasts (made of ooids or underlying lithology)	uni- and bidirectional cross-laminations	ooids tangential, tightly packed up to 5 laminae ooid nuclei echinoderms, peloids	tidal deltas, bars, and channels lagoons	Evans and others, 1973 Loreau and Purser, 1973 Purser and Evans, 1973 Wagoner and van der Togt, 1973
Intraclast Packstone	< 1 m	erosional (up to 0.3 m relief)	Major - intraclasts Minor - peloids, ooids	imbricated intraclasts some layers discontinuous fine-upwards into smaller intraclasts and peloids	intraclasts up to 4 cm long, rounded, made of micrite, ooid peloid packstone, or laminite locally channel morphology	supratidal levee tidal channel beach ridge ?	James, 1984 Shinn, 1973, 1983, 1986 Shinn and others, 1969
Peloid Packstone	< 3 m	gradational to abrupt	Major- peloids Minor - intraclasts (near base), ooids	burrowed	subtidal offshore - dark gray, often completely dolomitized, very fine grained subtidal lagoonal - buff to light gray, fine to coarse grained, often assoc. w/ small intraclasts	subtidal offshore subtidal lagoonal	Shinn, 1973, 1986 Shinn and others, 1969 Purser and Evans, 1973 Shinn, 1973
Mudstone	< 1 m	gradational	micrite	none, burrow homogenized?	commonly completely dolomitized	protected subtidal	Logan, 1974 Shinn, 1983, 1986
Exposure-altered interval	< 0.5 m	gradational	precursor particles, pisoids shrinkage features (Fig. 3.4D)	aveolar septal structure?	extensive fabric-selective and wholesale dissolution (Fig. 3.4E) developed in ooid packstone, mudstone, and peloid packstone common near top of peritidal package, at 33.3 at SR section	subaerial exposure	Esteban and Klappa, 1983 Read, 1974 Chapter 6, this thesis

Figure 3.4 - Photomicrographs of representative lithologies, peritidal package. Long axis on all photos is 4.5 mm.

A. Peritidal package. Cryptalgal laminite intraclast in ooid-intraclast grainstone. Note truncated cement (arrow) and fenestrae in intraclast. Shelter porosity filled with coarse blocky dolomite. From IS section, at 21 m from base.

B. Peritidal package. Mudcrack (M), filled with sediment from above. Note laminar fenestrae (F) also. From SR section, 43.3 m from base.

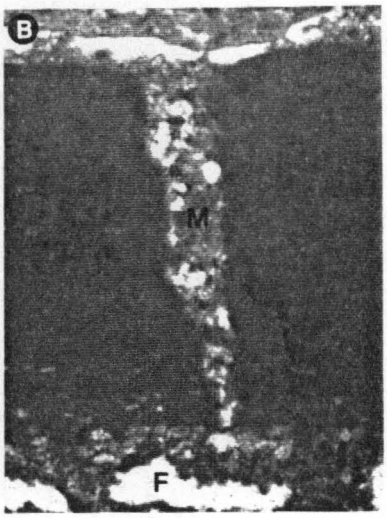
C. Peritidal package. Anhydrite pseudomorphs (A). Anhydrite has been dissolved and replaced by vadose silt (V) and iron-poor calcite (as indicated by staining). Note crust-like appearance of some molds; others appear as isolated acicular molds. From SR section, 13.2 m from base.

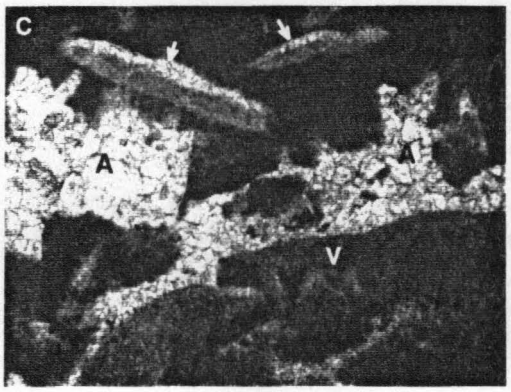
D. Peritidal package. Exposure-altered interval, associated with lower exposure surface. Note shrinkage (S) and fine-grained dolomite (D). From SR section, 33.3 m from base.

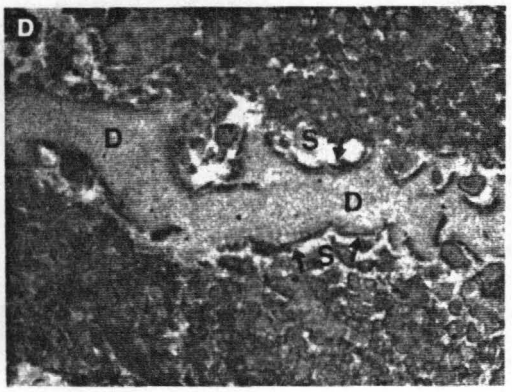
E. Peritidal package. Vadose silt, fabric-selective dissolution associated with upper exposure surface. From 61.3 m from base, SR section.

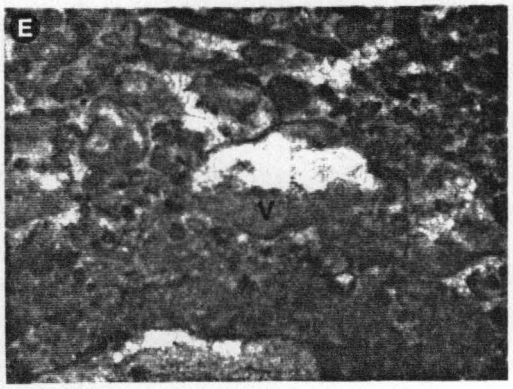
F. Peritidal package. Multigenerational intraclast, probably from a tidal delta or tidal channel. Intra-intraclast truncation surface indicated by arrow. Note that ooids in intraclast are similar to matrix. From SR section, 36 m above base.

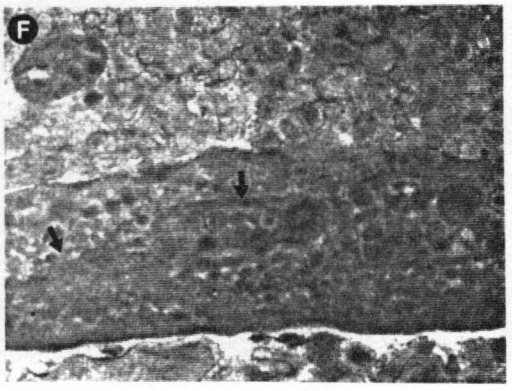

A


B
M
F


C
A
A
V


D
D
S
D
S


E
V


F

contain features probably developed by prolonged exposure, such as extensive fabric-selective and non-fabric selective dissolution (Figure 3.4E), vadose silt, and a reddish coloration. This exposure interval probably corresponds to that documented by Srinivasan and Walker (1993) at the top of the Maryville in basinward areas because it signals a unique and distinct change in platform dynamics in both areas (discussed later). Chapter 4 contains a detailed discussion of parasequence stacking patterns in the peritidal package.

Backstepping platform/shelf package

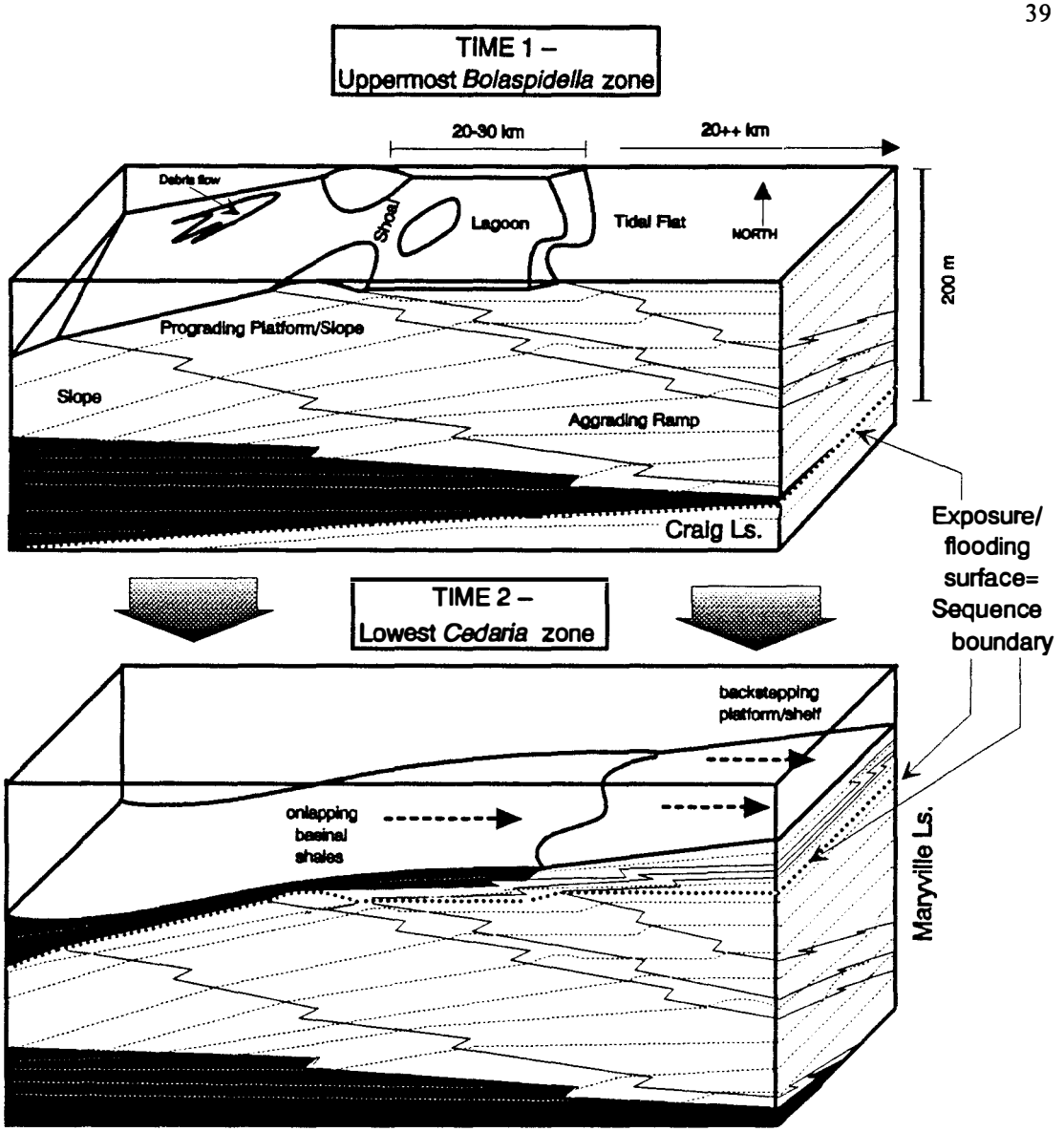
This package (Table 3.1; Fig. 3.2F) occurs above the peritidal package and below the shales and deep-water limestones of the Nolichucky Formation (Walker and others, 1990). It is up to 25 m thick in the Dumplin Valley fault zone, but thins to absent to the west and thickens to the northeast..

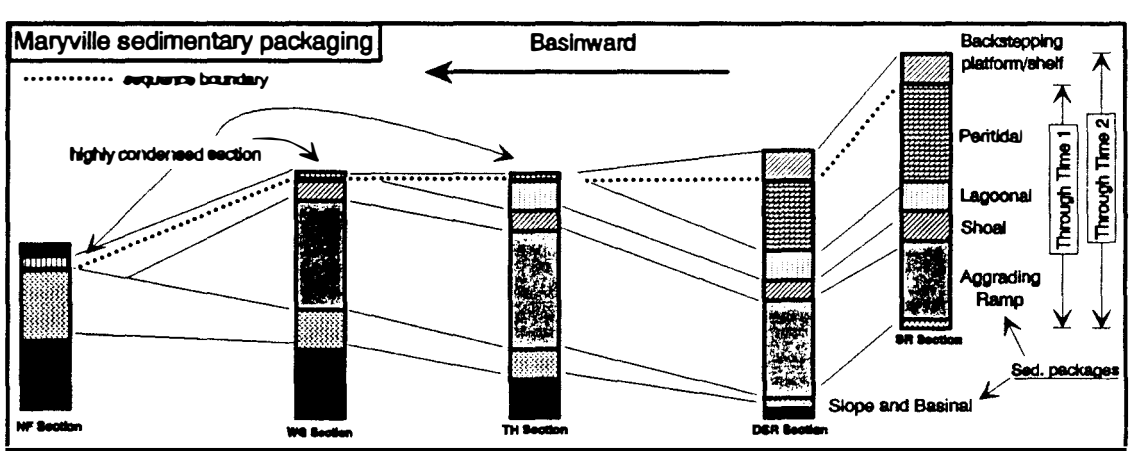
These rocks are interpreted to represent a rapid deepening-upward trend to deeper-water deposition following demise of the platform but before deposition of the shaly to quartz-silty carbonate deposits of the Nolichucky Shale (Walker and others, 1990). Its distibution suggests that it was deposited in areas where platform-drowning, tectonic subsidence was less pronounced, within range of allochthonous carbonates from areas still producing carbonate sediments. This package is overlain by the deeper water or down-ramp basinal shales of the Nolichucky Shale.

MODEL FOR EVOLUTION OF THE MARYVILLE SHELF

This study of the sedimentary packages exposed in the Dumplin Valley fault zone permits development of a more complete model for the evolution of the Maryville carbonate shelf. The purpose of this section is to present a model for the development of these stratigraphic packages, and thus for the Maryville shelf (Fig. 3.5).

Figure 3.5 - Model for the development of the Maryville shelf. Dashed lines represent inferred time-lines. The sedimentary packages defined in this study are shown. Note the south/southwesterly progradation of the platform, and the thinning carbonate sections and thickening shale sections in that direction. The columns underneath the diagram schematically represent stratigraphic sections measured for this thesis [DSR-1 and SR] and by Srinivasan (1993) [TH, WG, and NF].


TIME 1 –
Uppermost *Bolaspidella* zone
20-30 km
20++ km
Debris flow
Shoal
Lagoon
Tidal Flat
NORTH
200 m
Prograding Platform/Slope
Slope
Aggrading Ramp
Craig Ls.
Exposure/
flooding
surface=
Sequence
boundary
TIME 2 –
Lowest *Cedaria* zone
backstepping
platform/shelf
onlapping
basinal
shales
Maryville Ls.


Maryville sedimentary packaging
Basinward
sequence boundary
highly condensed section
Backstepping
platform/shelf
Peritidal
Lagoonal
Shoal
Aggrading
Ramp
Through Time 1
Through Time 2
BR Section
Sed. packages
Slope and Basinal
NF Section
WG Section
TH Section
DSR Section

Deposition of the basal Maryville took place on a gently sloping ramp (Srinivasan and Walker, 1993). The contact with the underlying shales is abrupt. In platformward areas, the slope package is thin (< 3 m), but thickens significantly towards the basin. In more distal areas, slope sediments are interbedded with basinal shales and these together comprise the entire Maryville (Figure 3.5; see Srinivasan and Walker, 1993).

In platformward areas, slope deposits are overlain by relatively thick (up to 45 m) mid-ramp and aggrading ramp sediments. These predominantly muddy rocks represent the beginning of shoaling in the Maryville and correspond to the aggrational stacking pattern of Srinivasan and Walker (1993). These areas provided sediment transported basinward and deposited as distal storm deposits and debris flows (slope package). Aggradation led to the development of a very shallow ramp across much of the shelf.

Overlying the mid-ramp and aggrading ramp deposits are ooid shoal deposits. These ooid shoals represent times of maximum aggradation, probably up into constantly agitated waters less than 5 m deep, as in modern shoals (Harris, 1977; Hine, 1979). The great thickness of the Maryville shoal deposits probably reflects infilling of available acommodation space as shoals aggraded into the zone of maximum wave action.

The lagoon package was deposited in protected environments platformward of the ooid shoals. This lagoon was probably 20-30 km wide and up to 10 m deep. Lagoonal sediments were not subaerially exposed and no peritidal caps developed, suggesting that wave sweeping and redistribution mechanisms (Enos, 1977, 1989; Osleger, 1991) were effective in keeping the sediment-water interface below sea-level.

The peritidal package is limited to the studied part of the Dumplin Valley area, where it occurs immediately above lagoonal deposits. Its overall progradational nature is demonstrated by its across- and along-strike thinning. It probably prograded from the southeast in tongues or may represent migration of large tidal islands. The meter-scale components of this package are neither vertically nor laterally rhythmic, and are not

correlative, even within 5 km (palinspastic) distance, as discussed in Chapter 4.

From the slope to the peritidal package, then, aggradation and progradation were the primary controls on development of the Maryville sedimentary packages (Figure 3.5 top). Aggradation on the initially ramp-like profile was driven by prolific sediment production typical of many carbonate shelves (Schlager, 1981, 1992). Concomitant progradation was driven by excess sediment production in shallower areas, and transport and deposition basinward, ahead of the rapidly shallowing shoals. The end result of these two processes is the regional shoaling-upward trend observed in the development of the slope through peritidal facies of the Maryville.

At the top of the peritidal package, a prominent exposure surface is present. This surface is present in other lithologies across the entire shelf, and has been documented in shelf-edge and lagoonal facies by Srinivasan and Walker (1993).

The transition from peritidal to backstepping platform/shelf packages reflects a significant change in platform dynamics. Platform exposure provided a shutdown of carbonate production, which resumed at a much slower rate after platform re-inundation (Rankey and others, 1992; Srinivasan and Walker, 1993). The decreased *rate* of sedimentation ("lag time" of Schlager, 1981) led to an accentuation of the effects of tectonically induced relative sea-level rise coupled with thermal subsidence (see Chapter 5 for more detailed discussion of the evidence for episodic subsidence and its tectonic implications). Thus, above the exposure surface, the rate of sediment production fell below the rate of sea-level rise and resulted in a deepening-upwards trend (backstepping platform/shelf package; Figure 3.5 middle). The biostratigraphically younger age of the upper Maryville to the north/northeast (Derby, 1965; Palmer, 1981) is the result of the continued deposition of this package consisting largely of allochthonous sediment in these areas.

CONCLUSIONS

Six stratigraphic packages are defined in the Maryville Limestone based sedimentary structures, component particles, and bed thicknesses. The stratigraphic packaging is interpreted to represent a general *shoaling*-upwards trend from the slope package through the peritidal package. A regionally extensive exposure surface occurs at the top of the peritidal package. Above this exposure surface is a *deepening*-upwards trend, related to a decreased rate of sedimentation after reflooding of the old platform and regional tectonic downdropping. Aggradadation and progradation were the dominant controls on depositional styles, but platform exposure and tectonism also effected the final stacking patterns and spatial distribution of the Maryville Limestone.

Chapter 4

Can eustatic, tectonic, and autocyclic processes be resolved from the stratigraphic record in peritidal cycles of the Maryville Limestone (Middle Cambrian), southern Appalachians?

ABSTRACT

The Maryville Limestone (Middle Cambrian) of the southern Appalachians contains numerous shallowing-upward peritidal cycles in a tidal flat package that reaches up to 58 m thick. Cycles are not correlative between sections, and display no systematic vertical or lateral thickening, thinning, or "bundling." Stacking patterns, lack of correlation of cycles, and regional trends documented herein suggest that these cycles were created by a combination of eustatic, tectonic, and autocyclic processes. No evidence for regular (Milankovitchian) eustatic forcing or localized tectonism is present. Instead, the random "facies mosaic" was produced by regional sediment loading and/or tectonism associated with regional extension combined with autocyclic processes and irregular eustatic sea-level fluctuations. Because the peritidal package as a whole is discontinuous along strike, it likely represents progradation of "tongues" of peritidal islands. Autocyclic processes associated with tidal island migration are *probably* the dominant control on final stacking patterns.

INTRODUCTION

Statement of problem

Meter-scale cycles in peritidal carbonate rocks are ubiquitous from the Proterozoic to Holocene (Fischer, 1964; Ginsburg, 1975; James, 1984; Grotzinger, 1986; Osleger and Read, 1991, 1993; Koerschner and Read, 1989; Goldhammer and others, 1990; Hardie and others, 1986; many others). Although these cycles are widely recognized and studied, the processes that lead to their development are still the subject of much debate (Hardie, 1986; Koerschner and Read, 1989; Kozar and others, 1990; Read and others, 1986; Hardie and others, 1991; Read and others, 1991; Wright, 1992). Several mechanisms have been proposed to explain the origin of such cycles: 1) eustatic sea-level fluctuations (Fischer, 1964; Grotzinger, 1986; Read and others, 1986; Koerschner and Read, 1989; Osleger and Read, 1991); 2) tectonic variations (Cisne, 1986; Hardie and others, 1986); and 3) autocyclic processes, such as tidal island migration, tidal channel migration, etc. (Ginsburg, 1971; Matti and McKee, 1976; Hardie, 1986).

Geologic setting

In the study area (Figure 1.1), the Maryville is up to 211 m thick, but some of the uppermost 45 m is probably duplicated due to faulting. The lower 165 m consists of slope, mid-ramp, aggrading ramp, shoal, lagoon, and peritidal lithologies in a shoaling-upward trend (Chapter 3; Figure 3.1). Above the peritidal package, a prominent shelf-wide exposure surface (and sequence boundary) is present. Above the exposure surface in this area, carbonates of the upper Maryville represent a deepening-upward trend that culminates in deposition of the deeper-water shales of the Nolichucky Shale. Elsewhere, the Nolichucky rests directly on the exposure surface (Srinivasan and Walker, 1993). The distribution of various facies was controlled by the overall progradation of the Maryville

platform. The peritidal facies, on which this study is based, was likewise controlled by progradation of the peritidal environments. Thickness trends of the peritidal package (Figure 4.1) indicate a "wedge" shape of peritidal deposits in the Dumplin Valley area, probably related to tidal island distribution and progradation. Thin lenses of peritidal lithologies are present near the top of the Maryville in areas further west, but probably represent isolated peritidal caps associated with the relative sea-level fall that terminated the Maryville platform.

LITHOFACIES AND STRATIGRAPHIC PACKAGING IN THE PERITIDAL PARTS OF THE MARYVILLE

The peritidal package of the Maryville consists of several lithologies (Table 3.2), all of which represent environments similar to those documented in modern tidal flats in the shallow marine, intertidal, or supratidal environment. Much of the peritidal package is dolomitized, probably by penecontemporaneous dolomitization. These sediments are extremely varied, but are "lumped" here for discussion.

Peritidal cycles (Figure 4.2) commonly have a scalloped base (with up to 30 cm relief) and may contain intraclasts composed of the lithology of the underlying bed, indicating erosion prior to, or concomitant with, sedimentation. Intraclastic lithologies are much more common at the IS section, and ooid-rich lithologies are more abundant at the SR section (Table 3.3; Figure 4.2). Other cycles contain a homogenous dark gray mudstone as the basal unit. The grainstone and packstone layers are comprised of ooids, peloids, and intraclasts in varying amounts (Figure 3.4A-F), and are commonly cross-laminated. None of these lithologies contains mudcracks, fenestrae, or other indicators of subaerial exposure, and are thus interpreted to represent subtidal deposition in environments such as lagoons and tidal channels, deltas, or bars. The thickness of the

Figure 4.1 - Regional exposures and distribution of the peritidal package, Maryville Limestone, Dumplin Valley TN. Roads along which the exposures are present are indicated. Pattern indicates areas in which peritidal sediments are present. Numbers next to sections indicate the thickness of peritidal sediments. Note the "wedge" shape (thinning to the SW, NE, and NW) of the peritidal package. A "+" indicates that the base of the peritidal package could not be conclusively located; thus, these measurements represent minimum thicknesses.

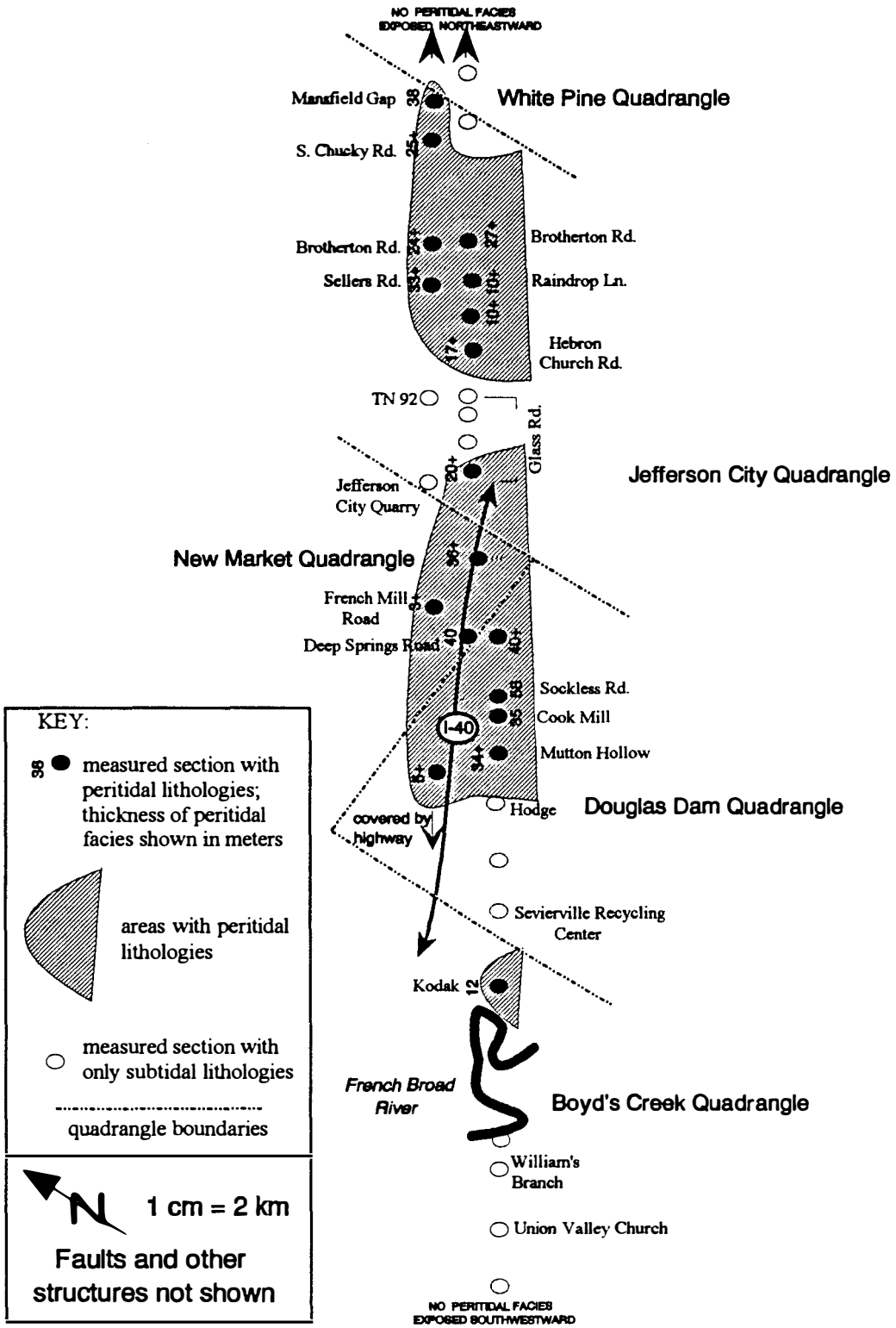
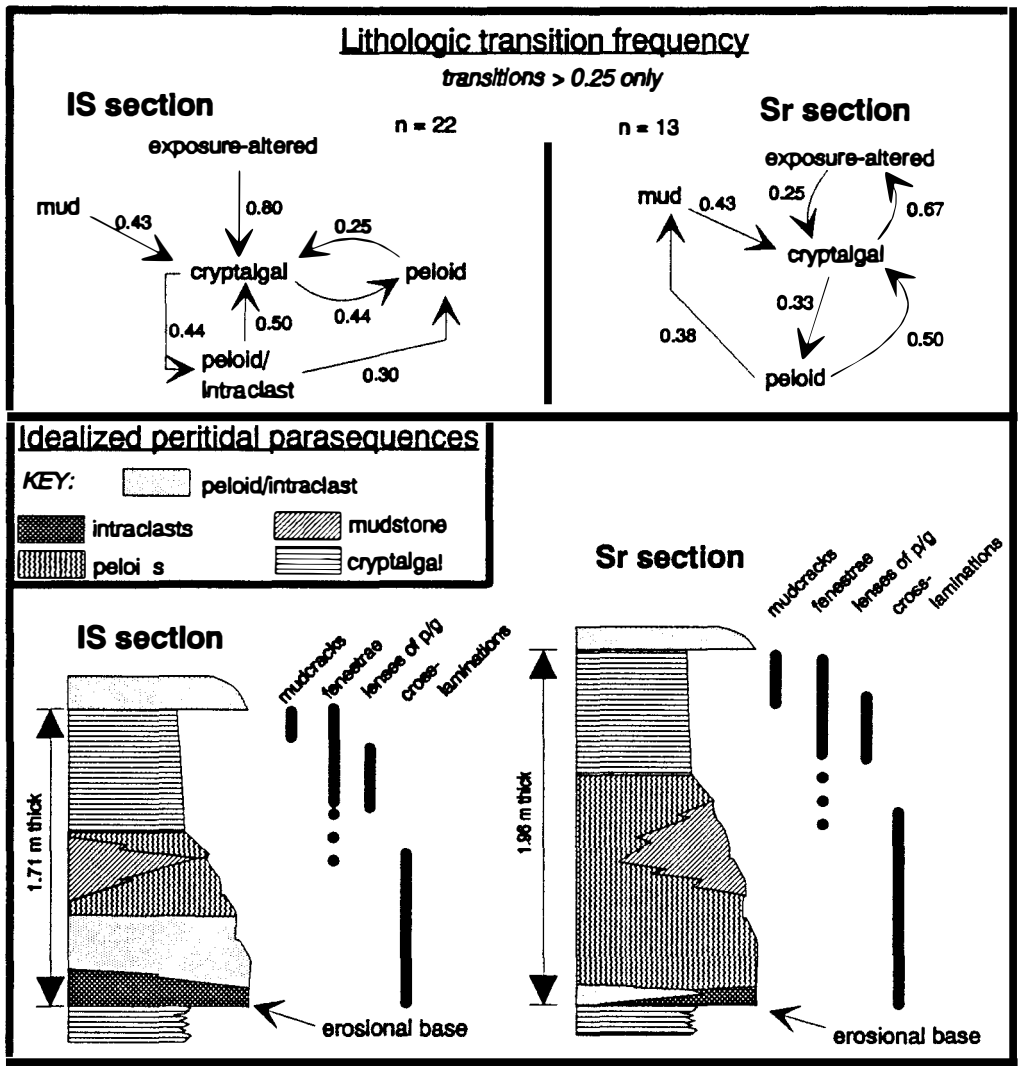

NO PERITIDAL FACIES EXPOSED NORTHEASTWARD
Mansfield Gap
38
White Pine Quadrangle
S. Chucky Rd.
25+
Brotherton Rd.
24+
27+
Brotherton Rd.
Sellers Rd.
23+
10+
Raindrop Ln.
10+
17+
Hebron Church Rd.
TN 92
Glass Rd.
20+
Jefferson City Quarry
Jefferson City Quadrangle
New Market Quadrangle
36+
French Mill Road
5+
Deep Springs Road
40
40+
Sockless Rd.
38
35
Cook Mill
I-40
Mutton Hollow
34+
5+
Hodge
Douglas Dam Quadrangle
covered by highway
Sevierville Recycling Center
Kodak
12
French Broad River
Boyd's Creek Quadrangle
William's Branch
Union Valley Church
NO PERITIDAL FACIES EXPOSED SOUTHWESTWARD
KEY:
38 measured section with peritidal lithologies; thickness of peritidal facies shown in meters
areas with peritidal lithologies
measured section with only subtidal lithologies
quadrangle boundaries
N
1 cm = 2 km
Faults and other structures not shown

Figure 4.2 - Characteristics of peritidal "cycles"

(upper) Semi-quantitative analysis of lithologic transition frequency. Only transitions representing >24% (0.24) of total transitions from a given lithology are shown for simplicity. Lithologies indicate only the dominant allochem, and thus are quite simplistic. Arrows point *towards* the lithology *which overlies* the given lithology. Numbers represent how often the given transition occurs (1.00 = 100% of the time *from a given lithology*). As Appendix C (raw lithologic transition data) shows, however, many other variations are possible. Note that transitions and frequencies vary between the two sections.

(lower) Diagram showing idealized peritidal cycles or parasequences. As suggested above, such cycles are merely simplistic representations of actual "cycles," which show complex transitions and lithologies. Wedges represent less common transitions. Note the more common intraclastic lithologies in IS section, and the thicker SR cycles.


Lithologic transition frequency
transitions > 0.25 only
IS section
n = 22
exposure-altered
mud
0.43
0.80
0.25
cryptalgal
peloid
0.44
0.50
0.44
peloid/
intraclast
0.30
Sr section
n = 13
exposure-altered
mud
0.43
0.25
0.67
cryptalgal
0.33
0.38
0.50
peloid
Idealized peritidal parasequences
KEY:
peloid/intraclast
intraclasts
mudstone
peloi s
cryptalgal
IS section
mudcracks
fenestrae
lenses of p/g
cross-
laminations
1.71 m thick
erosional base
Sr section
mudcracks
fenestrae
lenses of p/g
cross-
laminations
1.96 m thick
erosional base

subtidal portions of cycles ranges from 0 to 3.3 m, and averages 0.7 m (Appendix B).

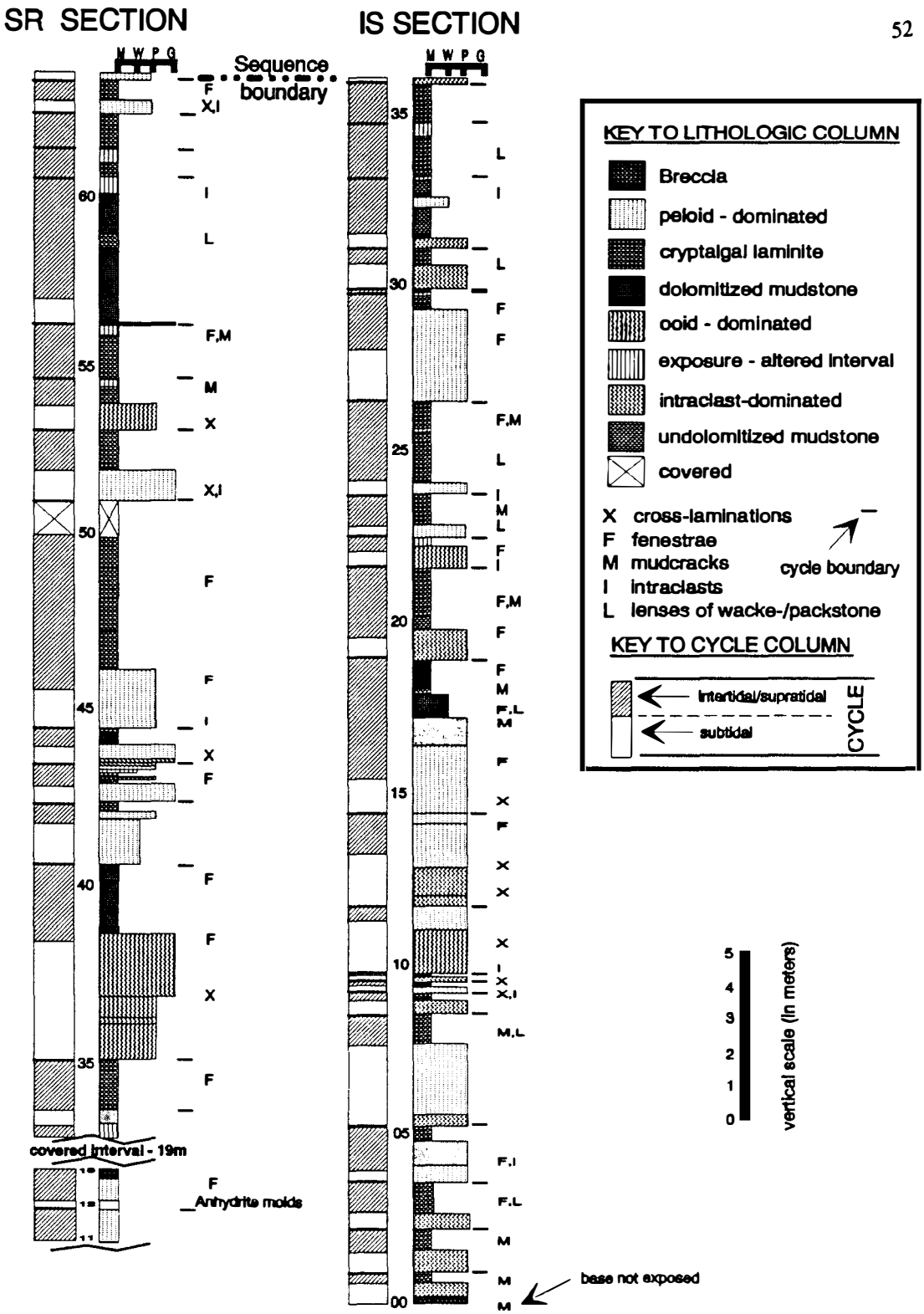
The upper parts of most cycles consist of cryptalgal laminite or peloid-ooid packstone/grainstone with fenestrae, mudcracks, and rare tepee structures (chevron-shaped features formed by dessication of mud polygons; Bates and Jackson, 1984). The uppermost parts of these units are commonly the most subaerially altered (mudcracks, tepee structures, etc.), although evidence for extended periods of exposure is relatively rare. These lithologies gradationally or abruptly overlie the subtidal portions of the cycles, and are interpreted to represent intertidal to supratidal deposition. Intertidal/supratidal thicknesses range from 0 to 3.8 m, and average 1.1 m (Appendix B).

Subtidal and intertidal/supratidal parts together comprise a complete cycle, although in approximately 15 percent of the cycles, the subtidal portion is not present. A "typical" cycle consists of a basal ooid-peloid-intraclast packstone-grainstone which grades upward into fenestral peloid packstone or cryptalgal laminite. Cycle thicknesses average 1.8 m, but cycles range in thickness from 0.2 to 5.5 m (Appendix B). Cycles are not correlative between sections (Figure 4.3), and no systematic thickening or thinning up-section is evident. Instead, cycles appear to be arranged in a random "mosaic" of lithologies. In the lowermost part of the IS section, subtidal lithologies (intraclast packstone and peloidal packstone) in the same stratigraphic interval are laterally adjacent to cryptalgal laminite. Contemporaneous sediments in subtidal settings in advance of the prograding tidal flat likewise show no evidence for regular cyclicity (Srinivasan and Walker, 1993; Chapter 3 of this thesis).

CYCLE MODELS AND MARYVILLE STACKING PATTERNS

Three models have been proposed to explain the origin of similar peritidal "cycles" in other sequences: Milankovitch-induced eustatic sea-level fluctuations (Fischer, 1964;

Figure 4.3 - Detailed comparison of peritidal cycles, IS and SR sections. Sections from the IS (Interstate 40) and SR (Sockless Road) sections (see Figure 1.1), located approximately 3 km apart, no more than 5 km apart palinspastically. Base of peritidal package at IS section not exposed. Note that cycles do not correlate between sections across even this short distance, and that systematic vertical thickening and thinning are not evident.


SR SECTION
IS SECTION
M W P G
Sequence boundary
covered interval - 19m
Anhydrite molds
base not exposed
KEY TO LITHOLOGIC COLUMN
Breccia
peloid - dominated
cryptalgal laminite
dolomitized mudstone
ooid - dominated
exposure - altered interval
intraclast-dominated
undolomitized mudstone
covered
X cross-laminations
F fenestrae
M mudcracks
I intraclasts
L lenses of wacke-/packstone
cycle boundary
KEY TO CYCLE COLUMN
intertidal/supratidal
subtidal
CYCLE
vertical scale (in meters)

Koerschner and Read, 1989; Osleger and Read, 1991), episodic tectonism (Cisne, 1986; Cloetingh, 1986, 1988), and autocyclic processes (Ginsburg, 1971; Hardie, 1986; Selg, 1988; Kozar and others, 1990; Hardie and others, 1991). The purpose of this section is to briefly describe the three major models for repetitive meter-scale peritidal cycles, and comment on their applicability to the patterns observed in the Maryville.

Milankovitch-driven eustatic fluctuations

Orbital variations leading to changes in climate that drive sea-level fluctuations have been well documented in the Quaternary (Broeker and von Donk, 1970; Hays and others, 1976; Berger and others, 1984), and many workers have used these variations as an analog to explain cyclic deposits preserved in the older rock record (Fischer, 1964; Grotzinger, 1985; Goldhammer and others, 1986, 1990; Hardie and others, 1986; Read and others, 1986; Koerschner and Read, 1989; Fischer and Bottjer, 1991; Osleger and Read, 1991). Systematically varying cycle thicknesses and bundling have been related to stratigraphic forcing by glacioeustatic oscillations driven by the 19, 23, 41, 100, and 413 ka (and longer) Milankovitch rhythms.

Several theoretical problems exist concerning the ways that these Milankovitch cycles are commonly "recognized" in the rock record. First, these cycles are commonly defined by Fischer plots (Fischer, 1964; Read and others, 1986; Koerschner and Read, 1989; Osleger and Read, 1991). Although useful as an *illustrative* tool for showing changes in cycle thicknesses through a given stratigraphic section (Steinhauff and Walker, in press), these diagrams do **not** necessarily define sea-level excursions. A fatal flaw with Fischer plots is the assumption that cycles represent equal amounts of time (Hardie and others, 1991). This relation may be valid if creation of accommodation space (eustasy + tectonism) is linear, but clearly is not in the realistic case when this relation is nonlinear, or when progradation (as is common in tidal flat environments such as in the Maryville)

results in time-transgressive deposits.

Alternatively, cycle thickness is commonly assumed to be directly proportional to time, so cycle thicknesses are directly translated into time (discussed by Hardie and others, 1991). Commonly, "cycle periods" defined in this manner fall within the Milankovitch band, and therefore, Milankovitch control is assumed. As Algeo and Wilkinson (1989) have pointed out, however, "cycle period" is largely meaningless, because for cycles between one and twenty meters "cycle period" will almost always fall within the Milankovitch cycle band given realistic values of accumulation rates.

A second fundamental problem with Fischer plots is that more than one cycle can be created from a single sea-level rise, and thus the conventional method of using a series of discrete shoaling-upwards cycles to define sea-level variations may be incorrect, as described by Drummond and Wilkinson (1993). They defined *lag depth* as the depth of the sediment-water interface established during flooding, prior to resumed sediment production. By using a constant lag depth of one meter, their modelling shows that lag depth can be achieved (and a new cycle created) two and even three times during a **single** sea-level excursion. Thus the tacit assumption that each cycle was caused by a distinct eustatic rise and fall of the sea is likely an oversimplification.

Finally, although Fischer plots may be useful for illustrating changes in cycle thicknesses, a fundamental assumption is not met in the Middle Cambrian. Fischer plots assume (short term) linear thermal subsidence; perturbations from a linear pattern of sediment (cycle) thickness are then interpreted as excursions in creation of accommodation space created by eustatic sea-level variations. Recent work (Chapter 5 and the stacking patterns discussed in this chapter) has shown that the Cambrian passive margin was not fully mature (subsiding by short-term "linear" thermal subsidence alone) until the Late Cambrian. As discussed below, Cambrian sea-level "fluctuations" defined by Fischer plots may actually represent tectonic events or changes in the *rate* of subsidence.

The fundamental assumption of linear thermal subsidence in defining Fischer plots may therefore be flawed.

As this theoretical discussion shows, although Fischer plots may be useful for displaying *trends* in cycle *thicknesses*, they do **not** define sea-level fluctuations caused by **eustatic** (Milankovitch or other) mechanisms over definitive time periods. In addition to these theoretical concerns, this eustatic-forcing model does not fit the observed Maryville cycle trends in several ways.

First, the Maryville peritidal meter-scale cycles contain no systematic thickness variations within or between sections (Figures 4.3 and 4.4). If composite eustasy were responsible for the stacking patterns in the Maryville, systematic thinning- or thickening-upward of packages should be evident, especially in this area of relatively rapid subsidence (3.5 cm / 1000 yrs) where "missed beats" would be minimized and sea-level would be most accurately recorded (Osleger and Read, 1991; Read and others, 1991). A major exposure surface such as that at the top of the Maryville peritidal package should be underlain by stratigraphically upward thinning "cycles" approaching this major ("third order") boundary, but Maryville strata contain no such pattern. Alternatively, this sequence boundary may represent minor base level uplift rather than sea-level fall. The effects of a eustatic driving mechanism are not evident between sections, either. If eustatic sea-level variations were controlling accommodation space (and hence cycle thickness), cycles should be correlative across the shelf, as suggested by Osleger and Read (1991), who correlated cycles "as subparallel bands for many kilometers" and subtidal cycles for "greater than 45 km," and by Goodwin and Anderson (1990), who correlated cycles "for 100s of kilometers." In the Maryville, however, across only 5 km (palinspastic) distance, cycles *do not* correlate, as shown by Figures 4.3 and 4.4.

Second, as mentioned before, the dominant control on tidal flat development was progradation. If an external forcing mechanism such as eustasy were responsible for

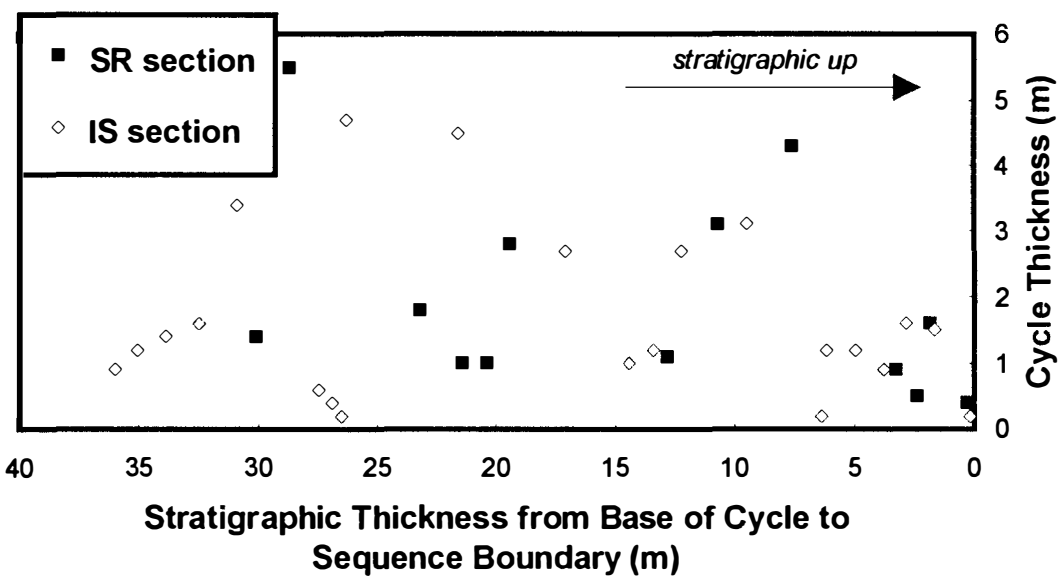


Figure 4.4 - Cross plot of distance from base of cycle to sequence boundary versus cycle thickness. No systematic vertical variations within or lateral changes between sections are evident, suggesting that regular eustatic sea-level fluctuations were not the driving mechanism in cycle development. Likewise, cycles are not time equivalent across even this short distance.

development of the meter-scale peritidal cycles, then correlative "cycles" should be evident in subtidal areas just seaward of the tidal flat (Read and others, 1986; Osleger and Read, 1991; Read and others, 1992). In those areas and further off platform, however, these regular "cycles" are *not* represented by the Maryville stacking patterns (Chapter 3 of this thesis; Srinivasan and Walker, 1993; Srinivasan, 1993).

Finally, in the non-glacial Cambrian, a climatic mechanism for driving short-term sea-level fluctuations is absent (Hardie, 1986; Osleger and Read, 1991). Instead, three mechanisms have been proposed to explain "cyclicity" in the Cambrian and other ice-free periods: 1) Thermal expansion or contraction of the ocean related to changing insolation; this process may explain longer-term (Ma) sea-level trends, but is probably not important in short-term fluctuations (Hardie, 1986); 2) Changing volumes of alpine glaciers; this process may provide a mechanism for small-scale sea level fluctuations, but then cannot account for larger-scale (3rd order) depositional sequences requiring large sea-level fluctuations (Osleger and Read, 1991); and 3) climate-induced changing volumes of lake and groundwater storage (Jacobs and Sahagian, 1993); this mechanism may have been active in the Triassic, but has yet to be proven for other periods such as the Cambrian.

In summary, although eustatic sea-level fluctuations **undoubtedly** influenced Maryville deposition, there is no evidence for a *regular* eustatic forcing mechanism in the meter-scale cycles of the Maryville peritidal package. Thus, other mechanisms must have controlled the final repetitious sedimentation patterns in these deposits.

Tectonism

Bosselini (1967), Cisne (1986), Hardie (1986), and Hardie and others (1986; 1991) have proposed that tectonic cycles, or "jerky subsidence," may have controlled cyclic deposition typical of peritidal sections. In these models, accommodation space

created by either episodic thermal or nonthermal subsidence is rapidly filled as the tidal flat progrades seaward.

Several models attempt to explain how tectonic activity might control cyclic sequences. One model proposes that episodic vertical movement on faults could result in random meter-scale accommodation events (Bosselini, 1967; Cisne, 1986; Hardie and others, 1991). According to this model, however, the repetitive sequences would be best developed near a fault zone and die out away from it. The apparent vertical noncyclic nature of peritidal package thicknesses suggests noncyclic controlling mechanisms, but the lack of lateral continuity of subpackages across small distances argues against dominance of the Cisne mechanism. Within 5 km, accommodation potential and tectonic frequency would have been similar (Cisne, 1986), but, as noted, such similarities over this distance were not observed in the Maryville. In addition, this model cannot explain the regional distribution of "cyclic" carbonates across the entire shelf (Hardie, 1989a).

In another variation, Hardie (1989a) proposed that thermal subsidence may occur at sporadic intervals instead of being a gradual, constant process. Strain would build up in the basement until a critical threshold was reached, when a rapid subsidence event would ensue. The range of subsidence associated with Middle Cambrian "thermal subsidence" in the southern Appalachians (0.01 - 0.06 m/ ka; Koerschner and Read, 1989) falls within the range defined by Cloetingh (1986) for relative sea level changes driven by intraplate stress mechanisms (0.01 - 0.1 m/ka). It may be, then, that such stepwise, thermal subsidence events were influenced by stress fields through achievement of a critical threshold due to changing horizontal tensional stress field orientation and magnitude. These subsidence events would result in creation of accommodation space, and lead to progradation of peritidal environments and the production of shallowing-upward "cycles" as this space was filled.

Alternatively, it is possible that stepwise tectonism was controlled by *vertical*

stresses due to sediment loading. It is well established that sediment loading amplifies subsidence caused by other mechanisms (Barrell, 1917; Sawyer and others, 1983; Walker and others, 1983; Stephenson, 1989; Reynolds and others, 1991; Bott, 1992). The scale at which this enhancement occurs is, however, not well understood. It is clearly recognizable and resolvable at larger (100s to 1000s of m) scales, but must proceed at smaller time increments *during* sedimentation. The great thickness of Middle Cambrian sediment in the Tennessee depocenter relative to adjacent areas (Hasson and Haase, 1988) suggests that sediment loading would have been active in these areas during deposition of the Maryville.

Theoretical considerations suggest that for every 1 m of sediment deposited, an additional 0.6 m of accommodation space is created because of sediment loading alone (Walker and others, 1983; Sawyer and others, 1983; Reynolds and others, 1991). In the case of meter-scale cycles, although this accommodation space was probably not created concomitant with deposition of *each* cycle (at the 10-100ka scale), the effects and nature (episodic, linear, or merely changing rates of subsidence) of sediment loading are very difficult to ascertain from the stratigraphic record. In the Conasauga basin, shale overpressuring followed by episodic pressure release may have provided meter-scale accommodation space during the development of the overlying limestones. Either stepwise tectonism *or* changing rates of subsidence would effect peritidal cycle stacking patterns.

Further evidence for the effects of increased subsidence (due to sediment loading?) is that near the Virginia "arch", a "cycle" was created, on the average, once every 130 ka (determined by the methods outlined in Koerschner and Read, 1989). Southward, the frequency consistently declines (Koerschner and Read, 1989), and in the area covered by this thesis, a "cycle" was created, on average, once every 38 ka (Figure 4.5). As discussed earlier, although every cycle does **not** represent the same amount of

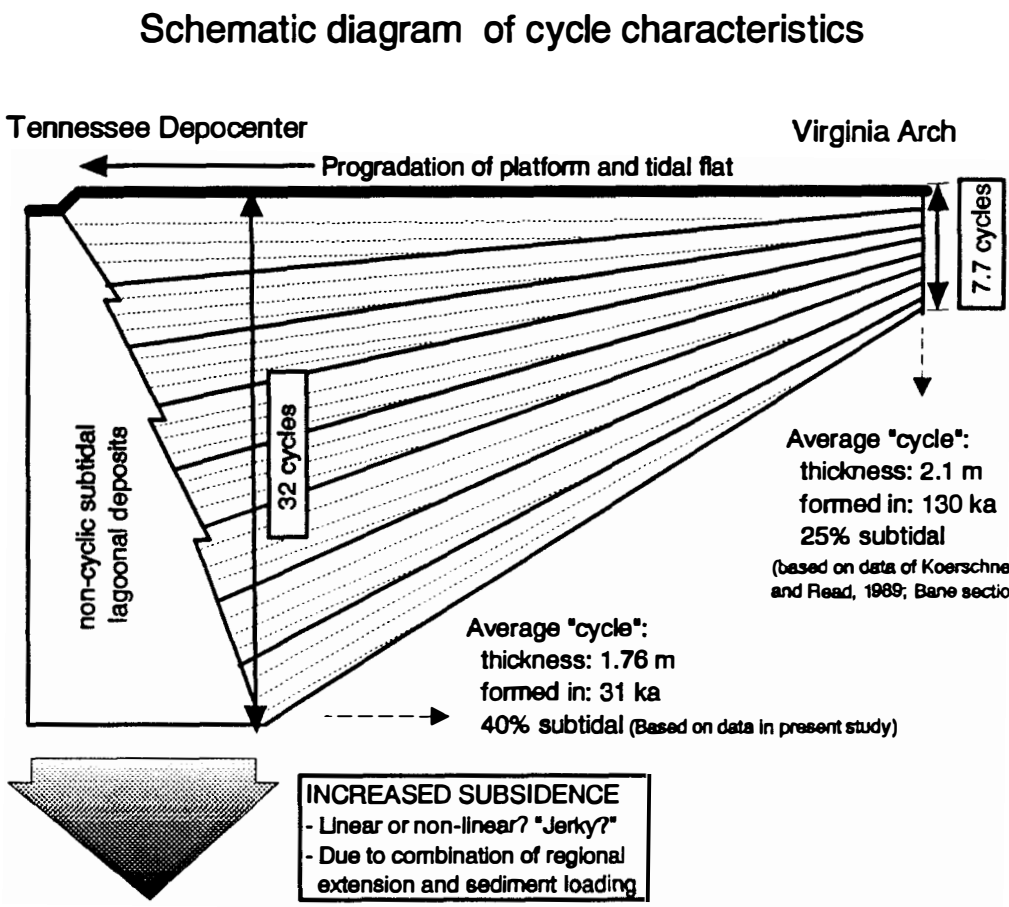


Figure 4.5 - Diagram showing regional cycle characteristics. Based on time of 1 Ma (and an assumption that thickness = time). The southwestward increase in cycle number per million years and increase in relative subtidal portions of cycles are interpreted to represent the influence of non-thermal tectonism associated with sediment loading and/or regional extension towards the Tennessee depocenter. Cycles are *not* correlative across even short distances, however, as shown in Figures 4.3 and 4.4 and discussed in the text. See text for discussion.

time and cycle thickness is **not** proportional to time, the general trend indicates that an accommodation threshold (lag depth?) was achieved more often to the south, towards the Tennessee depocenter. These data are similar to those in the model presented by Drummond and Wilkinson (1993), who noted that cycle stacking patterns and total number of cycles is driven by the rate of subsidence. The larger proportion of subtidal lithologies in the Tennessee depocenter likewise suggests that: 1) time before progradation of the tidal flat wedge was longer; 2) "lag depth" was achieved more commonly due to increased "linear" thermal subsidence; 3) episodic tectonism was more common; or 4) a combination of two or three of these factors was operative.

At the top of the peritidal package, a prominent, shelf-wide exposure surface is present (Srinivasan and Walker, 1993; Rankey and others, 1992; Chapters 3, 5 of this thesis). The relative sea-level fall that caused this exposure may have been eustatic or the result of minor tectonic uplift. Hardie (1986) and Hardie and others (1986) suggested that similar tectonism, and relative uplift, may have controlled stacking patterns in the Triassic of northern Italy.

Autocyclic processes

Although there is no way to conclusively prove that autocyclic mechanisms controlled stacking patterns, the lack of lateral continuity of cycles, the lack of systematic vertical cycle thickening or thinning, and the absence of contemporaneous subtidal cycles preclude stratigraphic forcing by Milankovitch eustatic sea-level fluctuations or localized tectonism. Thus, although probably influenced by small, irregular eustatic sea-level variations and minor tectonism, the dominant controls on meter-scale stratigraphic packages in the Maryville appear to be autocyclic processes, as suggested for other sequences by Ginsburg (1971), James (1984), Hardie (1986), Kozar and others (1990), and Hardie and others (1991). Mechanisms include processes documented in modern tidal

flats: progradation (Shinn and others, 1969; Purser and Evans, 1973; Shinn, 1983, 1986; Hardie and Shinn, 1986; Strasser and Davlaud, 1986), erosion and sediment redistribution by storms, waves, and tidal channels (Purser and Evans, 1973; Shinn, 1973, 1983, 1986; Shinn and others, 1969; Strasser and Davlaud, 1986), tidal island and tidal channel migration (Enos, 1977, 1989; Enos and Perkins, 1979; Pratt and James, 1986), sedimentary aggradation (Evans and others, 1973; Shinn, 1973, 1983, 1986), and variations in sedimentation rate and/or lag depth (Enos and Perkins, 1979; Enos, 1991). Several autocyclic models exist, and all rely on tidal flat progradation, as observed in modern settings, and as documented above for the Maryville tidal flat.

The classic autocyclic model (Ginsburg, 1971) suggests that the shallowing-upward trend in platform carbonates is the result of the interplay of continuous subsidence, sediment production, and "lag time." As the tidal flat progrades, it decreases the size of the subtidal lagoon sediment "factory" which will then "shut down" until subsidence deepens the lagoon enough for carbonate production to resume. Given subsidence rates similar to those in the Middle Cambrian and progradation rates similar to those in modern environments, time scales of tens- to hundreds-of thousands of years would be expected (Hardie, 1986).

Matti and McKee (1976) and Hardie (1986) proposed a modification to the "shrinking lagoon" model. They suggest that as a tidal flat progrades seaward, it moves towards deeper lagoonal water. The increasing volume of sediment required to maintain a constant progradation rate in combination with the shrinking lagoonal "factory" (the area of abundant sediment production) would halt tidal flat advance well before the shelf-edge.

Both of these mechanisms would produce laterally continuous deposits, assuming regular seaward progradation. The laterally discontinuous Maryville cycles, like those documented by Selg (1988), suggest that Maryville stacking patterns were controlled by other, even more local factors. These processes might be similar to processes documented

in Pleistocene and Holocene environments by other workers (see references above). Autocyclic mechanisms would create shoaling-upward cycles that are non-time equivalent across the shelf. Autocyclic processes can likewise lead to localized subaerial exposure surfaces in areas accreted above sea-level, even with continually rising sea-level, as documented in the Holocene by Enos and Perkins (1979), Enos (1989), and Ginsburg (1957). Cycles and exposure-altered intervals thus formed would not be correlative from place to place, as is the case in the Maryville (an exception is the major shelf-wide exposure surface, which, in the study area, is at the top of the Maryville peritidal package).

SUMMARY AND CONCLUSIONS

The peritidal package present in part of the the Dumplin Valley area probably does not represent deposition in an elongate, linear tidal flat "attatched" to a coastline. Rather, its lateral discontinuity suggests that it represents deposition on tidal islands. These islands may be analgous to restricted settings such as modern Florida Bay, but their distribution *may* be controlled by block faulting or tilting. Those areas in Dumplin Valley with peritidal facies might be areas with less (relative) subsidence, those with only subtidal facies might reflect greater (relative) subsidence. With the great progradation rate of Holocene peritidal sequences (measured in km/ka; Shinn, 1986), the lens shape of Maryville peritidal facies (Figure 4.1) may best be explained by such faulting or tilting. No faults were observed bounding these depositional packages.

Maryville cycles are thus interpreted to be the result of tidal island migration in a zone between the attatched tidal flat (the Honaker Dolomite) and the lagoon. The decrease in abundance of intraclastic lithologies in more restricted settings (SR section) may represent less reworking by tidal channels or wave activity. Likewise, the thin lenses of peritidal lithologies in more near shelf-edge areas probably represent small islands

formed at the time of maximum restriction and sea-level fall associated with the termination of the Maryville platform.

The fundamental hypothesis of this chapter is that several processes (tectonic, eustatic, and autogenic) acted in concert to produce the peritidal cycles and stacking patterns in the Maryville. No evidence (such as systematically stratigraphically thickening or thinning cycle thicknesses or cycles correlative across wide areas) indicative of *regular* Milankovitch-controlled eustatic forcing is present. Instead, episodic subsidence associated with sediment loading and/or regional extension combined with autocyclic processes and eustatic sea-level fluctuations to create the peritidal "facies mosaic." Distribution of Maryville peritidal facies apparently was controlled by sedimentary aggradation and progradation in a tidal island setting.

This study suggests that the controls on sedimentation patterns during Maryville deposition were numerous and temporally and spatially variable. Sediment loading, tectonism associated with regional extension, thermal subsidence, irregular eustatic sea-level fluctuations, and autogenic processes all exerted an influence on meter-scale stacking patterns. The absolute input of each of these factors on stacking patterns is probably *unresolvable* from the stratigraphic record.

CHAPTER 5

Episodic tectonism on Cambrian "passive" margin, southern Appalachians: Implications for passive margin development and sequence analysis

ABSTRACT

Many early Paleozoic passive margins are characterized by limestone/shale alternations (grand cycles), but tectonic and eustatic controls on development of these repetitions are poorly understood. Field, petrographic, and geochemical evidence from the Middle Cambrian Craig Limestone Member (Rogersville Shale) and Maryville Limestone indicates that subaerial exposure, followed by drowning, terminated platform development, and led to the limestone-to-shale transition. Evidence documented herein suggests that these two transitions were driven by *episodic pulses of subsidence*, rather than eustasy, as suggested by other geologists.

Like the Conasauga depocenter, most cratonic depocenters and grabens associated with Late Proterozoic-Early Cambrian continental breakup were active into the Late Cambrian. The passive margin is interpreted to have evolved in three stages: rift (active continental rifting), immature passive (no new rifts, but with nonthermal tectonism associated with sediment loading and/or regional extension), and mature passive (a truly thermally subsiding margin). Sequences developed on immature passive margins may predominantly record the effects of nonthermal tectonism, which may vary spatially and temporally. Non thermal tectonic components are commonly not resolvable on burial or "geohistory" curves based on formation-level stratigraphic measurements. Instead, detailed stratigraphic data, combined with chronostratigraphic data, is necessary to reveal details of subsidence history that effect sequence development. Detailed stratigraphy is

best studied on older, exposed passive margins; seismic stratigraphic data from younger margins may not provide the resolution necessary for such interpretation. The "eustatic" signal documented by Vail and co-workers on similar, younger passive margins may thus represent the combined effects of tectonism and eustasy.

INTRODUCTION

Passive margins form following a period of rifting associated with continental breakup. Once the newly-formed active spreading center migrates away from the continental margin and active rifting ceases, the continental margin is assumed to subside uniformly at an exponentially decreasing rate (thermal subsidence). This subsidence continues until plate configurations change and the passive margin becomes an active margin, characterized by nonthermal subsidence associated with convergent plates (Bott, 1992).

Our knowledge of the subsidence histories of Mesozoic and Cenozoic passive margins is obtained largely through seismic reflection and refraction methods, along with magnetic and gravity methods (Bott, 1992). On older, less well preserved passive margins, burial curves are commonly used to evaluate the effects of thermal subsidence (ie. Bond and Kominz, 1984; Levy and Christie-Blick, 1991). Sleep (1971) and McKenzie (1978) provided quantitative models for the development of sedimentary basins following a stretching event. The predicted subsidence was considered to be due to cooling and thermal contraction of the lithosphere, and is exponentially decreasing, or "thermal." Because the first-order subsidence patterns of most passive margins follows this generalized pattern (Bond and Kominz, 1984; Steckler and others, 1988; Bond and others, 1988; 1989; Levy and Christie-Blick, 1991), these models have found widespread acceptance.

In general, then, passive margins are assumed to follow a simple, predictable thermal subsidence history. Because the subsidence is assumed known and quantifiable, studies of sediments and sequences are concentrated on passive margins. In these sequences, perturbations from predicted patterns are interpreted to be the result of extra-basinal mechanisms. In particular, eustatic sea-level fluctuations have often been considered to be the primary control on sedimentary sequence development (Vail and others, 1977; Haq and others, 1988; Vail, 1987; Van Wagoner and others, 1988; Sarg, 1988; Mitchum and Van Wagoner, 1991; Koerschner and Read, 1989; Osleger and Read, 1991; many others).

My research on parts of Cambrian strata of the southern Appalachians has led me to the conclusion that, although some seqences are indeed related to eustasy, tectonism was also a controlling factor on sedimentary packaging, from third-order sequences to fifth-order sequences (see Chapter 4) on this "passive" margin. The purpose of this chapter is twofold: 1) to document Middle Cambrian tectonism in the Conasauga basin and to suggest that this tectonism may reflect the waning stages of the effects of continental breakup; and 2) to develop a model for the evolution of the Cambrian southern Appalachian passive margin.

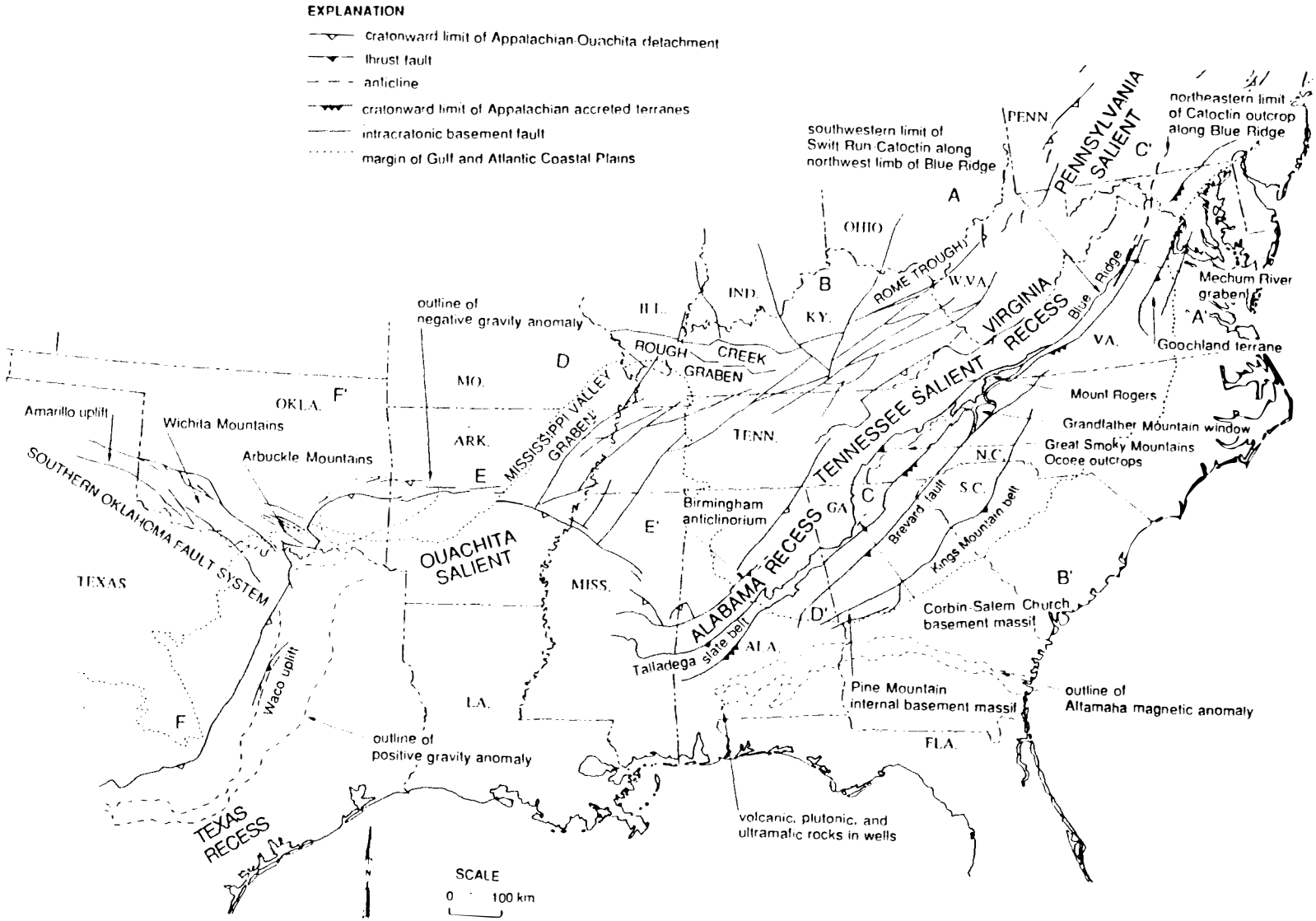
LATE PROTEROZOIC-EARLY CAMBRIAN CONTINENTAL BREAKUP AND CAMBRIAN TECTONISM

Rifting associated with the separation of Laurentia from the supercontinent Rodonia began during the Late Proterozoic (Odom and Fullagar, 1984; Bond and others, 1984; Hatcher, 1989). The stratigraphic evidence of rifting consists of numerous relatively narrow rift-basins containing thick accumulations of latest Proterozoic sediments and lava flows along the newly formed margin (Table 5.1, part A). In the southern

Table 5.1 Extensional features in the southeastern United States associated with Late Proterozoic-Early Cambrian continental breakup

Feature	dimensions	age of origin	age of termination	sed. thickness	references
Part A - Near craton-edge features					
Ocoee Basin	250 X 100 km?	late Proterozoic	late Proterozoic	12 km	Rankin and others, 1989 King, 1964 Rast and Kohles, 1986
Grandfather Mtn. Basin	150 X 75 km?	late Proterozoic	late Proterozoic	9 km (+volcanics)	King, 1970 Rankin, 1970, 1975 Neton, 1992
Mt. Rogers	150 X 75 km	late Proterozoic	late Proterozoic	3 km	Rankin, 1970, 1975, 1976 Schwab, 1976
Part B - cratonic features					
Rome trough	100 X 300+?	late Proterozoic	late Cambrian	up to 3200 m	Webb, 1980
Rough Creek graben	100 X 200 km	?	late Cambrian	> 2.5 km	Colinson and others, 1989
Birmingham fault system	100 X 300km	early Cambrian	late Cambrian	1.5 km?	Thomas, 1991
Mississippi Valley graben	50 X 200 km	late Proterozoic	late Cambrian	> 1 km	Braile and others, 1986 Hildenbrand, 1985
Tennessee depocenter	?	?	late Cambrian	900 m + (M. and U. Camb.)	Hasson and Haase, 1988 this thesis
Cincinnati Arch basin	48 X 160 km	late Proterozoic?	late Cambrian	> 3 km	Shrake and others, 1991
MS-AL-TN graben	?	? — defined geophysically —		?	Johnson and others, 1992

Figure 5.1 - Location map showing features associated with Late Proterozoic-Early Cambrian continental breakup and later Appalachian-Ouachita orogenesis (from Thomas, 1991).


EXPLANATION
cratonward limit of Appalachian-Ouachita detachment
thrust fault
anticline
cratonward limit of Appalachian accreted terranes
intracratonic basement fault
margin of Gulf and Atlantic Coastal Plains
southwestern limit of Swift Run-Catoctin along northwest limb of Blue Ridge
northeastern limit of Catoctin outcrop along Blue Ridge
PENNSYLVANIA SALIENT
PENN.
OHIO
W.VA.
ROME TROUGH
IND.
ILL.
KY.
VIRGINIA RECESS
Blue Ridge
VA.
Mechum River graben
Goochland terrane
outline of negative gravity anomaly
ROUGH CREEK GRABEN
MISSISSIPPI VALLEY GRABEN
MO.
OKLA.
ARK.
TENN.
TENNESSEE SALIENT
Mount Rogers
Grandfather Mountain window
Great Smoky Mountains
Ocoee outcrops
N.C.
S.C.
GA
Amarillo uplift
Wichita Mountains
Arbuckle Mountains
SOUTHERN OKLAHOMA FAULT SYSTEM
Birmingham anticlinorium
Brevard fault
Kings Mountain belt
OUACHITA SALIENT
ALABAMA RECESS
MISS.
TEXAS
Corbin-Salem Church basement massif
Talladega slate belt
ALA.
Waco uplift
Pine Mountain internal basement massif
outline of Altamaha magnetic anomaly
LA.
FLA.
outline of positive gravity anomaly
TEXAS RECESS
volcanic, plutonic, and ultramafic rocks in wells
SCALE
0 100 km
A
A'
B
B'
C
C'
D
D'
E
E'
F
F'

Appalachians, these grabens contain the sediments of the Ocoee Supergroup, Mount Rogers Formation, and Grandfather Mountain Formation (Figure 5.1). Inboard from the continental edge, the location of the successful rift, several other basins developed in the late Proterozoic, because of the regional crustal extension associated with the breakup of the supercontinent Rodonia (Table 5.1, part B). These basins commonly contain much thinner sediments, and are not associated with volcanics. They include the Mississippi Valley graben, the Reelfoot rift, the Rome trough, the Birmingham fault system, and several others (Figure 5.1), all which became active in the late Proterozoic-early Cambrian.

Most published accounts suggest that the rift-passive margin transition in the southern Appalachians occurred in the Early Cambrian (Fichter and Diecchio, 1986; Walker, 1990; Cudzil and Driese, 1987; Simpson and Erikkson, 1989; Hatcher, 1989; Walker and Driese, 1991). Active Middle Cambrian extension and related stratigraphic expression have been documented in the Rome trough (Webb, 1980), the Birmingham fault system (Thomas, 1991), the Conasauga basin (this thesis), and the Reelfoot rift (Nelson and Zhang ,1991). The data in Table 5.1 likewise suggests that all of the identified rift basins were active as depocenters until at least the *Late* Cambrian. At that time, transgressive carbonates or siliciclastics overstepped the graben walls without significant thickness variations, suggesting that basin-sustaining mechanisms were active across much of the passive margin to this time.

DEVELOPMENT OF SEQUENCE BOUNDARIES IN THE CONASAUGA BASIN

Field, petrographic, and geochemical evidence from both the Craig and the Maryville (presented here and within Chapter 6, this thesis) indicates that the carbonate-shale contacts in many areas are actually exposure/drowning surfaces. In more platform-

interior sections, the exposure/drowning surface is *within* the carbonates, and the carbonate-shale transition occurs several meters above this surface. Because these carbonate-shale transitions reflect significant changes in sedimentary processes and patterns (from basinward-prograding shallow-water carbonates to platformward-onlapping basinal shales), they are interpreted to represent sequence boundaries (Srinivasan and Walker, 1993).

Lower Rogersville-Craig cycle top

The top of the Craig Limestone shows evidence for subaerial exposure of subtidal sediments. The uppermost 0.2 m of the Craig exhibits vuggy pores up to 3 cm diameter and small-scale brecciation, all present only immediately below the surface. The dissolution voids (Figure 5.2A, 5.2B) are filled with clear to slightly turbid equant calcite spar, some of which is erosionally truncated (Figure 5.2B), indicating a very early diagenetic origin. Fabric-selective dissolution stabilized oncoids and attacked ooids up to 5 m below the top of the Craig (Figure 5.2A). Oxygen and carbon stable isotope ratios from these equant cements (including truncated cements) have $\delta\ ^{18}O$ ratios of -10.3 ‰ to -12.3 ‰ (mean -11.3 ‰; n=12) (Peedee Belemnite; PDB) and $\delta\ ^{13}C$ ratios of -0.2 ‰ to -0.9 ‰ (mean -0.4 ‰) (PDB) (Figure 5.3). These oxygen values are depleted relative to Cambrian marine carbonate values of -5 ‰ (Lohmann and Walker, 1989) by 4 to 6 ‰. In contrast, there is very little variation in carbon isotopic composition of these cements, which can be attributed to the absence of light organic carbon associated with land plants (Srinivasan and Walker, 1993). $^{87}Sr/^{86}Sr$ ratios from these cements are 0.7095, comparable to Cambrian marine carbonate strontium ratios of approximately 0.7092 (Burke and others, 1982), but significantly different from burial phases in this sequence, which have ratios of 0.7111 to 0.7139 (Srinivasan and Walker, in press).

Above the exposure surface is a thin (0.2 m) bed of packstone/grainstone

Figure 5.2 - Photomicrographs showing petrographic features of meteoric diagenesis and later drowning. Scale: 2.6 mm across base for A-D, 5.3 mm for E. Stratigraphic up is to top of page.

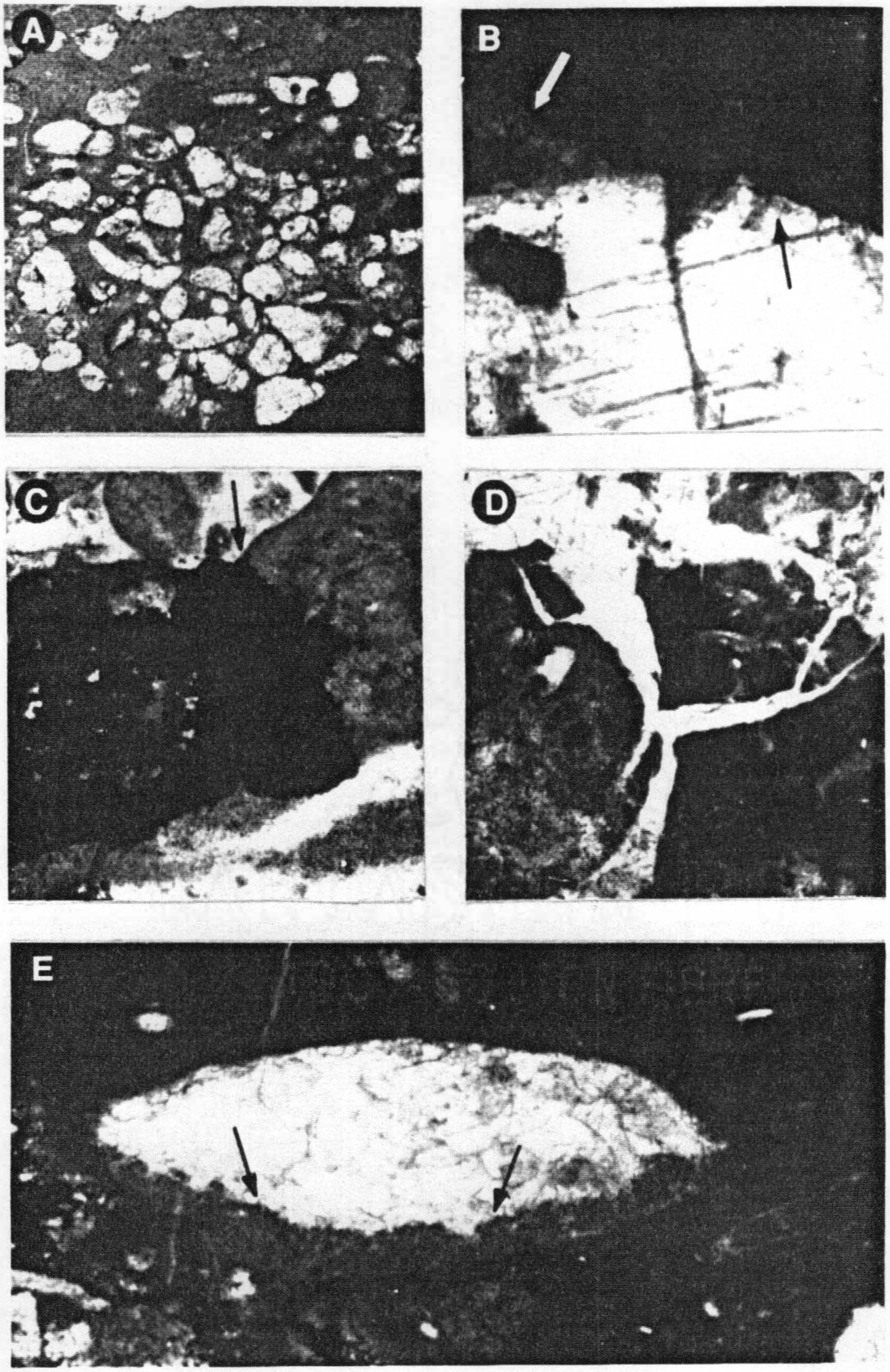
A) Fabric-selective dissolution voids filled with meteoric blocky calcite from 0.2 m below exposure surface; Craig, DSR section.

B) Truncated meteoric blocky cement; truncation surface marked by arrows; Craig, DSR section.

C) Truncated (arrow) framboidal pyrite (black) from 1 cm above exposure surface; Craig, DSR section.

D) Small-scale internal brecciation and meteoric blocky calcite; Maryville, WG section.

E) Fabric-selective dissolution, vadose silt (arrow) and meteoric drusy clear calcite; Maryville, WG section.


A
B
C
D
E

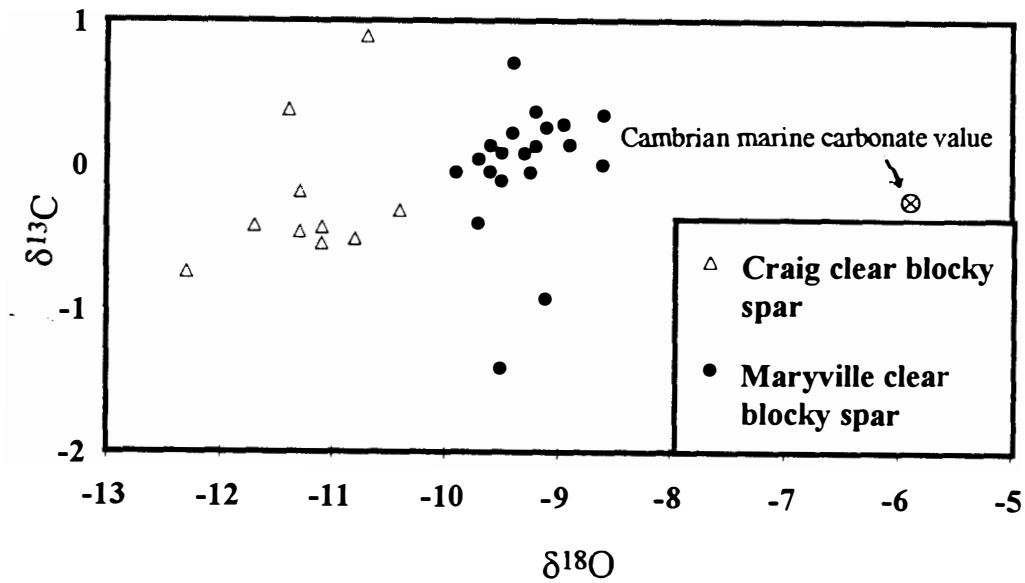


Figure 5.3 - Cross-plot of carbon and oxygen isotope ratios of equant to drusy calcites in dissolution voids, Craig and Maryville. Plot includes erosionally truncated cements. Craig ratios are from DSR sections. Maryville cements from Woods Gap, TN and Thorn Hill, TN (from Srinivasan, 1993). Note depleted values relative to Cambrian marine carbonate values. See text for discussion.

consisting of allochthonous trilobite fragments and oncoids encrusted with manganese and phosphate, and cemented by fibrous marine calcite. Truncation surfaces, some of which cut framboidal pyrite (Figure 5.2C) are common, but no dissolution voids are present. Immediately above these sediments are the shales of the upper Rogersville, which represent basinal lithologies that onlapped the drowned platform during a time of significant deepening.

Upper Rogersville-Maryville cycle top

Like the top of the Craig, the upper Maryville shows evidence for exposure/drowning. Exposure at the top of the Maryville is indicated by fabric-selective dissolution and small scale-brecciation (Figures 5.2D, 5.2E), developed only immediately below the exposure surface. Blocky to (less commonly) drusy calcites occluding porosity in dissolution voids have depleted oxygen isotope ratios of -8.7 ‰ to -9.9 ‰ (mean -9.2 ‰, n=19) (PDB) and carbon isotope ratios of -1.2 ‰ to +0.8 ‰ (mean +0.1 ‰) (PDB) (Figure 5.3). These oxygen ratios are depleted relative to Cambrian marine carbonate (delineated by Lohmann and Walker, 1989). Like the Craig meteoric calcites, these cements have $^{87}Sr/^{86}Sr$ ratios of 0.7095, very similar to the Cambrian marine value.

The exposure surface is overlain by the onlapping basinal shales of the Nolichucky Formation (basinal sections; see Srinivasan and Walker, 1993) or the backstepping platform/shelf package (platform-interior sections, in turn overlain by the Nolichucky Shale) reflecting significant deepening.

MODEL FOR THE ORIGIN OF THE LIMESTONE/SHALE TRANSITION

Given the evidence presented, I propose that a similar mechanism is involved in the end of these two grand cycles. Subaerial exposure during a sea level fall terminated

carbonate deposition. During exposure, a freshwater lens developed in the lithified sediments and led to early meteoric diagenesis. A relatively rapid sea-level rise then flooded the platform, which subsided during the "lag time" before carbonate deposition (Schlager, 1981), allowing siliciclastics characteristic of the adjacent basin to onlap the drowned platform sediments. Platform-central areas in which no siliciclastics encroached provided a nucleus from which platform sediments could prograde and, in time, reestablish carbonate deposition.

GRAND CYCLE CORRELATIONS

Evidence for a eustatic driving mechanism for sequence sevelopment consists of synchronous sequences and sequence boundaries in geographically widespread areas (Sloss, 1963; Vail, 1988). Many workers have speculated on the continent-wide correlation of grand cycles, but, as shown in Figure 5.4, there is considerable disagreement. The lower Rogersville-Craig cycle does not appear to have a biostratigraphically equivalent cycle elsewhere on the cration. The shales of the upper and lower Rogersville contain *Ehmaniella*. The top of the Craig, which must then occur within the *Ehmaniella* zone, cannot be biostratigraphically equivalent to cycle top 8 or 8' of Palmer (1981), which occurs at the top of the *Ehmaniella* zone. It is possibly biostratigraphically equivalent to cycle top 7 (top of the Dome Fm.) of Palmer (1981) which he recognized only in the House Range of Utah. The **base** of the Ehmaniella zone is 25 m above the base of the Dome, however (Robison, 1976), and thus the deepening at the top of the Dome does not appear to represent the same deepening event as that at the top of the Craig.

The Maryville Limestone does not lack possible correlatives; instead, it has been correlated with many different units by different geologists, and no consensus is present

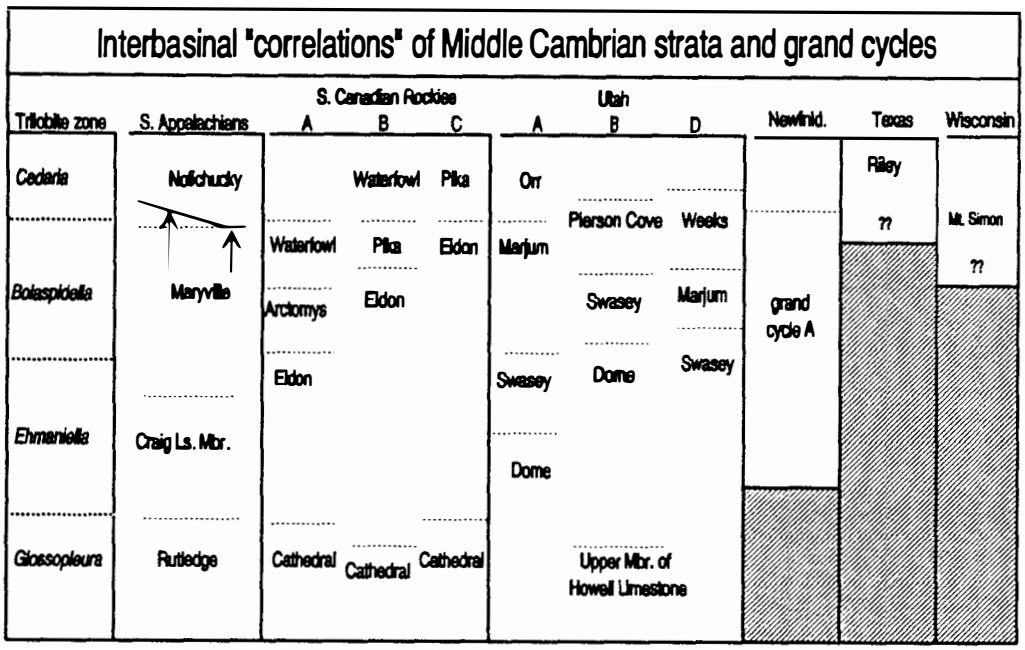


Figure 5.4 - Interbasinal "correlations" of Middle Cambrian grand cycles and strata. Note that there is no consensus on correlation of units across wide areas, or the actual age of any unit. Flooding of craton-interior locations (Texas and Wisconsin) in latest Middle Cambrian or early Late Cambrian is related to long-term (Sauk) sea-level rise (Sloss, 1963). Pierson Cove Fm. in Utah is biostratigraphically equivalent to the lower part of the Marjum (Robison, 1976). Top of Maryville (solid line) is time-transgressive, but sequence boundary (dotted line) is isochronous. Column A = Palmer (1981); B = Bond and others (1989); C = Aitken (1981); D = Hinze and Robison (1975); Newfoundland data from Chow and James (1987); Texas data from Palmer (1954); Wisconsin data from Ludvigson and Westrop (1985); southern Appalachian data from Resser (1938), Rasseti (1965), Palmer (1981), and interpretation in this thesis.

(Figure 5.4). Aitken (1981), for example, correlated the Maryville with the Eldon in the Canadian Rockies based on grossly similar ages. Bond and others (1988) used sedimentary "perturbations" from geophysically modelled subsidence to correlate the Maryville with the Eldon, with an age "shift of ... no more than 1.8 million years." (p.153) Bond and others (1989), using similar methods, correlated the Maryville with the Pika. Palmer (1981), using biostratigraphic data, suggested that the Maryville top is closest to that of the Waterfowl Formation. In spite of these disagreements, many of these geologists use their correlations to suggest eustatic control and relatively "isochronous" platform response (Aitken, 1981; Bond and others, 1988; 1989), yet the data do not *conclusively* support such contentions. Biostratigraphic resolution is not sufficiently precise to prove that two cycle tops that occur "near the top" or "near the base" of a trilobite zone were created by the same eustatic event. In addition, the cycle top might not actually be the sequence boundary, as shown by the present study. Correlating grand cycle tops is not necessarily the same as documenting synchronous development of sequences and their boundaries, and proving a eustatic control.

EXPOSURE, EUSTASY, TECTONICS, AND SEQUENCE BOUNDARIES

Drowning a carbonate ramp or platform requires an environmental crisis (such as rapid temperature or salinity variations), a rapid short-term sea-level rise of several tens of meters, clastic "poisoning" of carbonate environments coupled with continued subsidence, a pulse of tectonic subsidence, or a combination of two or more of these processes (Elrich and others, 1990; Read and others, 1991; Schlager, 1981; 1991; 1992). The thin bed of carbonate grains above the Craig and the backstepping platform package of the upper Maryville indicate that carbonate-producing environments were still present in more on-platform areas, and so an environmental crisis was apparently not a driving mechanism for

platform demise. The fact that these transported (Craig) and *in situ* to transported (Maryville) deposits occur between exposure surfaces and shales indicate that shales did not poison the carbonate factory and terminate the platform. Furthermore, significant deepening is required for the basinal shales to onlap the platform. Subaerial exposure, coupled with episodic tectonism, thermal subsidence, and possibly eustatic sea-level rise (in the case of the Maryville) caused the drowning of these two Middle Cambrian platforms. The top of the lower Rogersville-Craig grand cycle is marked by subaerial exposure followed by significant deepening. The relative sea-level fluctuations involved in the limestone-shale transition must have been on the order of 40-50 m (from holosubtidal deposition -> exposure -> basinal deposition). As discussed above, this cycle boundary does not appear to have a biostratigraphic equivalent elsewhere on the craton, with the *possible* but unlikely exception of the Dome Formation in Utah (Palmer, 1981). Although I do not propose that a eustatic cause for cyclicity necessitates a simultaneous craton-wide response, if eustasy on the order of 40-50 m were responsible for all inferred sea-level fluctuations in the Craig-upper Rogersville transition, undoubtedly a similar response (limestone-shale transition, or even deepening-upward) would be evident elsewhere. Because a response is **not** recognized, another factor apparently was responsible for platform demise (and grand cycle termination).

Non thermal tectonism may have influenced sequence boundary development in this intrashelf basin. In particular, episodic Cambrian tectonism associated with sporadic release of stresses concomitant with thermal cooling, sediment loading, and/or regional extension enhanced the drowning at the top of the lower Rogersville-Craig grand cycle (as well as the Maryville to Nolichucky sequence boundary; see below). Several lines of evidence support this hypothesis of Middle Cambrian tectonism in East Tennessee. First, the Middle Cambrian was a time of regional extension in the southeastern United States, as shown by Middle Cambrian tectonism in the Rome Trough/Rough Creek graben (north

of our study area; Webb, 1980; Collinson and others, 1989), the Birmingham fault system (south of our study area; Thomas, 1991), and the Mississippi Valley graben (west of our study area; Nelson and Zhang, 1991). It is likely that these tensional stresses were effectively transmitted across the southeastern part of the continent, including the Conasauga intrashelf basin. Second, deposition of "classic" grand cycles (deeper-water shale and shallower-water carbonate) in the Tennessee depocenter ended in the early Late Cambrian, the same time that all other craton-interior features noted above and associated with continental breakup ceased activity, suggesting that full stabilization (end of active extension) of the continental margin occurred during the Late Cambrian. Third, isopach maps (Hasson and Haase, 1988) indicate that up to 900 m of Conasauga sediment were deposited in eastern Tennessee (more than four times the amount in the adjacent Virgina arch; Read, 1989), indicating syndepositional differential subsidence. Modelling suggests that isostatic response to such sediment loading provides a feedback mechanism through enhancement of accommodation space (Walker and others, 1983; Reynolds and others, 1991), such as that we propose here for the Conasauga basin. Such enhancement would be most evident in condensed sections, such as those associated early platform reflooding after platform shutdown by subaerial exposure.

As at the top of the lower Rogersville-Craig cycle, the upper parts of the upper Rogersville-Maryville cycle contain evidence for significant deepening. Palmer (1981) and James and others (1989) noted that this cycle does not have a biostratigraphic equivalent in the Cordillera. The lithologically defined "top" of the Maryville is time-transgressive (Derby, 1965), becoming younger to the east/northeast. The **genetic** top of the Maryville (the exposure sufrace/sequence boundary) is within the *Bolaspidella* zone and hence it might be equivalent to cycle top 9 of Palmer (1981), which occurs near the top of the *Bolaspidella* zone.

With the evidence for regional extension and the sediment loading in the

Conasauga basin, even though the top of the Maryville **may** correlate biostratigraphically with other units, the drowning at the top of the Maryville may have been controlled, or enhanced, by tectonism, coupled with eustatic sea-level rise. The confusion surrounding grand cycle correlation (Figure 5.4) and the relatively poor biostratigraphic resolution raise questions about eustatic control of Maryville cycle termination. Tectonism reflected as changing *rates* of subsidence (Palmer and Halley, 1979; Palmer, 1981) or "jerky subsidence" (coupled with platform shutdown caused by subaerial exposure) may also play an important role in development of grand cycles. Current litho-, bio-, and chronostratigraphic resolution are not sufficiently precise to unequivocally prove a consanguineous eustatic cause for the demise of the Maryville platform and some (Eldon? or Pika? or Waterfowl?; Pierson Cove? or Marjum?; see Figure 5.4) in the Cordillera.

Thus, for both of these cycles, following platform exposure during the "lag time" before the onset of carbonate production, episodic tectonism associated with sediment loading and/or extension progressively dropped these exposure surfaces further below sea level (Figure 5.5A, 5.5B). During this "lag time," basinal pelagic shale deposition continued, and, in time, onlapped the drowned platform (Figure 5.5C, 5.5D). Because of the lack of significant sedimentation in platformward areas, the relative sea level rises caused by these successive fault movements were compounded and appear as a stratigraphically "instantaneous" change from subaerial exposure to deeper basinal deposition. Subsequently, increased sedimentation in the basin led to sediment loading and tectonic subsidence (Figure 5.5D, 5.5E). This basinal subsidence created a ramp profile, on which carbonate sedimentation nucleating in platformward areas resumed (Figure 5.5E, 5.5F).

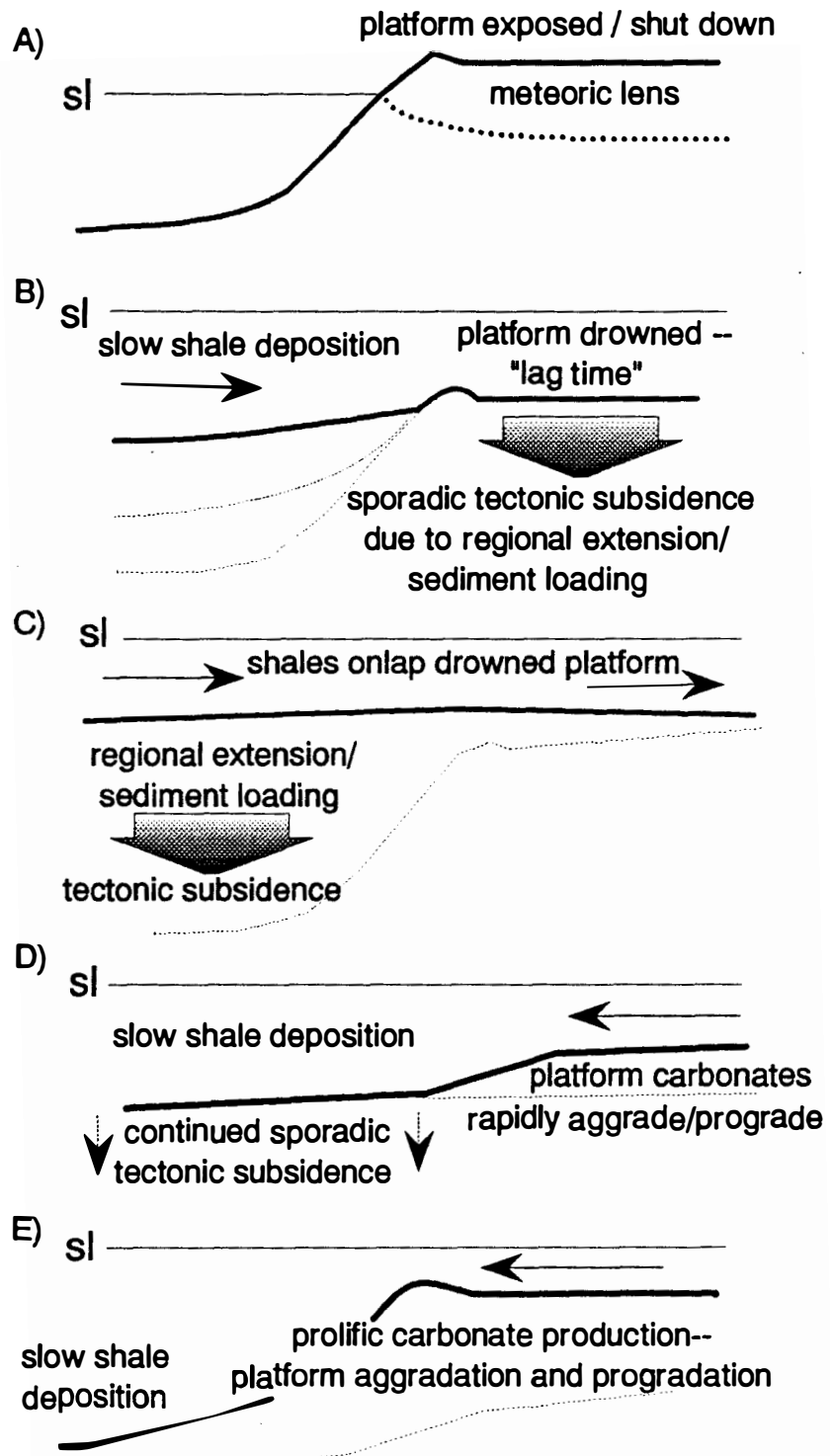


Figure 5.5 - Schematic diagram showing influence of exposure, "lag time" and tectonic subsidence on Tennessee grand cycle termination. Thermal subsidence not shown. Thicker cratonward sections and the deeper-water intrashelf basin are the result of this non-thermal tectonic component. See text for discussion.

MODEL FOR THE DEVELOPMENT OF THE CAMBRIAN PASSIVE MARGIN

Because most known early Paleozoic extensional features ended active subsidence in the Late Cambrian, and these features show evidence for nonthermally generated subidence, it seems probable that the true passive margin developed only in the *Late* Cambrian and not the Early Cambrian as suggested by other authors. The development of the passive margin proceeded in three steps.

The first stage of passive margin development was rifting of continental crust and the creation of oceanic crust in the successful rift. On the continent, this stage was characterized by attenuated crust and attenuation- created rift grabens, up to 500 km inboard (Thomas, 1991). In the most outboard areas (those closest to the continental edge), thick rift sediments accumulated, some associated with volcanics. In the early Paleozoic continental breakup, this stage ended in the Early Cambrian.

The second stage began when no more new grabens formed, and the ocean was open. It is characterized by broad warping of the lithosphere and depocenter development with episodic tectonism. Often, earlier structures were re-activated due to differential sediment loading and (?) continued extension. Thermal subsidence was a dominant control on regional sedimentation patterns, but episodic, non-thermal tectonism also controlled sedimentation patterns at the subregional and even local (?) scale. The relatively narrow depocenters may reflect low lithospheric rigidities, which tend to partition accommodation space created by sediment loading subregionally, as suggested by the modelling of Reynolds and others (1991). Sediments deposited in this intermediate phase are in most cases no more than 2 km thick and may be characterized by limestone-shale alternations or other changes reflecting sporadic deepening on the shelf. In the early Paleozoic of the southeastern U.S., this stage lasted into the Late Cambrian.

The third stage was the true passive margin, characterized by uniform thermal subsidence across the shelf. The end of subregional depocenters may be related to increasing lithospheric rigidities, which would tend to distribute accommodation space laterally, as modelled by Reynolds and others (1991). In the early Paleozoic of the southeastern U.S, this stage began in the Late Cambrian, and lasted into the Middle Ordovician. The sheet-like peritidal carbonates of the Knox Group and the oldest parts of the Chickamauga Group were deposited in this tectonic setting.

COMPARISON WITH MESOZOIC/CENOZOIC PASSIVE MARGINS

Because early Paleozoic passive margin sequences are typically complicated by later orogenesis, studies of Mesozoic and Cenozoic passive margins form the basis for much of our knowledge of passive margin genesis (Watkins and others, 1979; Watkins and Drake, 1982; Manspeiser, 1989). These margins are commonly studied by seismic reflection and refraction methods combined with gravity and magnetic data. In this regard, they provide a preserved image of the actual rifted margin, but with a resolution of +/- 20-30 m at best. In contrast, the development of Paleozoic margins is usually studied indirectly but at more stratigraphic detail, through sediment packages and patterns from outcrops (Bond and others, 1984; 1988, 1989; Levy and Cristie-Blick, 1991). Thus, I submit that the fine-scale development of passive margins might be better resolved in the record of these older dissected and exposed margins.

Two observations gleaned from studies of Mesozoic and Cenozoic passive margins can be related to the concepts of nonthermal subsidence and passive margin evolution in the Cambrian. First, the margins are riddled with faults and fault basins, up to 450 km inboard from the shelf-edge (Keen and others, 1987; Manspeiser, 1988). These rift basins formed in association with breakup of Pangaea. In the Precambrian-Cambrian breakup of

Rodonia, the inboard extent of rift basins is a similar 500 km (Figure 5.1) using the edge of the continent defined by pronounced gravity and magnetic anomalies as suggested by Taylor (1989). Thus, it is not surprising to find areas of attenuated crust as far inboard as the Rome trough or Mississippi Valley graben, and that intermediate areas such as the Tennessee depocenter were also characterized by extensional tectonics.

The second "theme" of Mesozoic and Cenozoic passive margin development relevant to discussion of tectonism on earlier passive margins is that Mesozoic and Cenozoic margins were characterized by episodic tectonism even during the traditional "drift" stage. Heller and others (1982), Keen and others (1987), Cloetingh and Kooi (1989; 1992), Hubbard (1988), Embry (1990), Aubry (1991), and Underhill (1991), among others, have documented episodic tectonism on reportedly mature passive margins that were characterized by "thermal" subsidence. These events are most commonly, although not exclusively, related to changes in horizontal stress fields caused by changing plate configurations.

It is not surprising, then, that Cambrian passive margins have similar responses to tectonic events. It is surprising, however, that these responses have not been as widely reported from more ancient passive margin sequences.

DISCUSSION

Although passive margins appear to be stable shelves and ideal places to study the stratigraphic responses to eustatic sea-level fluctuations, they are dynamic continental margins, responsive to extension, sediment loading, and "second-order" subsidence patterns (Stephenson, 1989), in addition to the familiar first-order exponentially decreasing thermal subsidence and eustasy. As this study in the Tennessee depocenter suggests, subsidence rate in one location is temporally and spatially variable. Likewise,

modelling studies of passive margins (Stephenson, 1989; Steckler, 1989) show that these margins are more complex than predicted by the pure-shear stretching model of McKenzie (1978).

Cloetingh and co-workers (Cloetingh, 1986; 1988; Cloetingh and Kooi, 1992) have quantitatively demonstrated that temporal fluctuations in lithospheric stress fields can result in significant deviations from predicted thermal subsidence patterns. Changing subsidence rates are then manifest as changes in relative sea-level. Modern world stress maps document the existence of pervasive, similarly oriented stress fields through the lithosphere across a wide area (Zoback and Zoback, 1989). The extensive active tectonism in the Middle and Late Cambrian of North America documented by Nelson and Zhang (1991), Thomas (1991), and this thesis suggests that tensional stresses were effectively transmitted across much of the southeastern part of the continent. It is likely that these stresses affected the lithosphere and caused deviations from predicted subsidence patterns in depocenters (where they are readily recognized) and areas that were more "stable."

In addition to horizontal stresses, vertical stresses associated with sediment loading also undoubtedly played a role in the development of these sequences. Five times as much Conasauga sediment was deposited in the Tennessee depocenter than in adjacent areas (Hasson and Haase, 1988). Modelling suggests that isostatic response to such sediment loading provides a feedback mechanism through enhancement of accommodation space (Reynolds and others, 1991). The time scale on which this enhancement occurs has not been resolved, but most two-dimensional modelling studies of the Cambrian passive margin (Read and others, 1991; Osleger and Read, 1991) assume that it is partitioned at a constant rate throughout deposition of the sequence. As Kendall and others (1992) suggested, and our studies of the Conasauga support, this response is probably not linear, but instead is sporadic, or possibly manifest through changing rates of subsidence. In

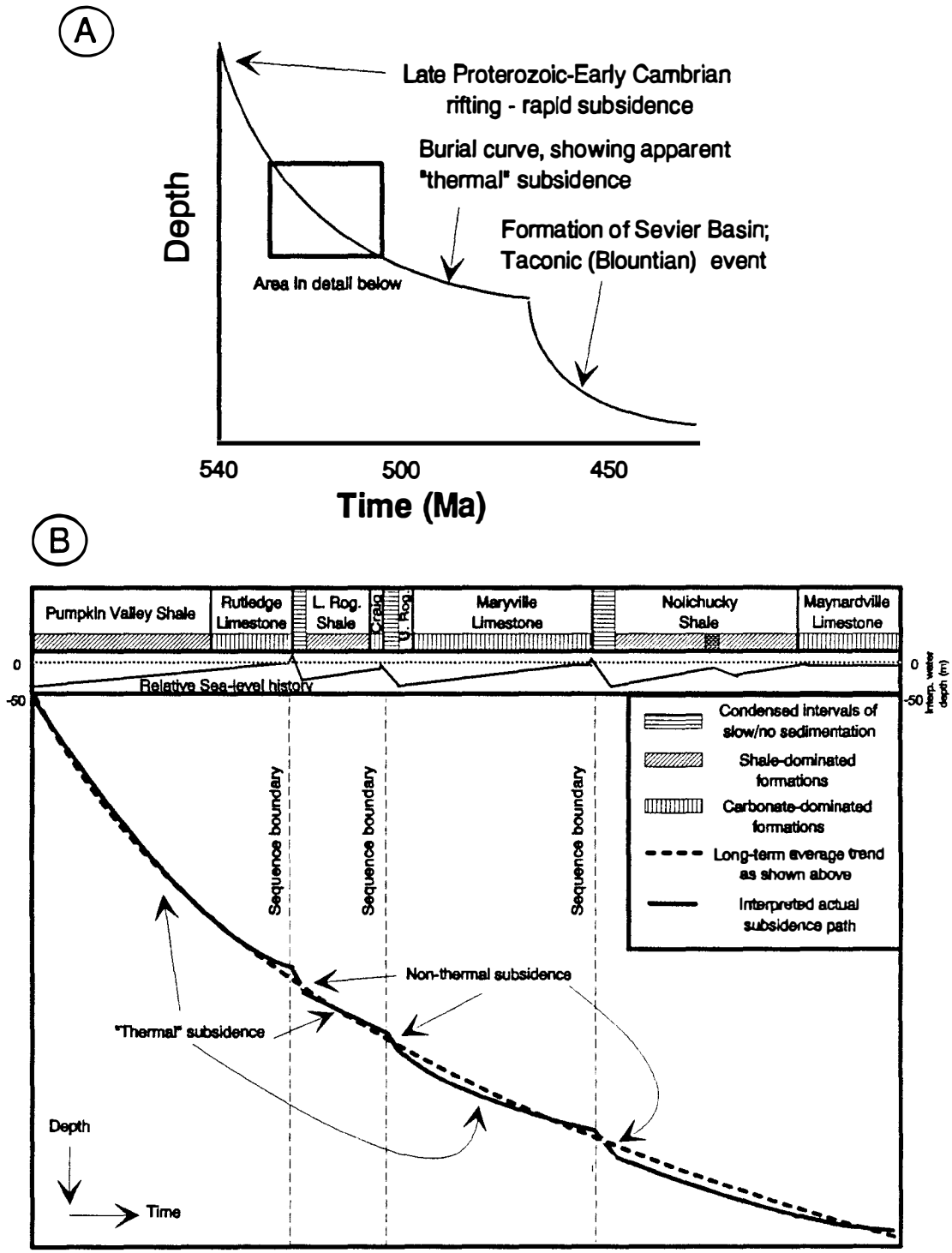
either case, sequence development would be effected.

Burial curves from the Iapetan passive margin of the southern Appalachians display apparently predictable thermal subsidence (Figure 5.6, curve A; see also Bond and others, 1988; 1989; Read, 1989; Walker and others, 1992; Srinivasan and Walker, in press). Stratigraphic, petrographic, and geochemical data (discussed above), however, suggest that actual subsidence "pathway" was much more complex than revealed by the burial curve (Figure 5.6, curve B). Comparison of the two curves suggests that burial curves mask non-thermal subsidence effects. As discussed above, yet another, unresolvable level of episodic subsidence may be present and manifest as meter-scale peritidal cycles.

On younger passive margins, Steckler and others (1988) evaluated uncertainties in backstripping techniques used to construct burial curves. They noted that the current resolution of such curves is only 10 percent, given uncertainties in compaction coefficients, densities, and flexural rigidities. On ancient passive margins, this error is possibly greater. Steckler and others (1988) observed that the two curves derived using different parameters differed "in detail," but that there was an "overall agreement in the shape and amplitude of the curves." As this thesis documents, however, the "detail" of subsidence histories (that is, within 10 percent of the "expected" thermal subsidence) is actually the driving mechanism of sequence development on the Cambrian Iapetan passive margin.

Classic sequence stratigraphy (Vail and others, 1977; 1984; Haq and others, 1987; Sarg, 1988) mandates that eustasy controls most changes in sedimentation patterns, and that tectonism controls only total sediment thickness. It also presumes that subsidence is thermal, linear, and predictable. On margins where non-thermal subsidence punctuates times of "normal" thermal subsidence, however, the possibility exists that stratigraphic responses to these relative sea-level changes could be misinterpreted as eustatic sea-level

Figure 5.6 Tectono-stratigraphic evolution, Conasauga basin, East Tennessee. Curves are qualitative, and estimated from measured sections at Thorn Hill, TN. A) Apparently "thermal" subsidence on Cambrian "passive" margin, southern Appalachians; modified from Walker and others, 1992 and Srinivasan and Walker, in press. Bond and others (1988; 1989) and Read (1989) document similar curves for areas further north/northeast. B) Interpreted episodic non-thermal subsidence "events" and their effects on third-order stratigraphy and sequence boundaries.


A
Late Proterozoic-Early Cambrian
rifting - rapid subsidence
Burial curve, showing apparent
"thermal" subsidence
Formation of Sevier Basin;
Taconic (Blountian) event
Area in detail below
Depth
540
500
450
Time (Ma)
B
Pumpkin Valley Shale
Rutledge Limestone
L. Rog. Shale
Craig
U. Rog.
Maryville Limestone
Nolichucky Shale
Maynardville Limestone
0
-50
Relative Sea-level history
Interp. water depth (m)
Condensed intervals of slow/no sedimentation
Shale-dominated formations
Carbonate-dominated formations
Long-term average trend as shown above
Interpreted actual subsidence path
Sequence boundary
Sequence boundary
Sequence boundary
Non-thermal subsidence
"Thermal" subsidence
Depth
Time

fluctuations. Until the effects of nonthermal tectonic processes can be resolved to the same scale as that desired for evaluating eustatic sea-level fluctuations, separation of the two is impossible. The chronostratigraphic resolution and eustatic sea-level histories suggested by classic sequence stratigraphy may not be present. Sequence stratigraphy (as currently practiced) might then be a limited, rather than a holistic, approach to interpreting the sea-level history of the earth.

CONCLUSIONS

1) Field, petrographic, and geochemical evidence suggests that the Craig ramp and the Maryville platform were terminated by platform exposure followed by drowning.

2) The "rapid" drowning, shown as deeper-water shales (basinal sections) or deepening-upward trend in carbonates then overlain by shales (platform interior sections), was caused by episodic pulses of subsidence, probably associated with regional extension, sediment loading, and/or thermal contraction of the lithosphere.

3) The effects of extension and nonthermal subsidence are recognizable in the style and extent of sedimentation into the *Late* Cambrian. The Cambrian passive margin evolved through three stages: the rift stage, the immature passive margin stage, and the mature passive margin stage.

4) Such nonthermal subsidence is not unique, but has been documented before on other, younger "passive" margins. Such "nonlinear" subsidence is potentially a source of error for studies of eustasy and passive margin evolution, if not carefully considered.

CHAPTER 6

Diagenetic patterns and their relation to stratigraphic packaging, Maryville Limestone (Middle Cambrian), East Tennessee

ABSTRACT

Petrographic study of diagenetic patterns reveals that there are four distinct diagenetic patterns (henceforth referred to as DP) within the Maryville Limestone in the Dumplin Valley area. Each pattern is characterized by (internally) similar petrographic features. DP 1 is characterized by hardgrounds and mineralized grains (in its lower part) and fibrous and bladed calcite, syntaxial overgrowths, and nonferroan equant calcite and dolomite. It probably represents early marine and later burial diagenesis. DP 2 contains early anhydrite and chert and is characterized by extensive dolomitization. It represents episodic very early meteoric and marine diagenesis on a tidal flat and later burial overprinting. DP 3 consists of clear equant calcite and common dissolution features associated with prolonged meteoric exposure. DP 4 is characterized by fibrous and bladed calcite, equant calcite and dolomite, and occassional truncation surfaces. Ferroan cements are common. These cements are of marine and burial origin. The distribution of diagenetic patterns is controlled in large part by factors that controlled depositional environment, which in turn influenced the extent and type of early cementation.

INTRODUCTION

A major goal of studies of carbonate diagensis is analysis of diagenetic patterns at a regional scale. Such analysis should present both interpretive and predictive results. The present study represents a preliminary attempt at such goals for diagenetic patterns

within the Maryville Limestone (Middle Cambrian) of East Tennessee. In particular, this chapter relates diagenetic patterns to stratigraphic packaging in the Maryville (described in Chapter 2). The results of this study suggest that the Maryville is characterized by four distinct diagenetic entities, and that the distribution of these diagenetic patterns is controlled by factors similar to those that controlled the distribution of the stratigraphic packages (thermal subsidence, episodic nonthermal subsidence, platform exposure, and sedimentary aggradation and progradation). This study represents primarily information from the Dumplin Valley area, but the work of Srinivasan (1993) supplemented my descriptions of DP 3 (see also Chapter 5).

DIAGENETIC PATTERNS

The diagenetic patterns (DP) described herein were studied by observation of 110 thin sections from the Maryville Limestone from three outcrops. The patterns were separated on the basis of petrographic characteristics and each pattern represents unique environment(s) of diagenesis. The purpose of this section is to describe the distribution and characteristics of each patterns. Figure 6.1 summarizes the Maryville paragenetic sequence in the Dumplin Valley area.

Diagenetic Features - DP 1 (slope-lagoon)

DP 1 is present in the slope through lagoon packages of the Maryville (see Chapter 3). In the basal parts of DP 1 (the slope package), hardgrounds, pyrite, and mineralized allochems are common. Hardgrounds (see Figure 3.2A) commonly truncate intraclasts, trilobites, and other allochems as an abrupt scalloped to subplanar surface. Some thin sections contain evidence for up to eight hardgrounds, indicating very slow deposition. Pyrite is another early diagenetic component. The pyrite is common in the slope package

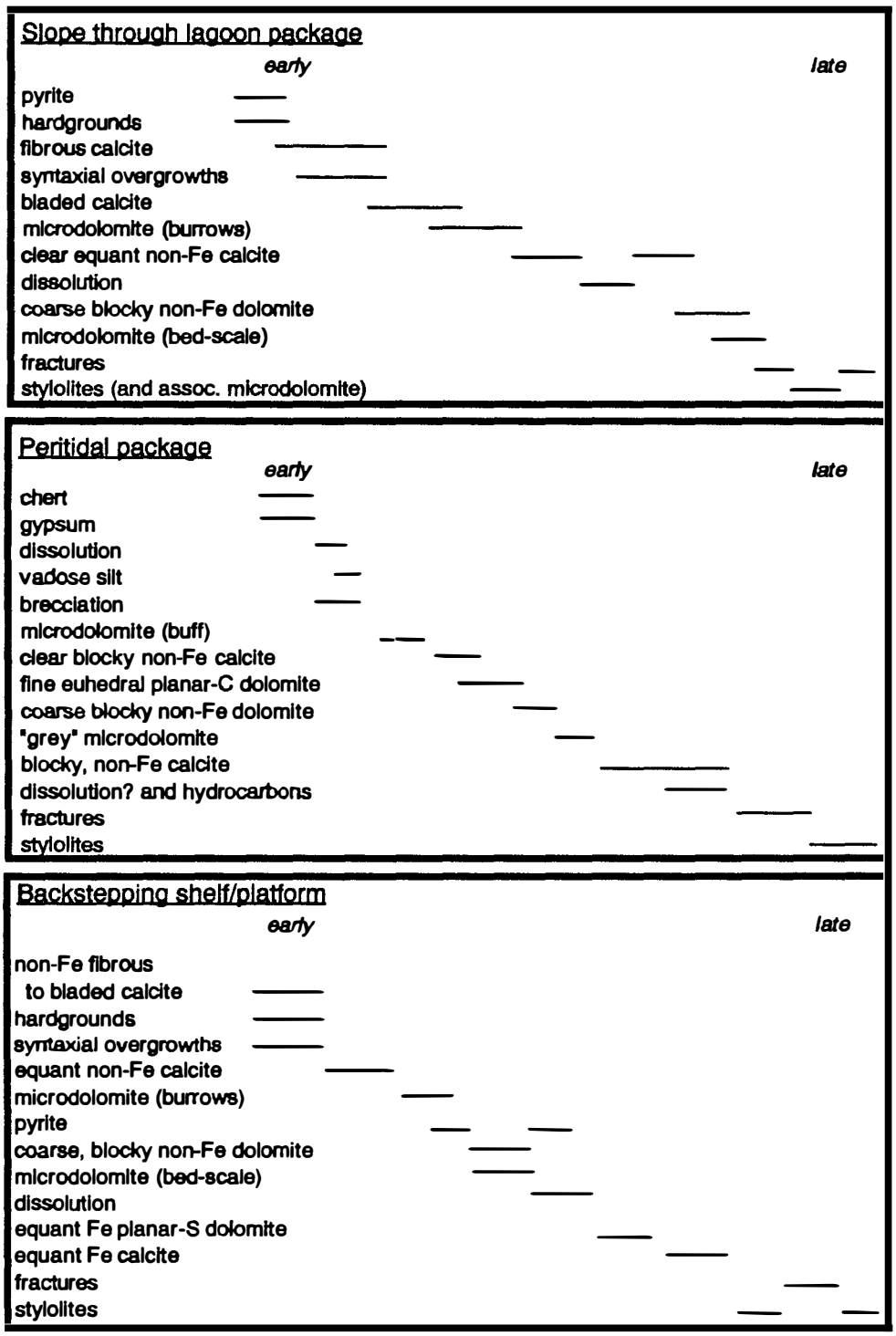


Figure 6.1 Paragentic sequence, Maryville Limestone, Dumplin Valley, TN. Sequence determined from study of three outcrops. Diagenetic features are listed on the left, and their relative timing is indicated by the bars to the right.

and becomes less common upwards (into the mid-ramp and aggrading ramp packges). The pyrite commonly occurs as small framboids up to 0.75 mm in diameter in mudstone or wackestone, and is rarely erosionally truncated or cross-cut by hardgounds. Less commonly, it occurs in packstones in intergranular spaces as small crystals. Mineralized grains are common in the slope package, but extremely rare above this package. These grains are coated with oxide minerals. Some grains contain numerous layers of coatings, some of which are truncated, indicating that more than one episode of mineralization occurred, probably related to slow deposition and episodic transport.

Cements in DP 1 consist of fibrous and bladed calcite (Figure 6.2A), syntaxial overgrowths, equant calcite, and coarse blocky dolomite (Figure 6.2A). Microdolomite and fracture fillings are also present. All are nonferroan as indicated by staining. Early micritic cements between allochems (especially peloids) are also common, and the resulting aggregate grains (Figure 6.2B) are quite common in the mid-ramp and lower aggrading ramp packages. Many of these grains are rimmed by truncated components (ooids, trilobites, etc.) indicating transport and abrasion before final deposition. The earliest cement phases are fibrous calcite (commonly isopachous) and syntaxial overgrowths. These two phases commonly line depositional components and occasionally develop competitive boundaries, indicating that they probably precipitated simultaneously (Walker and others, 1990b). Syntaxial overgrowths form exclusively on echinoderm grains. Many pores are commonly occluded by these two phases alone.

Like fibrous calcite and syntaxial overgrowths, bladed calcite may form the pore-lining phase (Figure 6.2C), but more commonly it overlies the fibrous calcite. It occurs as relatively small, elongate crystals that gradationally overlie fibrous calcite. Similarly, intergranular pores that were not occluded with fibrous and bladed calcite contain clear equant non-ferroan calcite (Figure 6.2B). No evidence for dissolution is present between the earlier phases and this phase. All cements mentioned above probably represent marine

Figure 6.2 Photomicrographs of diagenetic features, DP 1. Long axis of all photomicrographis is 4.5 mm; stratigraphic up is to top of page.

A) Fibrous calcite on oncoids; oncoids partly dissolved and filled with equant nonferroan calcite and dolomite. From sample 27.7.

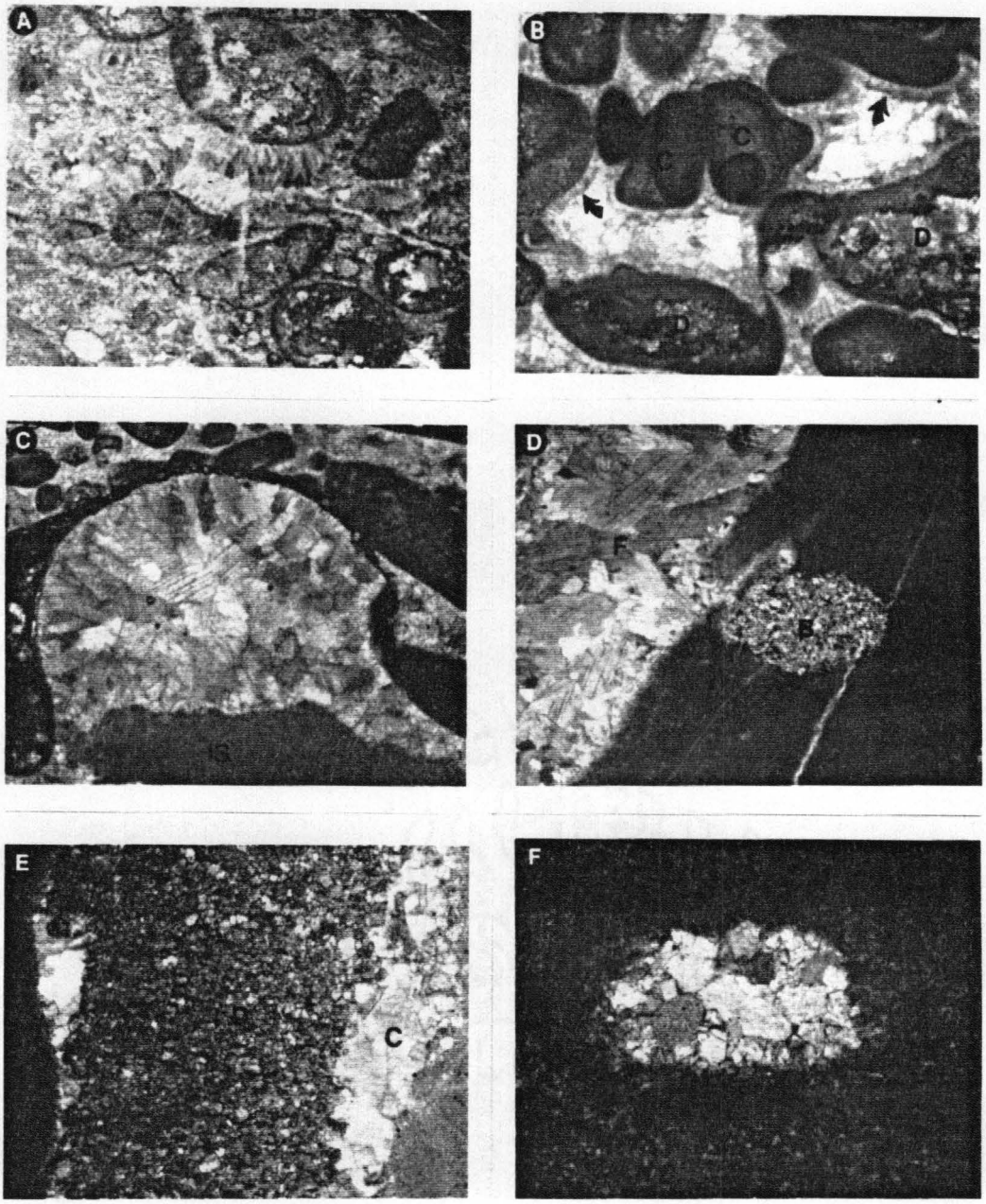
B) Isopachous rind of fibrous calcite (arrow), overlain by blocky, nonferroan calcite, which completely occludes intergranular porosity. Note partly dolomitized oncoids (D) and composite grains (C). From sample 75.8.

C) Bladed calcite (recrystallized fibrous calcite?) and internal sediment in shelter void. From sample 122.1L.

D) Dolomitized burrow in mudstone; fracture filled with nonferroan calcite. From sample 53.6.

E) Burrow filled with rim of nonferroan equant calcite and microdolomite. From sample 91.5.

F) Dolomitized peloids; void of uncertain origin filled with clear, equant non-ferroan calcite. From sample B3.5.


A
B
C
C
D
D
C
D
F
B
E
B
C
F

phases because of their morphologies (fibrous, bladed, etc.), competitive growth habits (i.e. between interpreted margin fibrous calcite and syntaxial overgrowths), and erosional truncation (where present) (Steinhauff, 1989).

In the mid-ramp, aggrading ramp, and lagoon packages, microdolomite is common. Many burrows are filled with microdolomite (Figure 6.2D) which weathers differently than the surrounding limestones to give the burrows their distinct buff, mottled field appearence. Microdolomite is comprised of subhedral to anhedral fine dolomite with irregular crystal boundaries (where resolvable). This microdolomite appears to be petrographically distinct from that which developed associated with stylolites, similar to the distinction between these two types elsewhere in the Maryville (Srinivasan, 1993; Srinivasan and Walker, in press). The stylolite-microdolomite appears to have a darker color, be slightly coarser grained, and contain more subhedral and even euhedral rhombs. Yet another type of microdolomite is that which completely replaces packstone-grainstone. The outline of allochems (most commonly peloids based on size and shape) remain as darker "ghosts," but most features are obscured (Figure 6.2F). This microdolomite, like that associated with stylolites, is darker and coarser grained than the burrow-fill dolomite.

Scattered through DP 1 are dissolved allochems filled with coarse blocky nonferroan calcite or coarse blocky nonferroan dolomite (Figures 6.2A, 6.2B). These allochems commonly retain a micritic envelope, and their shapes suggest peloid and ooid precursors. This pore-filling phase is commonly comprised of one to five equant crystals of calcite or dolomite and crystals have planar boundaries. A rim of insolubles is rarely present. These phases probably represent burial diagenesis.

Vertical distribution of cement and porosity types - DP 1

As discussed above, hardgrounds, mineralized grains, and pyrite are common only

in the lowest several meters of the parts of the Maryville examined in the Dumplin Valley area, probably related to the slow sedimentation rates. In areas where the slope package is thicker, such features would be common through a thicker interval.

From the base of the Maryville to approximately 15 m below the shoal package (the lower 38 m of the Formation), intergranular porosity is occluded by fibrous and bladed calcite along with syntaxial overgrowths. In this interval, many allochems are dissolved and filled with equant calcite and dolomite.

The shoal package, as well as the uppermost aggrading ramp package, is dominated by fibrous calcite, however, and intra- and inter-granular bladed and equant calcites are extremely rare. Unlike the slope, mid-ramp and lower aggrading ramp packages, these intervals contain very few dissolved allochems filled with coarse equant non-ferroan calcite or dolomite. This pattern is probably best explained by extensive early marine cementation (fibrous calcite), similar to that in modern ooid shoals (Harris, 1979) which occluded most porosity and inhibited later fluid flow through the rock. Some ooids in the shoal package are replaced with microdolomite which destroyed original ooid fabrics.

The diagenesis of the lagoon package differs from the underlying packages in that fibrous cements are less common, blocky cements are more common, and dolomitization is much more pronounced. In the lagoon package, many beds are completely dolomitized into fine to medium-grained anhedral to (less commonly) euhedral non-ferroan dolomite. The abundance of dolomitized beds increases upwards, towards the peritidal package, which is characterized by complete dolomitization. These dolomites differ from the peritidal dolomites in that they are much darker colored (in thin section as well as in the field) and generally finer grained.

One interval of sheared limestone is also present at the DSR section (Figure 6.3A). It consists of dolomitized ooids?, which are meshed in a "net" of fibrous, elongate

(sheared) nonferroan calcite. This deformation is probably related to Alleghanian tectonism.

Diagenetic Features - DP 2 (peritidal)

DP 2 is present only in the Maryville peritidal package and is characterized by extensive dolomitization. Unlike some dolomitized peritidal sequences, however, the Maryville dolomites are not comprised completely of coarse-grained sucrosic dolomite. Instead, many primary depositional and early diagenetic features remain undisturbed.

Because the peritidal package is composed of numerous shallowing-upwards cycles (see Chapter 4), the general terms "early" and "late" are somewhat ambiguous, as diagenesis of this package was strongly influenced by the *repetitive* submergence and emergence. **Several** cycles of relative sea-level fall and rise (and marine and meteoric diagenetic environments) related to development and evolution of subsequent cycles may thus be represented in a given sample.

A general paragenetic sequence for a given cycle can be developed (Figure 6.1). The first diagenetic process to effect some cycles (especially in the lower parts of the peritidal package) was precipitation of anhydrite. Although the anhydrite has been dissolved, crystal molds occur as euhedral acicular needles, most commonly in peloidal packstone, where they may form a 0.5 cm-thick crust-like fabric continuous across the outcrop (see Figure 3.4C) or occur as isolated acicular crystals (Figure 6.3B). These crystals do not appear to have displaced adjacent allochems as they grew. These molds are filled with clear equant nonferroan calcite, and commonly a floor of vadose silt is present. Some small-scale brecciation (in beds less than 0.1 m thick) is also present in the anhydrite zone, possibly related to evaporite dissolution. Chert is also present, but occurs through most of the DP only as small (<2mm) nodules observed only in thin section. At the DSR section, however, one covered interval contained abundant larger blocks of chert

Figure 6.3 Photomicrographs of diagenetic features, DP 1, 2, and 3. Figure 6.3A is from DP 1, Figures 6.3B, 6.3C, and 6.3D are from DP 2, Figures 6.3E and 6.3F is from DP 4. DP 3 is not illustrated here, but is shown in Figures 5.5E, 5.5F, 3.4D, and 3.4E. Long axis on A,B,C,E, and F is 4.5 mm, D is 1.0 mm; stratigraphic up is to top of page.

A) Dolomitized ooids (?) (arrows) in sheared, now-fibrous matrix; from sample 141.2.

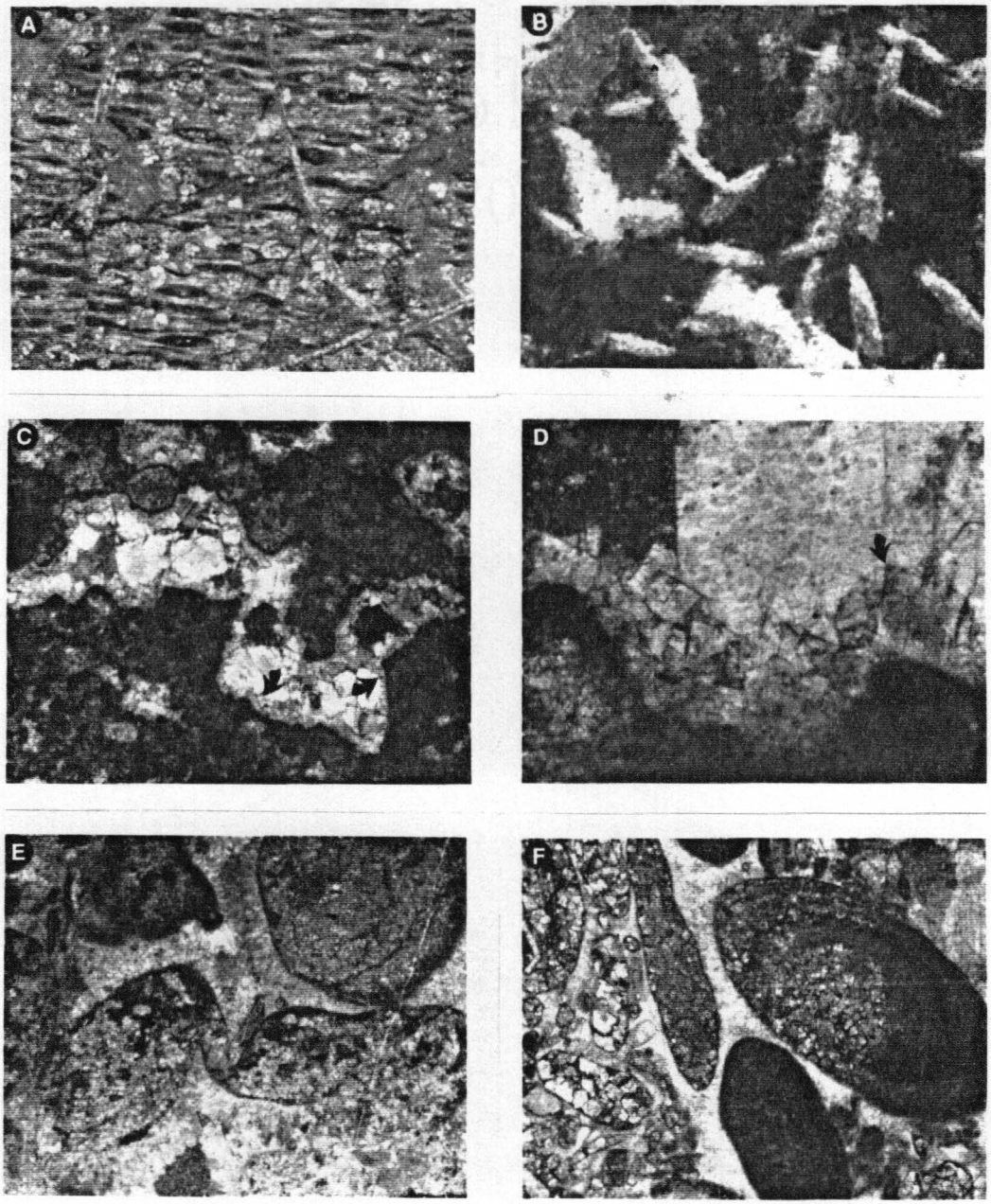
B) Acicular anhydrite crystal molds, now filled with clear, equant calcite and vadose silt. Matrix is dolomitized peloid packstone. See also Figure 3.4 C. From sample B13.1.

C) Pore-lining, fine, euhedral, planar-E dolomite and pore-filling coarse, equant planar-C dolomite. From sample B43.4.

D) Close up of rimming cements and part of coarse pore-central cements from area indicated in 6.3C . From sample B43.4.

E) Oncoids stabilized and filled with non-ferroan dolomite. Intergranular cement is mostly fibrous calcite. From sample Hy47.4.

F) Oncoids, some completely dolomitized, others partly dolomitized, some unaltered. Dolomite is mostly ferroan (as indicated by staining). Intergranular pores are filled with fibrous to bladed calcite. From sample Hy63.3.


A
B
C
D
E
F

float. A thin section of one float sample revealed "dirty" brown chert ? replacement of carbonate. A thin discontinuous band of replacement chert is also present at the IS section at 1.5 m from the base of the measured section.

Many intervals of the peritidal package are characterized by fine grained nonferroan microdolomite, which may occur as a replacement of bedded carbonate mud, as a replacement of peloids, ooids, etc., or within algal laminations. Microdolomite consists of very fine, anhedral crystals, most of which are approximately the same size (3-50 microns). Two distinct types of microdolomite are present: buff and gray. Both have distinct field appearances. Petrographically, buff dolomite is finer-grained and replaced allochems retain more of their fabrics. Gray dolomite is coarser-grained, contains crystal boundaries that cut across allochem boundaries, and obliterates most primary allochem fabrics. Gray dolomite occurs exclusively in subtidal sediments (those with no fenestrae, mudcracks, algal laminations, etc.) and appears to be petrographically identical to that developed in subtidal sediments in DP 1 and 3. An oxygen isotope ratio of -11.6 ‰ from a sample of brown dolomite (from Hy16.5) suggests that these dolomites are probably related to burial processes (see Srinivasan and Walker, in press), but this interpretation must be regarded as preliminary. Buff dolomite occurs in both subtidal or intra-supratidal sediments. This phase probably represents early replacement of orginally calcite components. Sample 43.3 contains both types and illustrates the differences.

Most pores, intra- or inter-granular or fenestral, contain an initial thin "rind" of small, euhedral planar-C (Mazzullo, 1992) dolomite (Figures 6.3C, 6.3D). Where this rind grows from a microdolomite base, it appears as a gradational transition into larger-size dolomite crystals. Where it grows from larger, nonmicrodolomite bases (such as peloids, ooids, intraclasts), it simply appears as an outward-coarsening rim. In both cases, however, the rind is thin, and porosity is commonly filled by coarse, equant, planar-S (Mazzullo, 1992), non-ferroan dolomite. These various dolomites are of very early origin

as indicated by truncation in intraclasts (see Figure 3.4A). All cements mentioned thus far in this DP probably represent precipitation from early meteoric, marine, "mixing zone(?)," or hypersaline tidal flat fluids, associated with the "cyclic" flooding and exposure of the tidal flat.

Burial phases include blocky nonferroan calcite commonly associated with coarse dolomite. Competitive boundaries (rarely) occur between these two phases. More often, however, the blocky calcite follows the dolomite with no evident dissolution between phases. This calcite is also commonly associated with dark hydrocarbon(?) residue, which appears as a black lining on pores, many of which still retain some original porosity. These residues are most common in intervals of sucrosic dolomite or zones with abundant coarse fenestral or intergranular dolomite. In these pores, the dolomite in contact with these dark linings is commonly euhedral and some porosity remains. Fluid migration through dolomitic pores thus appears to have been controlled by retention of primary porosity, rather than later dissolution. In contrast, the calcite associated with these residues is not euhedral, and migration might instead be related to creation of secondary porosity.

Coarse-grained sucrosic planar-E to planar-S (Mazzullo, 1992) dolomite is relatively rare, but where it does occur, it obliterates all other diagenetic features. Both stylolites and fractures cut all of the above-mentioned features. They are less common than in DP 1, 3, or 4, however, probably because of the lower solubility of dolomite and its greater mechanical strength.

Vertical distribution of cement and porosity types - DP 2

The distribution of cement and porosity types in DP 2 is more complex than that in DP 1 because of the repetitive exposure/flooding events associated with formation of cycles, although several broad generalizations are evident.

Anhydrite molds and breccia are present only in the lower parts of the SR and DSR sections. No anhydrite molds were observed at IS section, but the basal exposed bed is a breccia. The stratigraphically-limited distribution of these two features suggests that climate changed from arid to subarid, and conditions became unsuitable for evaporite precipitation.

Like anhydrite molds and breccia, the residues are stratigraphically limited. They are present only within 20 m of the top of the peritidal package at the SR and IS sections. Similarly, they are present almost exclusively in intragranular pores or voids created by (earlier) nonfabric selective dissolution in the lower parts of intra- supra- tidal parts of cycles. Nowhere were they observed in subtidal sediments. The reason for this trend is unknown.

Finally, coarse-grained sucrosic planar-E to planar-S dolomite, relatively rare through most of the peritidal package, is most common in the upper 12 m of this package. This distribution may be related to processes associated with the extended subaerial exposure that terminated the Maryville platform (Chapter 3). Alternatively, it may reflect a decrease in the rate of sea-level rise resulting in longer periods of exposure and alteration.

Diagenetic features - DP 3

DP 3 is characterized by meteoric diagenetic features associated with prolonged subaerial exposure. Similar diagenetic features have been recognized and documented before by Srinivasan (1993) in shelf-edge and lagoonal lithologies. In the studied part of the Dumplin Valley area, prolonged exposure is manifest only in the peritidal package.

As discussed above, DP 2 contains numerous examples of diagenetic features related to subaerial exposure. Thus, in areas where DP 3 is present within the peritidal package, it differs only in the *degree* of alteration. DP 3 contains several features not

present in DP 2, including extensive nonfabric selective dissolution, fabric-selective dissolution, shrinkage features, pisoids, and laminar calcrete features.

There are three distinct subDP of DP 3. SubDP 3A is developed in subtidal sediments, and is described in Chapter 5 and by Srinivasan (1993). It typically contains small-scale breccia (Figure 5.2D) and fabric-selective dissolution of allochems (Figure 5.2E). Clear equant to drusy calcite precipitated in dissolution voids have depleted oxygen isotope ratios (Chapter 5, Srinivasan, 1993). SubDP 3B is characterized by poorly developed pisoids, well-developed shrinkage features, and aveolar septal structure. Pisoids are generally small (<2 mm), but may contain several laminae. Shrinkage features are common (Figure 3.4D). They may be manifest as dolomite-filled spaces within distinct voids or between grain boundaries that appear to have been "fitted" at one time. These voids are comprised of an outer darker rim which is commonly torn, folded, or otherwise separated from the void edge filled with fine-grained buff microdolomite. Where the dark rims are separated from the void wall, the space is filled with coarse blocky dolomite rather than the microdolomite typical of the void interior. Aveolar septal structures are rare in this subDP.

SubDP 3C is characterized by nonfabric-selective and fabric-selctive (Figure 3.4E) dissolution voids, clotted textures, coarse blocky dolomite and calcite, concentrations of insolubles, grain-rotation features, laminar calcrete, and a distinct blood-red coloration, all of which are related to subaerial exposure and weathering. Nonfabric-selective dissolution is best developed in muddy rocks. Dissolution voids are commonly rimmed by insolubles and filled with coarse blocky nonferroan calcite and/or dolomite. They commonly have a dark red rim, which gives these rocks their distinct clotted field appearance. In more grain-rich rocks, leached allochems commonly contain vadose silt. Such geopetals may be rotated, probably related to churning. Laminar calcrete (?) is also associated with this subDP, but is less common. It is commonly dark brown to red and is comprised of

irregular discontinuous contorted laminae cut by fractures, which are erosionally truncated, indicating their early diagenetic origin.

Vertical and lateral distribution of cement and porosity types- DP 3

SubDP 3A is present across the platform, and has been documented in two horizons of subtidal sediments by Srinivasan (1993). SubDP 3B is recognized only at the SR section, at 33.3 m from the base of the measured section. This stratigraphic horizon may correlate with the lower occurrence of subDP 3C at Woods Gap, TN (Srinivasan, 1993), and may be related to prolonged relative sea-level fall and resulting meteoric exposure.

SubDP 3C is recognized at the top the peritidal package at both the SR and IS sections, and correlates with the upper occurrence of subDP 3C at Woods Gap, TN. This surface is the genetic top of the Maryville platform (the sequence boundary), and above it a significant change in platform dynamics occurs. Thus, diagenetic features and distribution of subDP 3C support the interpretation of subaerial exposure prior to platform flooding documented by Srinivasan (1993).

Diagenetic features - DP 4

DP 4 contains no features associated with meteoric diagenesis. Instead, it contains only marine and burial phases. It is distinct from DP 1 in that it contains common ferroan phases of both calcite and dolomite.

As in DP 1, the earliest diagenetic phases are syntaxial overgrowths and isopachous fibrous to bladed calcite. Fibrous to bladed calcite is extremely well-developed on ooids, and less well developed (but still common), on peloids, oncoids, and trilobites. These cements are occasionally erosionally truncated and cut by hardgrounds, indicating an early diagenetic origin. Syntaxial overgrowths are common only on echinoderm

grains. Planar boundaries between syntaxial overgrowths and fibrous cements suggest simultaneous growth. These cements and features represent early marine diagenesis.

Clear to turbid, equant nonferroan calcite commonly occurs overlying bladed calcite. No dissolution is evident between the bladed and equant phases.

Microdolomite is also common in this package and replaces either mudstones or packstones-grainstones. The microdolomite is gray and is petrographically identical to that developed in subtidal sediments in the peritidal package and upper lagoon package. Microdolomite in mudstones is typically finer grained than that in packstones and grainstones. It can be present as isolated burrow fills or as a wholesale replacement. That developed in the latter can be quite large, and replace the entire rock. In these examples, crystal boundaries commonly extend across allochem boundaries. Primary features of allochems (ooid laminae, etc.) are destroyed, and only "ghosts" remain.

Pyrite is also common in this DP. Some framboidal pyrite is associated with microdolomite, and probably represents an early phase. Other pyrite crystals occur with coarse, blocky nonferroan dolomite, and probably represents a deeper burial environment.

Coarse, blocky nonferroan dolomite occurs as the last phase in many intragranular pores. It also occurs in moldic pores created by dissolution of oncoids and ooids (Figure 6.3E). Pores are commonly filled by three to seven anhedral to subhedral planar-S dolomite crystals, and may contain insolubles around the pore lining. Within intragranular pores, no evidence for dissolution is present between the calcite phases and this last dolomite phase.

Coarse blocky ferroan calcite and dolomite (Figure 6.3F) are also present in some intragranular pores and in many moldic pores. These pores commonly contain evidence for dissolution prior to calcite or dolomite precipitation. Moldic pores created by the dissolution of oncoids and ooids commonly contain a rim of insolubles. The calcite and dolomite which fills these voids is commonly anhedral to subhedral with straight

compromise boundaries. Commonly, three to seven crystals fill these voids.

Stylolites and fractures cut through all of the above-mentioned features. They represent the latest stage of diagenesis of the rock.

Vertical and lateral distribution of cement and porosity types - DP 4

DP 4 is present only in the backstepping platform/shelf package of the Maryville, which is in turn present only in platform-interior areas (Chapter 2). It contains **no** evidence suggesting episode(s) of meteoric exposure.

In the lower parts of the backstepping platform/shelf package, replacement of mudstone with microdolomite and replacement of packstone-grainstone with coarse microdolomite is common. Above the basal 12 m, however, this bed-scale dolomitization becomes less common.

In the uppermost 10 m of the backstepping platform/shelf package, ferroan cements, both calcite and dolomite, become more common. This stratigraphic interval is the only range in which intragranular and moldic ferroan cements occur in any abundance in the studied Maryville of the Dumplin Valley area.

SEQUENCE STRATIGRAPHIC CONTROL ON DIAGENETIC FEATURES

The previous section subdivided Maryville diagenetic features into four distinct DP, each with characteristic cement mineralogies, cementation histories, and diagenetic environments. These *diagenetic* patterns are intimately associated with processes controlling the *deposition* of the various stratigraphic packages of the Maryville.

The lower parts of DP 1 are characterized by hardgounds, composite grains, and mineralized grains, all features that require slow sedimentation rates to form. Thus, their limited stratigraphic extent is due to sedimentation rates at the time of formation. When

rates increased, these features became less common. Similarly, the hardgrounds in DP 4 represent the slow sedimentation rates associated with platform drowning. These features may have effected later fluid flow by serving as impermeable boundaries.

All of DP 1 is characterized by marine and burial cementation. Fibrous and bladed calcite and syntaxial overgrowths were all probably precipitated in the marine diagenetic environment. This diagenetic environment was present through this time because of the constant rise in relative sea-level due to thermal (and non-thermal?) subsidence during the deposition of the mid-ramp and aggrading ramp packages. Just as no meter-scale shallowing upwards cycles are present (Chapter 2), no cyclic exposure surfaces are present in these depositional packages.

Marine cements are probably most abundant in the shoal package, where in many samples, intergranular pores are exclusively filled by marine fibrous to bladed calcite. This calcite was probably precipitated in the zone of intense water movement related to the development and migration of ooid shoals. In these environments, because most porosity was filled early with fibrous calcite, later phases are relatively rare. Early cementation is also suggested by the common ooid-rich intraclasts present in the aggrading ramp and lagoon packages. Many ooids are dolomitized by fine-grained dolomite. No diagenetic evidence for periodic exposure is present.

In the lagoon package, bed-scale dolomitization becomes more common upwards towards the peritidal package. This trend is probably related to: a) the movement of later fluids downward from the peritidal package (Dorag dolomitization; see Hardie, 1987b, however); b) early shallow-burial (<20m) dolomitization (Srinivasan, 1993); or c) later burial dolomitization. That such beds are common where no peritidal facies occur above (such as the SQ section) suggests that one of the burial explanations is probably more appropriate. Further isotopic and trace element studies should help clarify the origin of these dolomites (as well as how they might relate to the dolomites of DP 2).

The distribution of DP 2 is limited by the vertical and lateral extent of the peritidal package. The presence and abundance of hydrocarbon residue is also stratigraphically limited to the lower intertidal parts of cycles. This trend is related to retention or creation of pores in the sediments of this environment. Because cycles are not correlatable across even short distances (Chapter 3), these zones of migration are likewise probably not predictable across similar distances.

DP 2 does, however, contain several "predictable" trends. The first is the abundance of sucrosic dolomite in the upper parts of this package. This trend might be related to a decrease in the rate of sea-level fall during deposition of the upper parts of the peritidal package, or it may be related to processes associated with extended subaerial exposure (DP 3). A second trend is the limitation of anhydrite molds and breccia to the lower parts of the peritidal package. This pattern is probably related to climatic factors. A third trend is the presence of DP 3 at the top of DP 2. Finally, many cements in this package were formed very early, as indicated by their truncation by erosion, both as *in situ* deposits and in intraclasts. The probably exceptions to this are the calcites and dolomites associated with hydrocarbon residue. With further geochemical studies, it may be possible to delineate depositional controls on burial phases or early (tidal flat) phases.

DP 3 occurs at the top of and within DP 2 in the studied parts of the Dumplin Valley area. DP 3 was controlled by relative sea-level fall across the platform. SubDP 3A developed in subtidal sediments while peritidal sediments developed subDP 3B (on the lower exposure surface) and subDP 3C (on the exposure surface correlated with that at the top of the Maryville in platform-margin areas). SubDP 3B is probably not as well "developed" as subDP 3C because relative sea-level drop was less pronounced (lagoonal sediments were not exposed; Srinivasan, 1993), and possibly because of a shorter duration. Thus, the development of DP 3C is related to the same processes that led to platform termination.

SubDP 4 occurs only above DP 2 and 3. It contains no evidence for subaerial exposure, but contains exclusively marine and burial phases and common ferroan cements. The absence of meteoric diagenetic features is due to the rapid relative sea-level rise that drowned the platform (the deepening-upward trend). The upwards increase in abundance of ferroan cements may be related to proximity to the shales of the Nolichucky, that probably acted as fluid sources for burial fluids which effected the Maryville (Srinivasan, 1993). The limited abundance of ferroan cements in the lower Maryville may reflect the thin lower Rogersville Shale in the study area. One trend of SubDP 4 that might be of importance is the upwards (away from DP 1) decrease in bed scale dolomitization. Recall that a similar trend was present approaching DP 2 within DP 1.

CONCLUSIONS

The Maryville Limestone contains four distinct diagenetic patterns, defined on the basis of cement types and environments of diagenesis. DP 1 represents primarily marine and burial diagenesis. The extensive marine diagenesis was controlled by continual submergence below sea-level. The distribution of later burial phases is related to residual intragranular porosity and the extent of early marine cementation. DP 2 is characterized by extensive dolomitization, and is limited to areas where peritidal environments existed. DP 3 contains features formed due to extended subaerial exposure, and is manifest to varying degrees in subtidal and peritidal sediments in two distinct horizons. The distribution of DP 3 is related to the two major relative sea-level falls that exposed the platform. DP 4 is characterized by marine cementation, but contains more ferroan cements than any other DP. It occurs only in areas where carbonate sediments overlie the sequence boundary (the exposure surface), and was effected only by marine processes before burial due to the rapid relative sea-level rise.

CHAPTER 7

Summary and Conclusions

1) The lower 170 m of the Maryville Limestone displays a general shoaling-upwards trend from the slope package through the peritidal package in the study area. At the top of the peritidal package of the Maryville and limestones of the Craig Limestone Member, exposure surfaces are developed. Above the exposure surfaces are deepening-upwards trends.

2) Although aggradadation and progradation were the dominant controls on internal decameter stratigraphic packaging, tectonism also effected the final stacking patterns and spatial distribution of the Craig and Maryville limestones. In particular, episodic tectonism was responsible for the drowning represented by the abrupt transition from carbonates to shales above the Craig and from the peritidal package to the backstepping platform/shelf package of the Maryville.

3) A model for the carbonate-shale transitions involves exposure of the platform to provide shutdown of carbonate production that allowed Middle Cambrian nonthermal subsidence to be compounded during subsequent drowning and "lag time" and resulted in an apparently "instantaneous" substantial drowning of the platform.

4) Several processes (tectonics, eustasy, and autogenic) acted in concert to produce the peritidal meter-scale cycles and stacking patterns in the mid-Maryville of the study area. No evidence (such as systematically stratigraphically thickening or thinning of cycles or cycles correlative across wide areas) indicative of *regular* Milankovitch-controlled eustatic forcing is present. Instead, episodic subsidence associated with sediment loading and/or regional extension combined with autocyclic processes to create

the peritidal "facies mosaic."

5) This study suggests that the controls on sedimentation patterns during Maryville deposition were numerous and temporally and spatially variable. Sediment loading, tectonism associated with regional extension, thermal subsidence, irregular eustatic sea-level fluctuations, and autogenic processes all exerted an influence on meter-scale stacking patterns. The absolute input of each of these factors on stacking patterns is probably unresolvable from the stratigraphic record.

6) Tectonism associated with Maryville and Craig platform drowning does not represent isolated tectonism on the Iapetan margin. Cambrian strata of much of the southeastern United States margin contains evidence for spatially and temporally varying subsidence.

7) These effects of extension are recognizable in the style and extent of sedimentation into the *Late* Cambrian. Thus, I propose that the Cambrian passive margin evolved through three stages: the rift stage, the immature passive margin stage, and the mature passive margin stage.

8) Diagenetic patterns of the Maryville in the study area suggest four diagenetic "facies:" 1) DP 1, characterized by hardgrounds and mineralized grains (in its lower part) and fibrous and bladed calcite, syntaxial overgrowths, and non-ferroan equant calcite and dolomite probably representing early marine and later burial diagenesis; 2) DP 2 containing early anhydrite and chert and characterized by extensive dolomitization, representing episodic very early meteoric and marine diagenesis on a tidal flat and later burial overprinting; 3) DP 3, consisting of clear equant calcite and common dissolution features associated with prolonged meteoric exposure; and 4) DP 4, characterized by fibrous and bladed calcite, equant calcite and dolomite, and occasional truncation surfaces with common ferroan cements. DP 4 cements are of marine and burial origin. The

distribution of these cements is related to the same factors that controlled sedimentary package distribution.

REFERENCES

List of References

Aitken, J.D., 1966, Middle Cambrian to Middle Ordovician cyclic sedimentation, southern Rocky Mountains of Alberta: Bulletin of Canadian Petroleum Geology, v.14, p.405-441.

Aitken, J.D., 1967, Classification and environmental significance of cryptalgal limestones and dolomites, with illustrations from the Cambrian and Ordovician of southwestern Alberta: Journal of Sedimentary Petrology, v. 37, p. 1163-1178.

Aitken, J.D., 1981, Generalizations about grand cycles: *in* Taylor, M.E., ed., Short papers for the 2nd International Symposium on the Cambrian System: United States Geological Survey Open-File Report 81-743, p. 156-159.

Algeo, T.J., and Wilkinson, B.H., 1988, Periodicity of mesoscale Phanerozoic sedimentary cycles and the role of Milankovitch orbital modulation: Journal of Geology, v. 26, p. 515-542.

Aubry, M.P., 1991, Sequence stratigraphy: Eustasy or tectonic imprint?: Journal of Geophysical Research, v. 96, p. 6641-6679.

Ball, M.M., 1967, Carbonate sand bodies of Florida and the Bahamas: Journal of Sedimentary Petrology, v. 75, p. 583-597.

Barrell, J., 1917, Rhythms and the measurements of geologic time: Geological Society of America Bulletin, v. 745-904.

Bates, R.L., and Jackson, J.A., eds. 1984, Dictionary of geological terms: Anchor Press / Doubleday, New York, 571 p.

Beach, D.K., and Ginsburg, R.N., 1980, Facies succession of Plio-Pliestocene carbonates, northwestern Great Bahama Bank: American Association of Petroleum Geologists Bulletin, v. 64, p. 1634-1642.

Berger, A., Imbrie, J., Hays, J., Kukla, G., and Saltzman, B., 1984, Milankovitch and climate: Boston, Reidel Publishing Company, 895 p.

Black, M., 1933, The algal sediments of Andros Island, Bahamas: Royal Society [London] Philosophical Transitions, series B, v. 222, p. 165-192.

Bond, G.C., and Kominz, M.A., 1984, Construction of tectonic subsidence curves for the early Paleozoic miogeocline, southern Canadian Rocky Mountains: Implications for subsidence mechanisms, age of breakup, and crustal thinning: Geological Society of America Bulletin, v. 95, p. 155-173.

Bond, G.C., Kominz, M.A., and Grotzinger, J.P., 1988, Cambro-Ordovician eustasy: Evidence from geophysical modelling of subsidence in Cordilleran and Appalachian passive margins: *in* Kleinsephn, K.L. and Paola, C., eds., New Perspectives in Basin Analysis: New York, Springer-Verlag, p. 129-160.

Bond, G.C., Kominz, M.A., Steckler, M.S., and Grotzinger, J.P., 1989, Role of thermal subsidence, flexure, and eustasy in the evolution of early Paleozoic passive-margin carbonate platform: *in* Crevallo, P.D., Wilson, J.L., Sarg, J.F., and Read, J.F. (eds.) Controls on carbonate platform and basin development: Society of Economic Paleontologists and Mineralogists Special Publication No. 44, p. 39-61.

Bossellini, A., 1967, La tematica deposizionale della Dolomia Principale (Dolomiti e Prealpi Venete): Bollettino della societa geoloica italiana, v. 86, p. 133-169.

Bott, M.H.P., 1992, Passive margins and their subsidence: Journal of the Geological Society of London, v. 149, p. 805-812.

Braile, L.W., Hinze, W.J., Keller, G.R., Lidiak, E.G., and Sexton, J.L., 1986, Tectonic development of the New Madrid rift complex, Mississippi Embayment, North America: Tectonophysics, v. 131, p. 1-21.

Bridge, J., 1956, Stratigraphy of the Mascot-Jefferson City zinc district, Tennessee: U.S. Geological Survey Professional Paper 277, 277 p.

Bridge, J. and Hatcher, R.D., Jr., 1973, Geologic map of the New Market quadrangle, Tennessee: State of Tennessee, Division of Geology Quadrangle Map, scale = 1:24000.

Broeker, W.S., and van Donk, J., 1970, Insolation changes, ice volume, and O^{18} record of deep sea cores: Reviews of Geophysics and Space Physics, v. 8, p. 169-197.

Burke, W.H., Denison, R.E., Hetherington, R.B., Koepnick, R.B., Nelson, H.F., and Otto, J.B., 1982, Variation of seawater $^{87}Sr/^{86}Sr$ through Phanerozoic time: Geology, v. 10, p. 516-519.

Butts, C., 1940, Geology of the Appalachian valley in Virginia: Virginia Geological Survey Bulletin, v. 52, 568 p.

Campbell, M.R., 1894, Description of the Estillville Sheet (Kentucky, Virginia, Tennessee): U.S. Geological Survey Geologic Atlas, Folio 12.

Cattermole, J.M., 1962, Geology of the Maryville quadrangle, Tennessee: U.S. Geological Survey Geologic Quadrangle Map 163.

Cisne, J.L., 1986, Earthquakes recorded stratigraphically on carbonate platforms: Nature, v. 323, p. 320-322.

Chow, N., and James, N.P., 1987, Cambrian grand cycles: A northern Appalachian perspective: Geological Society of America Bulletin, v.98, p. 418-429.

Cloetingh, S., 1986, Intraplate stresses: a new tectonic mechanism for relative fluctuations of sea-level: Geology, v. 14, p. 617-620.

Cloetingh, S., 1988, Intraplate stresses: a new perspective in basin analysis: in Kleinspehn, K.L., and Paola, C. (eds.), New Perspectives in Basin Analysis: Springer, New York, p. 305-330.

Cloetingh, S., and Kooi, H, 1989, Intraplate stresses: A new perspective on QDS and Vail's third-order cycles: *in* Cross, T.A., ed., Quantitative Dynamic Stratigraphy: Prentice-Hall, p. 127-148.

Cloetingh, S., and Kooi, H, 1992, Intraplate stresses and dynamical aspects of rifted basins: Tectonophysics, v. 215, p. 167-185.

Collinson, C., Sargent, M.L., and Jennings, J.R., 1988, Illinois basin region: *in* Sloss, L.L., (ed.) Sedimentary Cover - North American craton, U.S.: Geological Society of America, The Geology of North America, Volume D-2, p. 383-426.

Cowan, C.A., and James, N.P., 1990, The Cambrian eustatic signal: Not so grand? [abst.]: American Association of Petroloeum Geologists Bulletin, v. 74, p. 634-635.

Cudzil, M.R., and Driese, S.G., 1987, Fluvial, tidal, and storm sedimentation in the Chilhowee Group (Lower Cambrian), northeastern Tennessee, U.S.A.: Sedimentology, v. 34, p. 861-883.

Derby, J.R., 1965, Paleontology and stratigraphy of the Nolichucky Formation in southwest Virginia and northeast Tennessee [Ph. D. dissertation]: Blacksburg, Virginia, Virginia Polytechnic Institute and State University, 468 p.

Droser, M.L, and Bottjer, D.J., 1986, A semiquantitative field classification of ichnofabric: Journal of Sedimentary Petrology, v. 56, p. 558-559.

Drummond, C.N., and Wilkinson, B.H., 1993, Carbonate cycle stacking patterns and hierarchies of orbitally forced eustatic sealevel change: Journal of Sedimentary Petrology, v. 63, p. 369-377.

Elrich, R.N., Barrett, S.F., and Ju, G.B., 1990, Seismic and geologic characteristics of drowning events on carbonate platforms: American Association of Petroleum Geologists Bulletin, v. 74, p. 1523-1537.

Embry, A.F., 1989, A tectonic origin for third-order depositional sequences in extensional basins - Implications for basin modeling: *in* Cross, T.A. (ed.) Quantitative dynamic stratigraphy, Prentice-Hall, New York, p. 491-502.

Enos, P., 1977, Holocene sediment accumulation sof the south Florida shelf margin: *in* Enos, P., and Perkins, R.D., eds., Quaternary sedimentation in south Florida:

Geological Society of America Memoir 147, p. 1-130.

Enos, P., 1983, Shelf environment: *in* Scholle, P.A., Bebout, D., and Moore, C.H., eds., Carbonate depositional environments, American Association of Petroleum Geologists Memoir v. 33, p. 268-295.

Enos, P., 1989, Islands in the bay - A key habitat of Florida Bay: Bulletin of Marine Science, v. 44, p. 365-386.

Enos, P., 1991, Sedimentary parameters for computer modelling, *in* Franseen, E.K., Wateney, W.L., Kendall, C.G.St.C., and Ross, W., Sedimentary modeling: Computer simulations and methods for improved parameter definition: Kansas Geological Survey Bulletin 233, p. 63-99.

Enos, P., and Perkins, R.D., 1977, Quaternary sedimentation in south Florida: Geological Society of America Memoir 147, 198 p.

Enos, P., and Perkins, R.N., 1979, Evolution of Florida Bay from island stratigraphy: Geological Society of America Bulletin, v. 90, p. 59-83.

Erwin, P.E., Jr., 1981, Stratigraphy, depositional environments, and dolomitization of the Maryville and Upper Honaker Formations, Tennessee and Virginia: [unpub. M.A. thesis] Duke University, 234 p.

Esteban, M., and Klappa, C., 1983, Subaerial exposure surfaces: *in* Scholle, P.A., Bebout, D., and Moore, C., eds., Carbonate depositional environments, American Association of Petroleum Geologists Memoir v. 33, p. 1-54.

Evans, G., Murray, J.W., Biggs, H.E.J., Bate, R., and Bush, P.R., 1973, Oceanography, eustasy, sedimentology, and geomorphology of parts of the Trucial Coast barrier island complex, Persian Gulf: *in* Purser, B.H., ed., The Persian Gulf - Holocene carbonate sedimentation in a shallow epicontinental sea: Heidelberg, Berlin, Springer-Verlag, p. 233-277.

Fischer, A.G., 1964, The Lofer cyclothems of the Alpine Triassic: Geological Survey of

Kansas Bulletin, v. 169, p. 107-149.

Fischer, A.G., and Bottjer, D.J., (eds.), 1991, Orbital forcing and sedimentary sequences: Journal of Sedimentary Petrology, v. 61, p. 1063-1252.

Fichter, L.S., and Deicchio, R.J., 1986, Stratigraphic model for timing the opening of the Proto-Atlantic Ocean in northern Virginia: Geology, v. 14, p. 307-309.

Fluegel, E., 1982, Microfacies analysis of Limestones: Springer-Verlag, New York, 633 p.

Ginsburg, R.N., 1957, Early diagenesis and lithification of shallow-water carbonate sediments in South Florida: Society of Economic Paleontologists and Mineralogists Special Publication 5, p. 80-100

Ginsburg, R.N., 1971, Landward movement of carbonate mud: new model for regressive cycles in carbonates (abstract): American Association of Petroleum Geologists Bulletin, v. 55, p. 340.

Ginsburg, R.N., 1975, ed., Tidal deposits: A casebook of recent examples and fossil counterparts: Springer-Verlag, New York, 428 p.

Ginsburg, R.N., and Hardie, L.A., 1975, Tidal and storm deposits, northwestern Andros Island, Bahamas: *in* Ginsburg, R.N., 1975, editor, Tidal deposits: A casebook of recent examples and fossil counterparts: Springer- Verlag, New York, p. 201-208.

Goldhammer, R.K., Dunn, P.A., and Hardie, L.A., 1986, High frequency glacio-eustatic sea-level oscillations with Milankovitch characteristics recorded in Middle Triassic platform carbonates, northern Italy: American Journal of Science, v. 278, p. 853-892.

Goldhammer, R.K., Dunn, P.A., and Hardie, L.A., 1990, Depositional cycles, composite sea level changes, cycle stacking patterns, and the heirarchy of stratigraphic forcing: examples from the platform carbonates of the Alpine Triassic: Geological Society of America Bulletin, v. 102, p. 535-562.

Goodwin, E.J., and Anderson, P.W., 1990, Characteristics of a field data base for

developing and evaluating quantitative stratigraphic models: *in* Cross, T.A. (ed.) Quantitative dynamic stratigraphy, New York, Prentice-Hall, p. 479-490.

Grotzinger, J.P., 1986, Cyclicity and paleoenvironmental dynamics, Rocknest platform, northwest Canada: Geological Society of America Bulletin, v. 97, p. 1208-1231.

Grover, G., Jr., and Read, J.F., 1978, Fenestral and associated vadose diagenetic fabrics of tidal flat carbonates, Middle Ordovician New Market Limestone, southwestern Virgina: Journal of Sedimentary Petrology, v. 48, p. 453-473.

Hall, G.M., and Amick, H.C., 1934, The section of the west side of Clinch Mountain, Tennessee: Journal of the Tennessee Academy of Science, v. 9, p. 157-220.

Haq, B.U., Hardenbol, J., and Vail, P.R., 1988, Mesozoic and Cenozoic chronostratigraphy and cycles of sea-level change: *in* C.K. Wilgus, Hastings, B.S., Kendall, C.G. St. C., Posamentier, H.W., Ross, C.A., and Van Wagoner, J.C. (eds.) Sea-level changes: An integrated approach: Society of Economic Paleontologists and Mineralogists, Special Publication 42, p. 71-108.

Hardie, L.A., 1986, Ancient carbonate tidal flat deposits: Colorado School of Mines Quarterly, v. 80, p. 37-57.

Hardie, L.A., 1989a, Cyclic platform carbonates in the Cambro-Ordovician of the central Appalachians: *in* Walker, K.R., Read, J.F., and Hardie, L.A., eds., Cambro-Ordovician carbonate banks and siliciclastic basins of the United States Appalachians: American Geophysical Union Field Trip Guidebook T161, p. 51-81.

Hardie, L.A., 1989b, Perspectives: Dolomitization: A critical review of some current views: Journal of Sedimentary Petrology, v. 57, p. 166-183.

Hardie, L.A, and Shinn, E.A., 1986, Carbonate depositional environments, modern and ancient, 3, Tidal Flats: Colorado School of Mines Quarterly, v. 81, 74 p.

Hardie, L.A, Dunn, P.A., and Goldhammer, R.K., 1991, Field and modelling studies of Cambrian carbonate cycles, Virginia Appalachians - Discussion: Journal of

Sedimentary Petrology, v. 61, p. 636-646.

Hardie, L.A., Bosseli, A., and Goldhammer, R.K., 1986, Repeated subaerial exposure of subtidal carbonate platforms: Evidence for high frequency sea-level oscillations on a 10^4 year scale: Paleoceanography, v. 1, p. 447-457.

Harris, L.D., 1964, Facies relations of the exposed Rome Formation and Conasauga Group of northeastern Tennessee with equivalent rocks in the subsurface of Kentucky and Virginia: U.S. Geological Survey Professional Paper 501-B, p. B25-B29.

Harris, P.M., 1979, Facies anatomy and diagensis of a Bahamian ooid shoal: Miami, Florida, University of Miami, Sedimenta VII, Comparative Sedimentology Lab, 163 p.

Hasson, K.O., and Haase, C.S., 1988, Lithofacies and paleogeography of the Conasauga Group (Middle and Upper Cambrian) in the Valley and Ridge province of east Tennessee: Geological Society of America Bulletin, v. 100, p. 234-246.

Hatcher, R.D., Jr., 1965, Structure of the northern portion of the Dumplin Valley fault zone in east Tennessee [Ph.D. dissertation]: Knoxville, University of Tennessee, 168 p.

Hatcher, R.D., Jr., 1989, Tectonic synthesis of the U.S. Appalachians, *in* Hatcher, R.D, Jr., Thomas, W.A., and Viele, G.W., (eds.) The Appalachian-Ouachita orogen in the United States: Geological Society of America, The Geology of North America, v. F-2, p. 233-318.

Hatcher, R.D., Jr., and Bridge, J., 1973, Geologic map of the Jefferson City quadrangle, Tennessee: State of Tennessee, Division of Geology Quadrangle Map, scale = 1:24000.

Hayes, C.N., 1891, The overthrust faults of the southern Appalachians: Geological Society of America Bulletin, v. 2., p. 141-154.

Hays, J.D., Imbrie, J., and Shackleton, N.J., 1976, Variation in the earth's orbit: Pacemaker of the ice ages: Science, v. 194, p. 1121-1132.

Heller, P.L., Wentworth, C.M., and Poag, C.W., 1982, Episodic post-rift subsidence of the United States Atlantic continental margin: Geological Society of America Bulletin: v. 93, p. 379-390.

Hildebrand, T.G., 1985, Rift structure of the northern Mississippi Embayment from the analysis of gravity and magnetic data: Journal of Geophysical Research, v. 90, p. 12607-12622.

Hine, A.C., 1977, Lily Bank, Bahamas: History of an active oolite sand shoal: Journal of Sedimentary Petrology, v. 47, p. 1554-1581.

Hinze, L.F., and Robison, R.A., 1975, Middle Cambrian stratigraphy of the House, Wah-Wah, and adjacent ranges in western Utah: Geological Society of America Bulletin, v. 86, p. 881-891.

Hubbard, R.J., 1988, Age and Significance of sequence boundaries on Jurassic and Early Cretaceous rifted continental margins: American Association of Petroleum Geologists Bulletin, v. 72, p.49-72.

Jacobs, D.K., and Sahagian, D.L., 1993, Climate-induced fluctuations in sea level during non-glacial times: Nature, v. 361, p. 710-712.

James, N.P., Stevens, R.K., Barnes, C.R., and Knight, I., 1989, Evolution of a lower Paleozoic continental margin carbonate platform, northern Canadian Appalachians, *in* Crevello, P., Wilson, J.L., Sarg, J.F., and Read J.F., eds., Controls on carbonate platform and basin development: Society of Economic Paleontologists and Mineralogists Special Publication No. 44, p. 122-146.

James, N.P., 1984, Shallowing-upwards sequences in carbonates, in Walker, R.G., ed., Facies models: Geoscience Canada, Reprint Series 1, p. 213-228.

Johnson, P.R., Zeitz, I., and Thomas, W.A., 1992, Grabens in N. Mississippi, N.W.

Alabama, and S.W. Tennessee: Geological Society of America Abstracts with Programs, Southeastern Section, v. 24, p.23.

Keen, C.E., Stockmal, G.S., Welsink, H., Quinlan, G., and Mudford, B., 1987, Deep crustal structure and evolution of the rifted margin northeast of Newfoundland: results from LITHOPROBE East: Canadian Journal of Earth Sciences, v. 24, p. 1537-1549.

Keith, A., 1895, Description of the Knoxville sheet (Tennessee, North Carolina): U.S. Geological Survey Atlas, Folio 16.

Kendall, C.G.St.C., and Skipworth, P.A.D'E., 1969, Holocene shallow water carbonate and evaporite sediments of Khor al Bazam, Abu Dhabi, southwest Persian Gulf: American Association of Petroleum Geologists Bulletin, v. 53, p. 841-869.

Kendall, C.G.St.C., Moore, P., Whittle, G., and Cannon, R., 1992, A challenge: Is it possible to determine eustasy and does it matter?: *in* Dott, R.H., ed., Eustasy: The historical ups and downs of a major geological concept: Boulder, CO, Geological Society of America Memior 180, p. 93-107

King, P.B., 1964, Geology of the central Great Smoky Mountains, Tennessee: U.S. Geological Survey Professional Paper 349-C, 148 p.

King, P.B., 1970, The Precambrian of the United States - Southeastern United States: *in* Rankama, K. (ed.) The geologic systems: The Precambrian, Volume 4: New York, Interscience, p. 1-71.

Koerschner, W.F., and Read, J.F., 1989, Field and modelling studies of Cambrian carbonate cycles, Virginia Appalachians: Journal of Sedimentary Petrology, v. 59, p. 654-687.

Kozar, M.G., 1986, The stratigraphy, petrology, and depositional environments of the Maryville Limestone (Middle Cambrian) in the vicinity of Powell and Oak Ridge, Tennessee: [unpublished M.S. thesis] University of Tennessee, Knoxville, 242 p.

Kozar, M.G., Weber, L.J., and Walker, K.R., 1990, Field and modeling studies of Cambrian carbonate cycles, Virginia Appalachians - Discussion: Journal of Sedimentary Petrology, v. 60, p. 790-794.

Kreisa, R.D., 1981, Storm-generated sedimentary structures in subtidal marine facies with examples from the Middle and Upper Ordovician of southwestern Virgina: Journal of Sedimentary Petrology, v. 51, p. 235-249.

Laporte, L.F., 1971, Paleozoic carbonate facies of the central Appalachian shelf: Journal of Sedimentary Petrology, v. 41, p. 724-740.

Levy, M., and Christie-Blick, N., 1991, Tectonic subsidence of the early Paleozoic passive continental margin in eastern California and southern Nevada: Geological Society of America Bulletin, v. 103, p. 1590-1606.

Lister, G.S., Etheridge, M.A., and Symonds, P.A., 1991, Detatchment models for the formation of passive margins: Tectonics, v. 10, p. 1038-1064.

Lohmann, K.C., and Walker, J.G.C., 1989, The $\delta^{18}O$ record of Phanerozoic abiotic marine calcite cements: Geophysical Research Letters, v. 16, p. 319-322.

Logan, B.W., 1961, Cryptozoon and associate stromatolites from the Recent, Shark Bay, Western Australia: Journal of Geology, v. 69, p. 517-532.

Logan, B.W., 1974, Inventory of diagenesis in Holocene-Recent carbonate sediments, Shark Bay, Western Australia: *in* Logan, B.W., and others, eds., Evolution and diagenesis of Quaternary carbonate sequences, Shark Bay, Western Australia: American Association of Petroleum Geologists Memoir 22, p. 195-249.

Logan, B.W., Hoffman, P., and Gebelein, C.D., 1974, Algal mats, cryptalgal fabrics, and structures, Hamelin Pool, Western Australia: *in* Logan, B.W., and others, eds., Evolution and diagenesis of Quaternary carbonate sequences, Shark Bay, Western Australia: American Association of Petroleum Geologists Memoir 22, p. 140-194.

Loreau, J.P., and Purser, B.H., 1973, Distribution and ultrastructure of Holocene ooids in

the Persian Gulf: *in* Purser, B.H., ed., The Persian Gulf - Holocene carbonate sedimentation in a shallow epicontinental sea: Heidelberg, Berlin, Springer-Verlag, p. 279-328.

Ludvigson, R., and Westrop, S.R., 1985, Three new Upper Cambrian stages for North America: Geology, v. 13, p. 139-143.

Manspeiser, W., 1989, Triassic-Jurassic rifting and opening of the Atlantic: An overview: *in* Manspeiser, W. (ed.) Triassic-Jurassic Rifting: Continental breakup and the origin of the Atlantic Ocean and passive margins, Part A: Elsevier, Developments in Geotectonics 22, p. 41-80.

Markello, J.R., and Read, J.F., 1981, Carbonate ramp-to-deeper shale shelf transitions of an Upper Cambrian intrashelf basin, Nolichucky Formation, southwest Virginia Appalachians: Sedimentology, v. 28, p. 573-597.

Markello, J.R., and Read, J.F., 1982, Upper Cambrian intrashelf basin, Nolichucky Formation, southwest Virginia Appalachians: American Association of Petroleum Geologists Bulletin, v. 66, p. 860-878.

Matti, J.C., and McKee, E.D., 1976, Stable eustasy, regional subsidence, and a carbonate factory: self-generating model for onlap-offlap cycles in shallow water carbonate sequences: Geological Society of America Abstracts with Programs, v. 8, p. 1000-1001.

Mazzullo, S.J., 1992, Geochemical and neomorphic alteration of dolomite: A review: Carbonates and Evaporites, v. 7, p. 21-37.

McKee, E.D., and Weir, J.W., 1953, Terminology for stratification and cross-stratification: Geological Society of America Bulletin, v. 64, p. 381-390.

McKenzie, D.P., 1978, Some remarks on the generation of sedimentary basins: Earth and Planetary Science Letters, v. 40, p. 25-32.

McReynolds, J.A., 1988, Paleoenvironments and facies relations of the Lower Cambrian

Rome Formation on the U.S. Department of Energy Reservation, Oak Ridge Area in Roane and Anderson Co., Tennessee: [unpublished M.S. thesis], Knoxville, University of Tennessee, 121 p.

McReynolds, J.A., and Driese, S.G., in press, Paleoenvironments and facies relations of the Rome Formation (Lower Cambrian) along Haw Ridge, Roane and Anderson Counties, Tennessee: Southeastern Geology.

Mitchum, R.M., Jr., and Van Wagoner, J.C., 1991, High frequency sequences and their stacking patterns: sequence stratigraphic evidence of high-frequency cycles: Sedimentary Geology, v. 70, p. 131-160.

Moore, R.C., 1949, Meaning of facies: *in* Sedimentary facies and geologic history: Geological Society of America Memoir 39, p. 1-34.

Mount, J.F., and Rowland, S.A., 1981, Grand cycle A (Lower Cambrian) of the southern Great Basin: A product of differential rates of relative sea level rise, *in* Taylor, M.E., ed., Short papers for the 2nd International Symposium on the Cambrian System: United States Geological Survey Open-File Report 81-743, p. 143-146.

Nelson, K.D., and Zhang, J., 1991, A COCORP deep reflection profile across the buried Reelfoot rift, south-central United States: Tectonophysics, v. 197, p. 271-293.

Neton, M.J., 1992, Late Proterozoic rifting of Laurentia: Source and deposition of conglomerate units of the Grandfather Mountain Formation, North Carolina Blue Ridge: [unpublished M.S. thesis], Knoxville, University of Tennessee, 180 p.

Odom, A.L., and Fullagar, P.D., 1984, Rb-Sr whole-rock and inherited zircon ages of the plutonic suite of the Crossnore Complex, southern Appalachians, and their implications regarding the time of the opening of the Iapetus Ocean: *in* Bartholomew, M.J., ed., The Grenville Event in the Appalachians and related topics: Geological Society of America Special Paper 194, 255-261.

Osleger, D.A., 1991, Subtidal carbonate cycles: Implications for allocyclic and autoclic

controls: Geology, v. 19, p. 917-920.

Osleger, D., and Read, J.F., 1991, Relation of eustasy to stacking patterns of meter-scale carbonate cycles, Late Cambrian, U.S.A.: Journal of Sedimentary Petrology, v. 61, p. 1225-1252.

Osleger, D., and Read, J.F., 1993, Comparative analysis of methods used to define eustatic variations in outcrop: Late Cambrian interbasinal sequence development: American Journal of Science, v. 293, p. 157-216.

Palmer, A.R., 1954, The faunas of the Riley Formation in central Texas: Journal of Paleontology, v. 28, p. 709-786.

Palmer, A.R., 1971, The Cambrian of the Appalachian and eastern New England regions, eastern United States, *in* Holland, C.H., ed., Cambrian of the New World: London, Wiley-Interscience, p. 289-332.

Palmer, A.R., 1981, On the correlatability of Grand Cycle tops, *in* Taylor, M.E., ed., Short papers for the 2nd International Symposium on the Cambrian System: United States Geological Survey Open-File Report 81-743, p. 156-159.

Palmer, A.R., and Halley, R.B., 1979, Physical stratigraphy and trilobite biostratigraphy of the Carrara formation (Lower and Middle Cambrian) in the southern Great Basin: United States Geological Survey Professional Paper 1047, 131 p.

Pratt, B.R., and James, N.P., 1986, The St. George Group (Lower Ordovician) of western Newfoundland: Tidal flat island model for carbonate sedimentation in shallow eperic seas: Sedimentology, v. 33, p. 313-343.

Purdy, E.J., 1963, Recent calcium carbonate facies of the Great Bahama Bank. 2. Sedimentary facies: Journal of Geology, v. 71, p. 472-497.

Purser, B.H., and Evans, G., 1973, Regional sedimentation along the Trucial Coast, southeast Persian Gulf, *in* Purser, B.H., ed., The Persian Gulf - Holocene carbonate sedimentation in a shallow epicontinental sea: Heidelberg, Berlin, Springer-Verlag,

p. 179-191.

Rankey, E.C., Srinivasan, K., and Walker, K.R., 1992, Coincident exposure/drowning surfaces within Middle Cambrian Grand Cycles, east Tennessee: A model for abrupt limestone/shale transitions/sequence boundaries: Geological Society of America Abstracts with Programs, v.24, p. 318.

Rankin, D.W., 1970, Stratigraphy and structure of Precambrian rocks in northwestern North Carolina, *in* Fisher, G.W., Pettijohn, F.J., Reed, J.C., Jr., and Weaver, K.N., Studies in Appalachian geology: Central and southern: New York, Interscience, p. 227-245.

Rankin, D.W., 1975, The continental margin of eastern North America in the southern Appalachians: The opening and closing of the proto-Atlantic Ocean: American Journal of Science, v. 275-A, p. 298-336.

Rankin, D.W., Drake, A.A., Jr., Glover, L., III, Goldsmith, R., Hall, L.M., Murray, D.P., Ratcliffe, N.M., Read, J.F, Secor, D.T., Jr., and Stanley, R.S., 1989, Pre-orogenic terranes, *in* Hatcher, R.D, Jr., Thomas, W.A., and Viele, G.W., (eds.) The Appalachian-Ouachita orogen in the United States: Geological Society of America, The Geology of North America, Volume F-2, p. 7-100

Rast, N., and Kohles, K.M., 1986, The origin of the Ocoee Supergroup: American Journal of Science, v. 286, p. 593-616.

Rasetti, F., 1965, Upper Cambrian trilobite faunas of northeastern Tennessee: Smithsonian Miscellaneous Collections 148 (3), 127 p.

Read, J.F., 1974, Calcrete deposits and Quaternary sediments, Edel Province, Shark Bay, Western Australia: *in* Logan, B.W., and others, eds., Evolution and diagenesis of Quaternary carbonate sequences, Shark Bay, Western Australia: American Association of Petroleum Geologists Memoir 22, p. 250-282.

Read, J.F., 1989, Controls on evolution of Cambrian-Ordovician passive margin, U.S.

Appalachians, *in* Crevello, P., Wilson, J.L., Sarg, J.F., and Read J.F., eds., Controls on carbonate platform and basin development: Society of Economic Paleontologists and Mineralogists Special Publication No. 44, p. 147-166.

Read, J.F., Osleger, D., and Elrick, M., 1991, Two-dimensional modelling of carbonate ramp sequences and component cycles: in Franseen, E.K., Watney, W.L., Kendall, C. G. St. C., and Ross, W., eds., Sedimentary modelling: Computer simulations and methods for improved parameter definition: Kansas Geological Survey Bulletin, v. 233, p. 473-488.

Read, J.F., Grotzinger, J.P., Bova, J.A., and Koerschner, W.F., 1986, Models for generation of carbonate cycles: Geology, v. 14, p. 107-110.

Resser, C.E., 1938, Cambrian system (resticted) of the southern Appalachians: Geological Society of America Special Paper 15, 140 p.

Reynolds, D.J., Steckler, M.S., and Coakley, B.J., 1991, The role of sediment load in sequence stratigraphy: The influence of flexural isostasy and compaction: Journal of Geophysical Research, v. 96, p. 6931-6949.

Robison, R.A., 1976, Middle Cambrian trilobite biostratigraphy of the Great Basin: Bringham Young University Geology Studies, v. 23, p. 93-109.

Robison, R.A., 1984, Cambrian Agnostida of North America and Greenland: Part I, Ptychagnostidae: University of Kansas Paleontological Institute, Paper 109, 59 p.

Rodgers, J., 1953, Geologic map of east Tennessee with explanatory text: Tennessee Division of Geology Bulletin 58, 168 p.

Rodgers, J., and Kent, D.F., 1948, Stratigraphic section at Lee Valley, Hawkins County, Tennessee: Tennessee Division of Geology Bulletin 55, 47 p.

Safford, J.M., 1856, A geological reconnaicance of the State of Tennessee: Nashville, State of Tennessee, 164 p.

Safford, J.M., 1869, Geology of Tennessee: Nashville, State of Tennessee, 550 p.

Sarg, J.F., 1988, Carbonate sequence stratigraphy, *in* C.K. Wilgus, Hastings, B.S., Kendall, C.G. St. C., Posamentier, H.W., Ross, C.A., and Van Wagoner, J.C. (eds.) Sea-Level Changes: An Intergrated Approach, Society of Economic Paleontologists and Mineralogists, Special Publication 42, p. 155-181.

Sawyer, D.S., Toksoz, M.N., Sclater, J.G., and Swift, B.A., 1983, Thermal evolution of the Baltimore Canyon trough and Georges Bank basin: American Association of Petroleum Geologists Memoir 29, p. 742-761.

Schlager, W. 1981, The paradox of drowned reefs and carbonate platforms: Geological Society of America Bulletin, v. 92, p. 197-211.

Schlager, W., 1991, Depositional bias and environmental change - important factors in sequence stratigraphy: Sedimentary Geology, v. 70, p. 109-130.

Schlager, W., 1992, Sedimentology and sequence stratigraphy of reefs and carbonate platforms: American Association of Petroleum Geologists, Continuing Education Course Note Series no. 34, 71 p.

Schwab, F.L., 1976, Depositional Environments, provenence, and tectonic framework: Upper part of the late Precambrian Mount Rogers Formation, Blue Ridge Province, southwestern Virginia: Journal of Sedimentary Petrology, v. 46, p. 3-13.

Selg, M., 1988, Origin of peritidal carbonate cycles: Early Cambrian, Sardinia: Sedimentary Geology, v. 59, p. 115-124.

Shinn, E.A., 1968, Selective dolomitization of Recent sedimentary structures: Journal of Sedimentary Petrology, v. 44, p. 904-916.

Shinn, E.A., 1973, Carbonate coastal accretion in an area of longshore transport, northeast Quatar, Persian Gulf, *in* Purser, B.H., ed., The Persian Gulf - Holocene carbonate sedimentation in a shallow epicontinental sea: Heidelberg, Berlin, Springer-Verlag, p. 179-192

Shinn, E.A., 1983, Recognition and economic significance of ancient carbonate tidal flats -

a comparison of modern and ancient examples: *in* Scholle, P.A., Bebout, D., and Moore, C., ed., Recognition of depositional environments of carbonate rocks: American Association of Petroleum Geologists Memoir 33, p. 172-210.

Shinn, E.A., 1986, Modern carbonate tidal flats: their diagnostic features: Colorado School of Mines Quarterly, v. 80, p. 7-35.

Shinn, E.A., Lloyd, R.M., and Ginsburg, R.N., 1969, Anatomy of a modern carbonate tidal flat, Andros Island, Bahamas: Journal of Sedimentary Petrology, v. 39, p. 1202-1228.

Shrake, D.L., Calrlton, R.W., Wickstrom, L.H., Potter, P.E., Richard, B.H., Wolfe, P.J., and Sitler, G.W., 1991, Pre-Mount Simon basin under the Cincinnati arch: Geology, v. 19, p. 139-142.

Simmons, W.A., 1984, Stratigraphy and depositional environments of the Middle Cambrian Maryville Limestone (Conasauga Group) near Thorn Hill, Tennessee: unpublished M.S. thesis, University of Tennessee, Knoxville, 275 p.

Simpson, E.L., and Erikkson, K.A., 1989, Sedimentology of the Unicoi Formation in southern and central Virginia: Evidence for late Proterozoic to Early Cambrian rift-to-passive margin transition: Geological Society of America Bulletin, v. 101, p. 42-54.

Sloss, L.L., 1963, Sequences in the cratonic interior of North America: Geological Society of America Bulletin, v. 74, p. 94-114.

Srinivasan, K., 1993, Depositional history, sequence stratigraphy, and diagenesis of the Maryville Limestone (Middle Cambrian), southern Appalachians: [Ph. D. dissertation] Knoxville, University of Tennessee, 139 p.

Srinivasan, K., and Walker, K.R., 1993, Sequence stratigraphy of carbonate ramp to rimmed-platform evolution: the Maryville Limestone (Middle Cambrian), southern Appalachians: Geological Society of America Bulletin, v. 105, in press.

Srinivasan, K., and Walker, K.R., in press, Petrographic and geochemical constraints for fluid source and possible pathways during burial diagenesis of Maryville Limestone (Middle Cambrian), southern Appalachians, USA: Sedimentology.

Srinivasan, K., Walker, K.R., and Foreman, J.L., 1991, Cambrian flooding event: implications for Middle and Upper Cambrian sequence stratigraphy, southern Appalachians: SEPM Midyear Meeting, Portland, OR, Abstracts, p. 34.

Steckler, M.S., 1989, The role of thermal-mechanical structure of the lithosphere in the formation of sedimentary basins, *in* Cross, T.A. (ed.) Quantitative dynamic stratigraphy, Prentice-Hall, New York, p. 89-112.

Steckler, M.S., Watts, A.B., and Thorne, J.A., 1988, Subsidence and basin modeling of the U.S. Atlantic passive margin, *in* Sheridan, R.E., and Grow, J.A., eds., The Atlantic Continental Margin, U.S.: Geological Society of America, The Geology of North America, v. I-2, p. 399-416.

Steinhauff, D.M., 1989, Marine cements: *in* Walker, K.R.,ed., The Fabric of Cements in Paleozoic Limestones: University of Tennessee Studies in Geology 20, p. 37-53.

Steinhauff, D.M., and Walker, K.R., in press, Sequence stratigraphy of and apparently non-cyclic carbonate succession: Recognizing subaerial exposure in largely subtidal stratigraphic sequences, Middle Ordovician, east Tennessee, *in* Witzke, B.J., and Ludvigson, G., eds., Paleozoic Sequence Stratigraphy, Geological Society of America Special Paper.

Stephenson, R., 1989, Beyond first order thermal subsidence models for sedimentary basins?: *in* Cross, T.A. (ed.) Quantitative dynamic stratigraphy, Prentice-Hall, New York, p. 113-125.

Strasser, A., and Davlaud, E., 1986, Formation of Holocene limestone sequences by progradation, cementation, and erosion: Two examples from the Bahamas: Journal of Sedimentary Petrology, v. 56, p. 422-428.

Taylor, S.R., 1989, Geophysical framework of the Appalachians and adjacent Grenville province: *in* Pakiser, L.C., and Mooney, W.D., Geolphysical Framework of the Continental United States: Geological Society of America Memoir 172, p. 317-348.

Thomas, W.A., 1991, The Appalachian-Ouachita rifted margin of southeastern North America: Geological Society of America Bulletin, v. 103, p. 415-431.

Underhill, J.R., 1991, Controls on Late Jurassic seismic sequences, Inner Moray Firth, UK North Sea: a critical test of a key segment of Exxon's original global cycle chart: Basin Research, v. 3, p. 79-98.

Vail, P.R., 1988, Seismic stratigraphy interpretation using sequence stratigraphy, Part 1: Seismic stratigraphy interpretation procedure: *in* Bally, A.W., ed., Atlas of seismic stratigraphy: Techniques papers and method oriented papers: American Association of Petroleum Geologists Studies in Geology, no. 27, v. 1, p. 1-10.

Vail, P.R., Hardenbol, J., and Todd, R.G., 1984, Jurassic unconformities, chronostratigraphy, and sea-level changes from seismic stratigraphy and biostratigraphy: *in* Schlee, J.S., ed., Interregional Unconformities and Hydrocarbon Accumulation: American Association of Petroleum Geologists Memoir 36, p. 129-144.

Vail, P.R., Mitchum, R.M., Jr., and Thompson, S. III, 1977, Seismic stratigraphy and global changes of sea level, Part 4: Global cycles of relative changes of sea level: in Payton, C.E., (ed.) Seismic stratigraphy -- Application to hydrocarbon exploration: American Association of Petroleum Geologists Memoir 26, p. 83-98.

VanArsdall, D.E., 1974, Lithostratigraphy of the Conasauga Group within the Hunter Valley and Copper Creek strike belts, northeastern Tennessee: [unpublished M.S. thesis], Richmond, Kentucky, Eastern Kentucky University, 83 p.

Van Wagoner, J.C., Posamentier, H.W., Mitchum, R.M., Vail, P.R., Sarg, J.F., Loutit, T.S., and Hardenbol, J., 1988, An overview of the fundamentals of sequence

stratigraphy and key definitions: *in* C.K. Wilgus, Hastings, B.S., Kendall, C.G. St. C., Posamentier, H.W., Ross, C.A., and Van Wagoner, J.C. (eds.) Sea-level changes: An integrated approach, Society of Economic Paleontologists and Mineralogists, Special Publication 42, p. 39-45.

Wagoner, C.W., and van der Togt, C., 1973, Holocene sediment types and their distribution in the southern Persian Gulf: *in* Purser, B.H., ed., The Persian Gulf - Holocene carbonate sedimentation in a shallow epicontinental sea: Heidelberg, Berlin, Springer-Verlag, p. 123-156.

Walker, J.D., 1990, The sedimentology and stratigraphy of the Chilhowee Group (Uppermost Proterozoic to Lower Cambrian) of eastern Tennessee and western North Carolina: The evolution of the Laurentian Iapetus margin: [unpublished Ph.D. dissertation], Knoxville, University of Tennessee, 274 p.

Walker, D., and Driese, S.G., 1991, Constraints on the position and timing of the Precambrian-Cambrian boundary in the southern Appalachians: American Journal of Science, v. 291, p. 258-283.

Walker, K.R., Shanmugam, G., and Ruppel, S.C., 1983, A model for carbonate to terrigenous clastic sequences: Geological Scoeity of America Bulletin, v. 94, p. 689-699.

Walker, K.R., Foreman, J.L., and Srinivasan, K., 1990a, The Cambrian Conasauga Group of eastern Tennessee: A preliminary general stratigraphic model with a more detailed test for the Nolichucky Formation: Appalachian Basin Industrial Associates, v. 17, p. 184-189.

Walker, K.R., Jernigan, D.G., and Weber, L.J., 1990b, Petrographic criteria for the recognition of marine, syntaxial overgrowths and their distribution in geologic time: Carbonates and Evaporites, v. 5, p. 141-152.

Walker, K.R., Steinhauff, D.M., and Roberson, K.E., 1992, Uppermost Knox Group, the

Knox unconformity, the Middle Ordovician transition from shallow shelf to deeper basin near Dandridge, Tennessee, and a possible source for mineralizing fluids: *in* Misra, K.C., Fulweiler, R.E., and Walker, K.R., eds., Zinc Deposits in east Tennessee: Society of Economic Geologists Guidebook Series no. 14, p. 66-76.

Watkins, J.S., Montadert, L., and Dickerson, P.W., 1979, Geological and Geophysical Investigations of Continental Margins: American Association of Petroleum Geologists Memoir 29, 709 p.

Watkins, J.S., and Drake, C.L., 1984, Studies in Continental Margin Geology: American Association of Petroleum Geologists Memoir 34, 541 p..

Webb, E.J., 1980, Cambrian sedimentation and structural evolution of the Rome trough in Kentucky [unpub. Ph.D. thesis]: Cincinnati, Ohio, University of Cincinnati, 98 p.

Wentworth, C.K., 1922, A scale of grade and class terms for clastic sediments: Journal of Geology, v. 30, p. 377-392.

Woodward, H.P., 1949, Cambrian system of West Virginia: West Virginia Geological Survey Bulletin, v. 20.

Wright, V.P., 1992, Speculations on the controls of cyclic peritidal carbonates: Ice-house versus greenhouse eustatic controls: Sedimentary Geology, v. 76, p. 1-5.

Zoback, M.L., and Zoback, M.D., 1989, Tectonic stress field of the continental United States: *in* Pakiser, L.C., and Mooney, W.D., eds., Geophysical framework of the continental United States: Boulder, CO, Geological Society of America Memoir 172, p. 523-543.

APPENDICES

Appendix A

Descriptions of measured sections

Descriptions are listed from the base to top of the measured section. The sample numbers represent the stratigraphic distance between the sampling interval and the base of the measured section; note that this position is *not always* the stratigraphic position above the base of the formation. Prefixes reflect from which section the sample comes:

<number> = DSR, on ramp
o <number> = DSR, off ramp
Hy <number> = IS section
B <number> = SR section
SQ <number> = Sevierville Quarry section

MEASUREMENT CONVENTIONS

Bed thicknesses used in the descriptions of measured section follow those used by McKee and Weir (1953), with the exception that I used "massive" for beds > 1 m thick. Grain size descriptions are based on the standardized terminology of Wentworth (1922).

Bed Thickness

Massive bedded	>1.0 m
Thick bedded	0.3-1.0 m
Medium bedded	0.1-0.3 m
Thin bedded	0.03-0.1 m
Very thin bedded	0.01-0.03 m
Laminated	0.003-0.01 m
Thinly laminated	< 0.003 m

Grain size

Coarse-grained ... grains visible with unaided eye and readily identifiable (> 1.0 mm)
Medium-grained .. grains visible only with hand lens (appx. 0.25-1.0 mm)
Fine-grained ..... grains visible only with difficulty with hand lens (appx. 0.1-0.25mm)
Very fine grained .. grains not distinguishable even with hand lens (appx. < 0.25 mm)

Base of units

I noted the base of units as:
gradational ... transitional across > 0.1 m
abrupt ..... distinct change in lithologies where a distinct line could be drawn at the contact; contacts (generally) linear on outcrop face
irregular ..... abrupt but non-linear contact; contact has amplitude < 1/3 wavelength; that is, the contact appears as a gently undulating line.

scalloped ..... abrupt but non-linear contact; contact has amplitude > 1/3 wavelength; that is, the contact appears as a rapidly undulating line

Most of the units that I defined are not separated by distinct bedding planes. Rather, much of the Maryville is massively bedded, especially on the newer road cuts (DSR, IS). The units herein are defined on the basis of their lithology. A bedding plane may or may not correspond to a unit boundary. Thus, to call a unit "thinly bedded" technically is not correct, because bedding planes do not subdivide the unit.

The descriptions herein are primarily field descriptions, but have been supplemented with slab and petrographic descriptions where available.

Deep Springs Road and I-40, On-Ramp Section

Section exposed in roadcuts along the on-ramp, from Deep Springs Road to I-40 east. The lower 115 m of the Maryville is very well exposed by the roadcut, but the upper 100 m is very poorly exposed on the hillside.

bed number	cumulative thickness	description
		————Lower Rogersville Shale————
		(base covered, not measured)
		dark gray to black to dark green clay shale; thin? interbeds of carbonates.
		————Craig Limestone Member————
1	0.0-2.0	burrow-mottled mudstone; dark gray; burrows dolomitized, horizontal; lower 0.1 contains abundant intraclasts (intraclast wackestone); not well exposed; SAMPLES 0, 1.0
2	2.0-3.5	covered interval
3	3.5-6.5	burrow-mottled mudstone; dark gray; burrows dolomitized, horizontal; several thin (1-3 cm) layers of peloid packstone at 4.5, 5.2, 5.5, 6.4 m from base of Craig; no fossils except within peloid layers; SAMPLE 5.5.
4	6.5-6.75	peloid packstone/grainstone; dark gray; abrupt to stylolitized base; peloids generally fine-grained; no burrows; packstone layer from 6.7-6.72 (peloid packstone with some burrows); burrows dolomitized, horizontal; SAMPLES 6.5, 6.75.
5	6.75-7.0	peloid packstone/grainstone; dark gray; rare burrows, dolomitized, some horizontal, most common near 6.85 m; several discontinuous mudstone lenses; uppermost 5 cm laminated.
6	7.0-7.05	burrow-mottled mudstone; dark gray; common pyrite/marcasite; irregular burrow pattern, some dolomitized.
7	7.05-7.5	peloid packstone/grainstone; dark gray; peloids well sorted; burrows, more common upwards; several pockets of mudstone, some with very regular to irregular (scalloped) upper boundaries; SAMPLE 7.5.

8 7.5-20.5 burrow-mottled mudstone light to dark gray; burrows dolomitized, horizontal; several thin, peloid packstone layers/lenses (at 7.9, 8.2, 11.9, 14.8, 17.7) with possible cross-laminae; pyrite/marcasite; numerous vugs (burrows) filled with blocky calcite; SAMPLES 7.9, 8.0, 10.9, 12.8, 14.8, 17.0, 19.1 (from 20.1), 17.7 (part of peloid packstone lens).

9 20.5-20.9 mudstone to peloid packstone; medium gray; some ooids; appears to have been sheared slightly, upper part distorted; SAMPLES 20.5, 20.9.

10 20.9-21.4 mudstone, extensively sheared; shearing is confined to within this bed and upper part of bed below; light gray with bluish tint; weathers slightly lighter than surrounding units; pinches and swells laterally, appears to pinch out in upper part of outcrop; SAMPLES 21.1, 21.2, 21.3.

11 21.4-22.0 burrow-mottled mudstone; dark gray; burrows horizontal, dolomitized; weathers buff; layer laterally onlaps ooid/peloid packstone (layer 12); SAMPLE 21.5.

12 22.0-22.5 peloid/ooid packstone to grainstone; medium gray; grain size appears tp decrease upwards fromappx. 3 mm to < 1 mm; numerous micritic stringers, some up to 3 cm high, some with scalloped upper boundary; intraclasts?; SAMPLES 22.0 (from 11-12 boundary), 22.4.

13 22.5-22.6 burrow-mottled mudstone; dark gray; burrows dolomitized, horizontal; fossil fragments in lowermost 1 cm.

14 22.6-22.9 peloid packstone/grainstone; dark gray; fossil fragments; base abrupt; SAMPLE 22.8.

15 22.9-24.4 burrow-mottled mudstone; dark gray; burrows dolomitized, horizontal; numerous thin ooid/peloid/fossil packstone layers which are usually not alterally continuous; SAMPLES 23.8, 23.7, 24.4 (from upper contact).

16 24.4-24.6 ooid/peloid (oncoid?) wackestone to packstone; medium gray; peloids appear to be between <1 mm to 5 mm; appears to be some segregation between ooid-rich layers and peloid-rich layers; SAMPLE 24.6.

17 24.6-25.3 burrow-mottled mudstone; medium to dark gray; burrows dolomitized,

horizontal; stylolitized boundary with 18; SAMPLE 24.7.

18 25.3-25.5 oncoid?/ooid wackestone to packstone; dark gray; stylolites; trilobites and echinoderms; SAMPLE 25.4.

19 25.5-25.7 ooid packstone/grainstone; light to medium gray; several thin (<2 cm) micritic layers, some dolomitized; SAMPLE 25.7 (from 19-20 boundary).

20 25.7-25.8 burrow-mottled mudstone; medium gray; burrows dolomitzied, horizontal; transitional lower contact, abrupt, stylolitized upper contact; some rare ooids.

21 25.8-25.9 ooid packstone/grainstone grading laterally into peloid packstone and burrowed mudstone; medium gray; SAMPLE 25.8.

22 25.9-26.2 mudstone; dark gray; some thin ooid-rich layers; orangish/reddish rimmed voids, filled with turbid white sparry calcite, up to 3 cm diameter; at 26.05 an 26.2, irregular iron oxide layers (exposure surfaces?); SAMPLES 26.1, 26.2.

23 26.2-26.21 oncoid/ooid/peloid packstone/grainstone; persistant thickness across outcrop; abundant pyrite.

24 26.21-26.4 oncoid/peloid grainstone; in general, oncoids increase in size upwards, largest oncoids app. 1.5 cm diameter; trilobite, echinoderm fragments; pyrite; stylolites (hardgrounds?) cut oncoids; no imbrication; upper surface (contact w/ upper Rogesrville) forms an oncoid "pavement"; allochems coated with darkened mineralized? rim; above this oncoid-rich layer is thin (<1cm) shale and another thin (<1cm) carbonate-rich layer with more oncoids; SAMPLES 26.4, 26.4b.

--------Upper Rogersville Shale---------

25 26.4-27.0 clay shale; medium olive gray weathered, brown fresh; laminated; micritic carbonate nodules, some up to 0.1 m diameter, most elongate; SAMPLE 27 (nodule).

---------Maryville Limestone---------

26 27.0-27.05 fossil wackestone/packstone; medium gray; some intraclasts; hardgrounds common; lower contact irregular, some load casts; upper boundary very irregular; SAMPLE 27A.

27 27.05-27.2 nodular mudstone; medium gray; laminated; separated into layers by hardgrounds.

28 27.2-27.5 intraclast/fossil/ooid/peloid wackestone to packstone to grainstone; medium gray; red intraclasts (up to 4 cm, some laminated) floating in fossiliferous matrix with no distict preferred orientation; several distinct ooid and fossil layers; pyrite; thin shaley parting at 27.3; SAMPLES 27.3U and 27.3L.

29 27.5-29.9 peloid/ooid packstone to grainstone, grading up into peloid wackestone to ooid/fossil/peloid packstone/wackestone; medium gray; well-developed oncoids, up to appx. 1 cm diameter; abundant fossil fragments in lowermost 7 cm; few/no oncoids near the top of unit; lower boundary sharp; SAMPLES 27.7, 29.0, 29.4, 29.9.

30 29.9-51.7 burrow-mottled mudstone with thin wackestone/packstone layers-lenses; light to dark gray; lower contact gradational;
mudstone: mostly medium to dark gray; common stylolites; burrows dolomitized; locally faint laminae; ichnofacies index ii3-ii5 (Droser and Bottjer, 1986).
wackstone/packstone: light to dark gray; allochems include intraclasts (<0.5cm, often rounded), peloids, fossils, and ooids; lower contacts of most of these layers are abrupt to scalloped, upper contacts gradational to abrupt to stylolitized; pinch and swell (boudin-like morphology) noted as PS below, often discontinuous across outcrop; layers present from: 32.4-32.5 (PS), 32.6-32.7, 32.8-32.85, 33.8-33.85 (PS), 34.2-34.3 (PS), 34.9-34.95, 35.7-35.75, 36.4-36.45 (PS), 37.2-37.25, 38.3-38.4, 39.3-39.35 (PS), 39.9-40.0 (PS), 40.5-40.55, 40.9-41.0 (PS), 41.7-41.9, 42.5-42.55 (PS), 43,8-43.85 (PS), 44.3-44.35 (PS), 44.75-44.8 (PS), 44.9-45.0, 45.2-45.3, 45.7-45.85 (PS), 46.1-46.25, 46.4-46.5, 46.6-46.65, 47.6-47.7, 48.9-48.95 (PS), 49.1-49.25, 50.1-50.15, 51.0-51.05, 51.5-51.6 (PS); SAMPLES 31.1, 32.3, 32.4, 34.2, 37.2, 39.1, 39.15, 39.2, 42.5, 44.3 (note packstone and mudstone), 46.5, 48.9, 50.1, 50.4 (burrows).

31 51.7-52.5 peloid/ooid/fossil packstone; medium gray; base planar to scoured to stylolitized to burrowed?; intraclasts up to 8 cm X 1 cm common near base; several thin (<0.1m) burrowed mudstone layers at 51.85-51.9, 52.25-52.3; contacts of these mudstone layesr are planar to scoured at base, undulatory and abrupt at top; some sorted beds, giving pseudo-laminar appearance; local small-scale cross-laminae; ooids/intraclasts less common upwards, peloids more common; SAMPLE 51.7 (note burrows? into mudstone).

32 52.5-52.6 burrowed mudstone; dark gray; burrows dolomitized, mostly horizontal; faint laminae?; two thin grainy layers - fossil/peloid/ooid packstone (52.65-52.7) and peloid packstone (53.2-53.3), both with irregular bases, gradational top; SAMPLE 53.6 (from 32-33 boundary).

33 52.6-54.5 ooid grainstone; light to medium gray; well-sorted, ooids only?; stylolites; small (<1cm) elongate intraclasts in lower 3 cm; cross-laminae?; SAMPLES 53.8, 54.5.

34 54.5-57.5 burrow-mottled mudstone; medium to dark gray; burrows dolomitized, horizontal; peloid/intraclast ooid packstone layers at 54.8-54.85, 55.5-55.55, 55.65-55.7, 56.25-56.3, 56.4-56.45, 56.9-57.0; these layers are mostly continuous, some laterally discontinuous; SAMPLE 55.7.

35 57.5-57.8 ooid/peloid/fossil packstone to grainstone; medium gray; base irregular, mostly stylolitized; ooids abundant at base, grading up into peloid-rich packstone, overlain by thin (<2mm) mud layer, and finally a fine-grained ooid? packstone; SAMPLES 57.6 (ooids and peloids; two samples), 57.7 (peloid, mud and fines).

36 57.8-58.6 mudstone and burrow-mottled mudstone intimately interlayered with thin peloid/ooid packstone and peloid/fossil wackestone to packstone layers; medium gray; burrows dolomitized, horizontal; lower contact sharp and planar; peloid/fossil layers have irregular, scalloped bases and often have micritic intraclasts up to 5 cm long; non-mudstone layers appear to thicken and thin laterally; SAMPLE 58.2 (from an ooid to unburrowed mudstone contact).

37 58.6-59.4 burrow-mottled mudstone; medium gray; burrows dolomitized; lower contact sharp to stylolitized; no grainy layers.

38 59.4-59.5 mudstone to peloid wackestone; dark gray; lower contact stylolitized; few to no burrows; SAMPLE 59.5 (from 38-39 boundary).

39 59.5-60.1 ooid grainstone; medium to dark gray; lower contact sharp, irregular, or stylolitized; basal 0.1 m contains fossil fragments and imbricated small (<1cm) intraclasts; cross-laminae?; discontinuous wackestone to mudstone layers at 59.7 and 60.0, with some burrows; SAMPLE 60.0 (from ooid-mud contact).

40 60.1-61.0 burrow-mottled mudstone to wackestone to packstone with interlayered ooid/fossil/peloid to peloid packstone; medium to dark gray; lower

contact gradational - several burrows from thin layer extend downward into bed 39; SAMPLE 60.25 (from mudstone/grainstone contact).

41 61.0-61.7 ooid grainstone; medium gray; sharp (scoured?) basal contact; lower 0.15 m rich in ooids, fossils, peloids, and intraclasts, grades up into pure oolite; small (<0.75 cm) intraclasts in upper 0.5 cm; stylolites; SAMPLES 61.0 (base), 61,2 (middle), 61.7 (upper).

42 61.7-61.9 burrow-mottled mudstone; medium gray; lower contact sharp to gradational; burrows dolomitized, horizontal; some very thin, discontinuous grainy layers.

43 61.9-62.2 ooid/fossil grainstone; medium grayl sharp lower contact; rare intraclasts; more ooid-rich upwards; SAMPLE 62.2.

44 62.2-63.3 burrow-mottled mudstone; medium gray; lower contact stylolitized to scalloped; scattered ooid/fossil/intraclast packstone layers in lowest 0.2m, none above.

45 63.3-63.45 peloid/fossil packstone; medium gray; gradational lower contact; one thin (<1 cm) discontinuous burrowed mudstone layer; stylolited; SAMPLE 63.45.

46 63.45-63.5 mudstone; dark gray; lower contact very sharp planar; few burrows; thin (<5 mm) grainy lag layer.

47 63.5-63.7 peloid/fossil packstone to grainstone (lower half) and intraclast/peloid/fossil packstone (upper half); medium gray; stylolitized lower contact; SAMPLE 63.7 (note intraclasts).

48 63.7-63.9 burrow-mottled mudstone; dark gray; abrupt lower contact; burrows dolomitized.

49 63.9-64.05 peloid/intraclast/fossil packstone to grainstone; dark gray; scalloped abrupt lower contact; coarse grained; upper contact has fibrous texture (small fault movement?); SAMPLE 64.0.

50 54.05-67.5 burrow-mottled mudstone; dark gray, abrupt, fibrous lower contact; burrows dolomitized; locally laminated; several thin, continuous peloid/intraclast/fossil packstone layers at 64.3-64.35, 66.05-66.1, 66.4-66.45, 66.7-66.75, 66.9-66.95 -- all have sharp, scalloped base and abrupt, irregular top; intraclasts <2 cm, most less than 1 cm; SAMPLE 64.3 (grains and mud).

51 67.5-68.3 ooid grainstone; medium gray; lowermost 0.1 m consists of scalloped, irregular base overlain by ooid/intraclast (<0.5 cm max size) packstone fining upward to wackestone with some burrows; above this thin wackestone is stylolitized contact with ooid grainstone; thin dolomitized layers; SAMPLES 67.5, 67.6, 68.3.

52 68.3-69.1 burrow-mottled mudstone to wackestone; dark gray; abrupt lower contact; locally laminated; burrows dolomitized, horizontal.

53 69.1-69.8 ooid packstone to grainstone; medium gray; lower contact irregular to scalloped; rare small (<1.5 cm) intraclasts in lowest 0.1m; SAMPLE 69.8.

54 69.8-70.4 burrow-mottled mudstone; medium gray; burrows dolomitized, horizontal; fossil/ooid wackestone packstone lens at 70.3; SAMPLE 70.2.

55 70.4-71.1 ooid grainstone; medium gray; irregular scalloped base; fossils in lower .05m; SAMPLE 70.9

56 71.1-71.8 burrow-mottled mudstone; medium gray; burrows dolomitized, horizontal; SAMPLE 71.2.

57 71.8-72.2 peloid/fossil packstone; medium gray; lower contact obscured; more ooid-rich upwards; SAMPLES 79.1, 72.1.

58 72.1-73.7 burrow-mottled mudstone; medium gray; burrows dolomitized, horizontal; sharp base; prominent bedding plane at 72.3; some thin (<1cm) wackestone lenses; at 73.4, persistent red (FeO?) 0.5 cm-thick layer; SAMPLES 73.3 (just below red layer), 73.4 (wackestone lens).

59 73.7-73.9 peloid/ooid/fossil packstone; medium gray; irregular to scalloped base; rare intraclasts; SAMPLE 73.4.

60 73.9-73.95 burrow-mottled mudstone; medium gray; burrows dolomitized, horizontal; scalloped to irregular base.

61 73.95-74.1 peloid/fossil/ooid? packstone; medium gray; irregular base; laminated?; stylolites.

62 74.1-74.25 burrow-mottled mudstone; medium gray; burrows dolomitized, horizontal.

63 74.25-74.3 peloid/fossil/ooid packstone; medium gray; irregular base; SAMPLE 74.3 (from 63-64 boundary).

64 74.3-74.5 burrow-mottled mudstone; medium gray; burrows dolomitized, horizontal.

65 74.5-74.55 peloid/fossil/ooid packstone; medium gray; irregular base; small (<0.5 cm) intraclsts common; cross-laminae?.

66 74.55-75.6 burrow-mottled mudstone; medium gray; abrupt base; less burrowed towards base; burrows dolomitized, horizontal; locally laminated; peloid/fossil packstone layer at 74.95-75.0.

67 75.6-76.8 peloid/fossil/intraclast packstone; medium gray; intraclasts small (<1.5 cm); SAMPLE 75.8.

68 76.8-76.0 mudstone, burrowed in upper half; medium gray; stylolited; discontinuous packstone/grainstone lens at 75.9.

69 76.0-76.6 peloid packstone to grainstone grading up into peloid/ooid packstone to grainstone; medium gray; lower surface sharp, planar to scalloped; thin interlayered burrowed mudstone; intraclasts present in lowest 15 cm; SAMPLES 76.3, 76.5.

70 76.6-76.8 burrow-mottled mudstone; medium to dark gray; irregular, abrupt lower surface; burrows dolomitized, horizontal.

71 76.8-76.9 fossil/peloid wackstone to packstone; medium gray; abrupt lower surface; rare small intraclasts (<1cm).

72 76.9-77.2 burrow-mottled mudstone to wackstone; dark gray; lower contact sharp, irregular; rare intraclasts.

73 77.2-78.4 ooid grainstone; medium gray; abrupt, scalloped (and often stylolitized) lower contact; small intraclasts (<1.5 cm), fossils, and peloids common near base, grading up into pure oolite; in upper 25 cm, burrow-mottled mudstone interfingers with ooid grainstone; SAMPLE 78.1 (interfingering).

74 78.4-78.6 interlayered burrow-mottled mudstone and peloid/fossil packstone; medium gray; lower contact gradational.

75 78.6-83.4 ooid grainstone; massive; medium gray; peloids and intraclasts (<1.5 cm)

common near base; thin, dolomitic stringers in middle part; thin burrowed mudstone layer at 79.5-79.6; packstone in upper 20 cm; SAMPLES 78.6 (at base), 78.8 (near base), 80.6, 81.6 (dolomitic stringers), 83.4 (uppermost).

76 83.4-83.5 burrow-mottled mudstone; dark gray; burrows dolomitized, horizontal.

77 83.5-83.9 ooid/peloid packstone to grainstone with some wackestone and burrow-mottled mudstone layers/lenses; medium to dark gray; generally coarsening-upwards; SAMPLE 83.6.

78 83.9-84.2 burrow-mottled mudstone; dark gray; burrows dolomitized, horizontal; thickness varies laterally from 0.2-0.35 m.

79 84.2-88.1 ooid grainstone; light to medium gray; sharp lower contact, irregular, mostly stylolitized; no fossils or intraclasts in lower part; dolomitic stringers; many ooid dolomitized; cross-laminae; at 85.25, thin (2 cm) discontinuous burrowed mudstone layer; small (<1cm) intraclsts and some fossils in upper 10 cm; SAMPLES 85.6, 87.2 (stringers).

80 88.1-88.3 burrow-mottled mudstone; medium gray; burrows dolomitized, horizontal; thickness varies laterally from 0.2-0.35 m because of irregular lower contact; conspicuous bedding plane at 88.15.

81 88.3-89.2 ooid grainstone; medium gray; fossils, peloids, and small (<1.5 cm) intraclsts present, usually concentrated in layers; stylolites; thin dolomitic stringers; continuous, thickening (0-5 cm) burrow-mottled mudstone to wackestone layer at 89.05; SAMPLES 88.4 (note peloids and intraclsts), 89.1 (mudstone).

82 89.2-89.65 intimately interlayered burrow-mottled mudstone and fossil wackestone to packstone; medium to dark gray; abrupt lower boundary.

83 89.65-89.8 ooid/fossil/peloid/intraclast packstone to grainstone; medium gray; lower contact scalloped to irregular to stylolitized; intraclasts up to 3.5 cm long, most elongate; persistent burrow-mottled mudstone layer from89.75-89.8; SAMPLE 89.8 (actually from 89.75).

84 89.8-90.1 burrow-mottled mudstone to wackestone; medium gray; lower contact stylolitized; burrows dolomitized, horizontal; burrows decrease in size and are less continuous upwards; SAMPLE 90.0.

85 90.1-91.3 ooid grainstone; medium gray; massive; lower contact irregular to undulatory; locally cross-laminated; fossils and intraclasts (up to 7

cm long and elongate) locally; stylolites; dolomitic stringers fairly common; thin discontinuous burrow-mottled mudstone layers at 90.8, 90.9; thin (<1-3 cm) layer of fibrous calcite at top (some slip?); SAMPLES 91.3, 91.3 (big one and small one).

86 91.3-91.55 mudstone; medium to dark gray; lower contact commonly dolomitized burrow; moderately burrow-mottled; burrows dolomitized, mostly horizontal, some vertical; local thin (<2 cm) wackestone/packstone layers (PS?); stylolites; abundant white blocky spar; SAMPLE 91.5

87 91.55-92.15 peloid/ooid grainstone; medium gray; lower contact mostly stylolitized, but in areas where not, up to 3 cm relief; dolomitic stringers; SAMPLES 91.6, 91.9, 92.2 (from 87-88 transition).

88 92.15-92.8 burrow-mottled mudstone; medium to dark rey; gradational lower contact; burrows dolomitized; stylolites; several mm-thick peloidal, fossil grainy layers, PS with some cross-laminae.

89 92.8-92.85 ooid grainstone; medium gray; strong H2S odor when broken; thin cataclasite at top; SAMPLE 92.8.

90 92.85-92.95 ooid/fossil/intraclast grainstone; medium gray; elongate intraclasts up to 1.5 cm long; SAMPLE 92.9.

91 92.95-93.1 intraclast packstone; medium to dark gray; clasts imbricated; unit thickens and thins (from 0.1-0.3 m) at expense of everlying mudstone; SAMPLES 93.0 (from thinner area), 93.05 (from thicker area).

92 93.1-94.6 mudstone; medium to dark gray; irregular lower contact; stylolites abundant from 93.1-94.1, burrows from 94.1-94.6; wackestone to packstone layers: 93.3-93.4 (intraclast/fossil grainstone; peloids?; oncoids?; abrupt lower contact, swiftly gradational upper contact), 93.55-93.6 (intraclast/fossil wackestone), 93.75-93.85 (peloid/intraclast/fossil wackestone), 94.4-94.5 (ooid packstone to grainstone); SAMPLE 93.5 (packstone up to mudstone, with peloids, intraclasts near base).

93 94.6-95.8 ooid grainstone; medium to dark gray; base scalloped to irregular, with up to 4 cm relief; stylolites; scattered small intraclasts; dolomitic stringers; cross-laminated; many ooids dolomitized; thin burrowed mudstone layer at 93.35-93.4, lens shaped (3 cm X 1 m) with skeletal lag.

94 95.8-99.8 burrow-mottled mudstone to wckestone; medium gray; lower contact harp to stylolitized; burrows dolomitized; few/no burrows from 97.5-97.8; numerous geopetals in burrows; several grainy layers: 96.05-96.1 (ooid packstone; peloids and fossils also; sharp, scalloped base, sharp, irregular upper contact), 96.7-96.8 (peloid/ooid/intraclast packstone), 97.05 (3 cm thick lens of intraclast/peloid/ooid packstone), 98.9-99.2 (peloid/ooid/intraclast packstone, irregular lower contact, upper surface burrowed); SAMPLES 96.7 (packstone), 97.6, 99.2 (lobes into packstone).

95 99.8-100.2 ooid grainstone; medium gray; irregular sharp base; stylolites; peloids; rare small intraclasts.

96 100.2-100.35 burrow-mottled mudstone; medium gray; lower contact sharp to stylolitized; burrows dolomitized, horizontal; prominent bedding plane halfway through unit; laminations?; SAMPLE 100.2 (both 95 and 96).

97 100.35-101.2 ooid packstone; medium gray; sharp lower contact; peloids and small intraclasts near base; at 100.8, thin (5 cm) thick mudstone layer; upper half more fossil and peloid-rich; SAMPLE 100.9.

98 101.2-101.6 burrow-mottled mudstone; medium to dark gray; burrows dolomitized; numerous vertical burrows; prominent bedding plane.

99 101.6-102.5 ooid grainstone; medium gray; sharp irregular to stylolitized lower contact; cross-laminae; small (<1 cm) intraclasts common in basal 10 cm; burrowed mudstone lens (2 cm X 50 cm) at 102.3.

100 102.5-103.15 burrow-mottled mudstone; dark gray; irregular lower contact, some burrows extend down into unit 99; burrows dolomitized, horizontal; discontinuous ooid grainstone lenses (2 cm X 80 cm) with abrupt lower contact at 102.6 (see outcrop above "101.6").

101 103.15-104.0 peloid/intraclast packstone to grainstone grading into ooid packstone to grainstone; medium gray; abrupt scalloped to very scalloped base; intraclasts small (<2 cm); ooids only above 103.3; SAMPLES 103.15 (base), 103.6 (ooids).

102 104.0-105.2 burrow-mottled mudstone; dark gray; burrows dolomitized; grainstone layers: 104.45-104.5 (ooid/intraclast/peloid grainstone), 104.55-104.6 (ooid/peloid/intraclast/fossil? grainstone), 104.85-105.0 (ooid/peloid/intraclast grainstone); SAMPLE 104.45.

103 105.2-105.45 peloid/fossil/intraclast packstone to grainstone; medium gray; irregular toscalloped base with thin discontinuous mudstone layers in basal 5 cm; larger grains common near base and top of unit; SAMPLE 105.3.

104 105.45-106.6 burrow-mottled mudstone to wackestone; medium to dark gray; burrows dolomitized; at 105.8, peloid packstone to wackestone lenses (6 cm X 60+ cm), cross-laminated; similar, smaller lenses at 106.1.

105 106.6-107.3 peloid/intraclast packstone to grainstone; medium gray; sharp, undulatory (on meter scale) base gives the unit irregular thickness; intraclasts < 1 cm large, rounded; cross-laminae; SAMPLE 106.8.

106 107.3-108.6 burrow-mottled mudstone; medium gray; lower contact stylolitized; burrows dolomitized, horizontal.

107 108.6-109.1 peloid/ooid/intraclast packstone to grainstone; medium gray; lower contact sharp, planar to scalloped; small (<0.75cm) intraclasts common near base; larger (up to 2 cm) intraclasts abundant near 108.75; peloids domonate elsewhere; stylolites; dolomitic stringers; SAMPLE 108.8 (intraclast-rich layer).

108 109.1-109.4 burrow-mottled mudstone; medium to dark gray; abrupt to stylolitized base; burrows dolomitized, horizontal.

109 109.4-110.6 peloid/intraclast/fossil? packstone to grainstone; medium gray; lower contact sharp, scalloped; intraclasts up to 1 cm long, common near mudstone layers; locally cross-laminated; stylolites; dolomitic stringers; burrow-mottled mudstone layers at 109.6-109.65, 109.8-109.85, 110.25-110.3, 110.45-110.55 (locally laminated, burrows dolomitized); SAMPLE 110.4 (some mudstone).

110 110.6-111.2 mudstone, mostly burrowed; dark gray; sharp lower contact, burrows dolomitized, horizontal.

111 111.2-111.35 peloid/fossil/intraclast/ooid? wackestone to grainstone; medium gray; irregular sharp scalloped base; intraclasts up to 3 cm long, imbricated?; stylolites; thinburrowed mudstone lens at 111.3.

112 111.35-111.9 wackestone to mudstone grading up into burrow-mottled mudstone; gradational with 111; stylolites (especially in lower half); at 111.55, packstone/grainstone layer, lens shaped (3 cm X 1 m); SAMPLE 111.7.

113 111.9-112.3 fossil/peloid/intraclast packstone grading up into burrowed mudstone to wackestone; medium gray; lower contact sharp planar to irregular; intraclasts imbricated, up to 5 cm long (most smaller, however) and concentrated in lower half; burrows dolomitized, horizontal; SAMPLE 112.25.

114 112.3-112.45 ooid/fossil/intraclast grainstone; medium gray; abrupt, irregular lower contact; small (<1.5 cm) intraclasts common near base, larger (up to 3 cm) abundant near top, some imbricated(?); SAMPLE 112.4.

115 112.45-112.6 mudstone to wackestone; medium to dark gray; rare burrows; stylolites, spar? common.

116 112.6-118.2 intraclast packstone/grainstone quickly grading up into ooid grainstone; medium gray; stylolites; dolomitic srtingers; massive; cross-laminations; prominent stylolite and thin mudstone layer at 113.5; sparry calcite present locally; intraclasts and fossils also abundant in uppermost 0.1 m; 2 large (2 cm) continuous dolomitized layers at 113.5; SAMPLES 113.2, 114.0, 115.2, 117.8.

117 118.2-118.5 mudstone to wackestone; dark gray; burrowed lower portion, stylolitized upper part; SAMPLE 118.2 (116-117 bound).

118 118.5-119.2 ooid grainstone; medium gray; lower contact abrupt, planar to scourder (up to 2 cm relief); small (1 cm) intraclasts fairly common in lowermost 5 cm; SAMPLE 118.7.

119 119.2-119.7 burrow-mottled mudstone to wackestone; dark gray; lower contact abrupt possibly stylolitized (?); burrows dolomitized; ooid packstone layer at 119.4-119.45 (persistent thickness, lower contact gradational).

120 119.7-119.85 ooid grainstone; medium gray; gradational lower contact; intraclasts near top; SAMPLE 119.85 (120-121 boundary).

121 119.85-120.0 burrow-mottled mudstone to wackestone; medium to dark gray; stylolitized lower contact; burrows dolomitized, horizontal.

122 120.0-121.8 ooid grainstone; medium gray; dolomitic stringers; lower contact gradational (over 5 cm); H2S odor when freshly broken; buff dolomitic pods? near top (similar to bed 116); cross-laminae; SAMPLE 121.2

123 121.8-122.0 burrow-mottled mudstone; dark gray; lower contact abrupt, "conformable" where not stylolitized; scattered throughout unit are ooid packstone to grainstone lenses (PS, up to 2 cm X 30 cm, cross-laminae, sharp, planar to scalloped lower contacts, abrupt, planar upper contacts).

124 122.0-122.1 ooid grainstone; medium gray; lower contact scalloped to stylolitized; thin (2 cm) burrowed mudstone layer 2 cm from base; uppermost 2 cm contains abundant fossil, intraclast (?), cross-laminae (?); in general, more homogenous than bed 125.

125 122.1-122.3 fossil-intraclast grainstone; medium gray; lower contact abrupt, irregular to gradational?; abundant coarse sparry calcite; very coarse grains (up to fine pebble size); common grain-scale dolomitization; common discontinuous mudstone layers, some burrowed; weak H2S odor; SAMPLE 122.1 (note both 124 and 125).

126 122.3-125.3 burrow-mottled mudstone to wackestone interlayered with peloid/intraclast packstone to grainstone; medium to dark gray; burrowed mudstone to wackestone: burrows dolomitized, horizontal; lower contacts typically abrupt, planar; locally laminated; thin (<3cm) peloid/fossil/intraclast packstone to grainstone layers fairly common, often lens-shaped; packstone to grainstone: lower contacts scalloped to irregular to stylolitized; ooids locally abundant; intraclasts may be imbricated, up to 2 cm long; thin (<4 cm) mudstone lenses rare; abundant localized grain-scale dolomitization; these layers are from 122.5-122.8, 122.9-123.5, 123.65-123.85, 123.95-124.2, 124.25-124.5, 124.6-124.7, 124.75-124.8, 124.9-125.05, 125.1-125.3; SAMPLES 122.7, 123.4, 124.4, 125.0 (note intraclasts), 125.3 (upper contact).

127 125.3-125.9 burrow-mottled mudstone; dark gray; lower contact abrupt, stylolitized (?); burrows dolomitized, horizntal; abundant laminations; prominent bedding plane with fibrous calcite perpendicular to bedding at 125.7; SAMPLES 125.7 (fibrous calcite and right below), 125.7s (fibrous).

128 125.9-126.5 peloid/fossil packstone to grainstone; medium gray; lower contact stylolitized; H2S odor; rare small (<2 cm) intraclasts; many grains dolomitized; thin (2-3 cm) burrow-mottled mudstone layer 5 cm from top of unit; SAMPLE 126.45 (includes mudstone).

129 126.5-128.1 burrow-mottled mudstone; dark gray; lower contact sharp, irregular, stylolitized?; burrows appear elongate (height:width less than most others).

130 128.1-130.1 peloid/intraclast packstone; medium gray; lower contact abrupt to gradational; thin (<4 cm) laterally continuous burrowed (dolomitized) mudstone to wackestone layers at 129.1, 129.4 (sharp, planar base, stylolitized top); several other small, discontinuous lenses near base; dolomitic stringers throughout; many grains dolomitized; lenses of dolomitic material (up to 4 X 11 cm) fairly common; fewer intraclasts, more fossil fragments upwards; SAMPLES 128.7, 129.2, 129.6 (note dolomite).

131 130.1-141.9 interbedded peloid/ooid packstone to burrow-mottled mudstone; medium gray; medium grained; poorly exposed; top not exposed; SAMPLES 130.4, 131.4, 132.1 (from behind pine tree); 141.8 (from 6 paces due west of highway ROW marker).

132 141.9-143.0 covered, but abundant chert float.

133 143.0-145.7 ooid packstone/grainstone; medium gray; poorly exposed; SAMPLE 144.6.

134 145.7-145.9 covered

135 145.9-154.7 dolostone; very hard; light gray to buff; less resistant, unit usually forms a ledge; poorly exposed, but abundant float, some chert; SAMPLE 147.1.

136 154.7-155.4 mudstone; dolomitic; medium gray; lower contact not exposed; fine grained; SAMPLE 155.0

137 155.4-159.0 covered

138 159.0-159.1 dolomitic mudstone; fine grained; light gray; anhydrite pseudomorphs; SAMPLE 159.1.

139 159.1-165.9 covered

140 165.9-166.9 dolomitic mudstone to cryptalgal laminite; light browninsh gray; fine grained; poorly exposed; SAMPLE 166.1.

141 166.9-172.4 covered

142 172.4-179.3 mudstone, grading up to wackestone/packstone in uppermost 0.5 m; light brownish gray; laminated (cryptalgally?); fine grained; peloids; SAMPLE 172.2, 179.1.

143 179.3-183.0 covered

144 183.0-191.3 dolostone; light tan; sucrosic texture; coarse grained; locally laminated; SAMPLES 184.5, 185.9, 189.8.

145 191.3-194.7 covered

146 194.7-197.2 ooid grainstone to mudstone; dolomitic; buff to light to medium gray; laminated; fine grained; poorly exposed; SAMPLE 195.9.

147 197.2-199.8 covered; fault??

148 199.8-201.2 mudstone to ooid packstone/grainstone; locally laminated; poorly exposed; SAMPLES 200.3, 200.8.

149 201.2-205.1 covered

150 205.1-206.5 mottled mudstone with scattered packstone to grainstone layers; medium to dark gray; laminated; poorly exposed; SAMPLE 205.8.

151 206.5-208.9 fossil/peloid/intraclast packstone to grainstone; medium gray; massive; cross-laminae?; SAMPLE 208.4.

152 208.9-210.1 covered

153 210.1-210.9 burrow-mottled mudstone; dark gray; fine grained; mottled dolomitized; SAMPLE 210.4.

154 210.9-213.2 covered

155 213.2-221.0 burrow-mottled mudstone; dark gray; laminae; burrows dolomitized; non-burrowed interval from 217.1-217.3; SAMPLE 219.8.

156 221.0-230.7 ooid grainstone; medium gray; massive; poorly exposed; SAMPLE 222.3.

157 230.7-231.2 burrow-mottled mudstone (dolostone); dark gray; laminae?; base not clear, poorly exposed.

158 231.2-238.6 fossil? packstone to grainstone, grading up into oncoid/trilobite grainstone; medium gray; base obscured; unit is very crumbly, many allochems apparently extensively dolomitized; intraclasts locally abundant; SAMPLES 232.6, 232.9, 236.0, 237.0.

----------Nolichucky Shale----------

159	238.6+	quartz siltly peloid packstone to shale; buff to brown; poorly exposed on hillslope.

I-40 at Deep Springs Road, off-ramp, south side

Section is very well exposed along the roadcut on the off-ramp from I-40 west to Deep Springs Road. The base of the Craig was not observed, and much of the Craig is faulted and contorted. Caution should be used in interpetations from this interval. The interval from approximately 8 m below the upper Rogersville (bed 5) to approximately 55 m above the base of the Maryville is *free* of major fault complications, however. The section above the 80 m mark (cumulative thickness) appears to be quite faulted, and so was not measured.

Bed number	cumulative thickness	description
		--- CRAIG LIMESTONE MEMBER ---
		-- base not exposed --
1	0-14.0	burrowed mudstone; medium to dark gray; base not exposed; pyrite/marcasite common, especially in lower 3 meters; massive; burrows dolomitized, horizontal; locally laminated; few burrows in interval from 9.4-9.8, open vugs, some filled with calcite in this interval also; another less burrowed zone from 11.5-11.9; fossil/peloid packstone to grainstone layers at 3.4-3.45, 3.7-3.8, 4.05-4.1, 4.35-4.4, 5.1-5.15, 5.6-5.65, 5.8-5.85, 6.3-6.35, 11.5-11.55, 11.8-11.85; intraclast packstone layers with scalloped base and planar top at 7.55-7.6, 7.9-7.95, 8.5-9.0, intraclasts up to 2 cm long; prominent bedding planes at 7.75, 9.8, 12.5; SAMPLES o2.5, o5.4, o7.75, o7.9, o9.8, o11.8.
2	14.0-14.25	intraclast/peloid packstone to grainstone; medium gray; abrupt irregular to scalloped to stylolitized base; intraclasts elongate to bean shaped, small (<5 cm), laminated (?); scattered thin dolomitic stringers; SAMPLES o14.1a, o14.1b.
3	14.25-16.0	burrowed mudstone; dark gray; base abrupt irregular to gradational; burrows dolomitized, horizontal, larger in lower 1.3 m; peloid/intraclast packstone to grainstone layer at 15.6-15.65; thin (<3 cm) ooid/intraclast/peloid lenses in uppermost 0.3 m, none continuous; reddish mm-thick layer at ~1-2 cm below top of unit; SAMPLES o15.9, o16.0.
4	16.0-27.0	burrowed mudstone to peloid to ooid to fossil packstones and grainstones; irregular, contorted bedding; SAMPLES o16.6, o16.1, o16.1b, o18.5, o19.5, o22.0, o22.1, o22.2, oA (from ~24.0), o25.7;

from ~25.3-27.2, locally undisturbed, lithologies include: sheared limestone (25.3-25.4), burrow-mottled mudstone, medium gray, some grainy layers (25.4-25.6), peloid/fossil packstone to grainstone (25.6-25.9), and burrowed mudstone to wackestone, medium gray, with peloid (oncoid??) layer at 26.7 (25.9-27.2).

5 27.2-27.55 burrowed mudstone; dark gray; lower contact prominent bedding plane; undeformed; burrows dolomitized, horizontal; in uppermost 0.1m, two prominent horizontal burrows accentuated by stylolites; forms first structurally "uncomplicated" layer; SAMPLE o27.3.

6 27.55-27.9 oncoid (?)/peloid/intraclast packstone to grainstone; medium gray; lower contact abrupt, irregular to scalloped; ooids, fossils in lowest 5 cm; stylolites; SAMPLE o27.7.

7 27.9-28.6 burrow-mottled mudstone; dark gray; lower contact sharp, undulatory; burrows dolomitized; uppermost 0.1 m unburrowed wackestone (?) packstone (?) with peloids (?); prominent bedding plane at 28.6; SAMPLE 28.6 (below BP).

8 28.6-28.85 ooid grainstone; lower contact stylolitized or with mm-thick sparry layer; irregular, small (<1 cm) intraclasts; some muddy layers in upper 0.1 m; SAMPLE o28.7.

9 28.85-29.0 burrowed mudstone; dark gray; burrows dolomitized, horizontal; lower contact stylolitized; SAMPLE o28.9 (includes some of be 8 in lower part).

10 29.0-29.03 peloid/ooid packstone to grainstone; medium to dark gray; lower contact stylolitized; persistent; SAMPLE o29.0 (bottom).

11 29.03-29.15 mudstone to wackestone; dark gray; lower contact abrupt, irregular to stylolitized; abundant spar-filled voids up to 2 X 1 cm; SAMPLE o29.0 (top), o29.1 (bottom).

12 29.15-29.18 ooid/fossil/intraclast packstone to grainstone; medium to dark gray; persistent; common spar-filled voids; SAMPLE o29.1 (top).

13 29.18-29.3 mudstone; dark gray; lower contact abrupt, irregular to undulatory to stylolitized; abundant sparry calcite-filled vugs; abundant pyrite/marcasite in upper 3 cm; SAMPLE 29.3b (from up on ledge).

14 29.3-29.5 intraclast grainstone, grading up into fossil/oncoid grainstone and then oncoid/fossil grainstone; medium to dark gray; planar base; oncoids

exposed on upper surface; iron oxide layer 1 cm from base; no thin grainstone layer as on on-ramp, south side; SAMPLE o29.5.

— Upper Rogersville Shale —

15 29.5-30.25 clay shale; gray to black; chippy.

— Maryville Limestone —-

16 30.25-30.3 fossil packstone; medium gray; base (contact with shale) abrupt, irregular, shows scour marks and load casts; rare intraclasts (?); thickens and thins slightly across outcrop.

17 30.3-30.5 ribbon wackestone/mudstone; medium gray; lower contact abrupt, irregular; abundant pyrite; 'ribbons' are thin (~1mm), very irregular, discontinuous, and often associated with pyrite; uppermost 4 cm grades into intraclast/fossil packstone; intraclasts elongate, imbricate (?), up to 2 cm long; SAMPLE o30.3.

18 30.5-30.8 fossil/intraclast/ooid(?) packstone/ grainstone; medium gray; lower contact abrupt, irregular to scalloped, it truncates intraclasts in bed below; lowermost ~2cm is echinoderm/intraclast packstone grainstone overlain by thin (<0.5cm) shale parting; above the shale parting is 10 cm intraclast/fossil packstone; intraclasts up to 5 cm by 2 cm, mostly flat lying; fossils include echinoderms, trilobites; the remainder of the unit is fossil/oncoid/intraclast packstone; sparse pyrite; oncoids increase in abundance upwards, and approach 1 cm in diameter; uppermost 5cm contains thin (<1cm) continuous dolomitic stringers.

19 30.8-31.1 oncoid/peloid/fossil packstone; medium gray; lower contact gradational with bed 18; packstone layers appear to be separated by thin (<1.5cm) discontinuous mudstone layers with gradational (?) bases and abrupt, scalloped tops; in general, oncoids larger, better developed (weathered???) laminae near base; oncoids approach 1 cm in diameter; SAMPLE o30.9.

20 31.1-33.2 fossil/oncoid grainstone to packstone to wackestone; medium gray; massive; lower contact prominent stylolite; unit appears to be intimately interlayered mudstone/wackestone layers and packstone/grainstone layers; common stylolites; oncoids appear to be dolomitized, not as well developed as in bed 19; some small (2 cm X 0.5 cm) sparry vugs and burrows near top of unit; SAMPLE o33.0.

21 33.2-54.7 mottled mudstone; medium to dark gray; lower contact gradational; less intensely burrowed from 35.2-35.6 also fairly common sparry voids; intensely/ completely burrowed from 37.4-37.5; locally laminated; massive bedded; upper parts of some burrows spar-filled; SAMPLES o34.5, o38.4, o45.2, o46.8, o48.9, o51.3 o53.6; numerous packstone/grainstone layers: **35.0-35.05** (peloidal packstone; discontinuous; fine grained), **35.1-31.15** (fossil/peloid packstone; continuous; gradational base and top; fine grained), **35.5-35.55** (intraclast/fossil/peloid grainstone; abrupt, irregular to stylolitized base; pinch and swell (PS)), **35.75-35.8** (intraclast/fossil/peloid grainstone; actually 2 close layers; medium grained; abrupt, scalloped base; PS; SAMPLE o35.8), **36.7-36.72** (fossil/peloid packstone; fine grained; PS), **37.25-37.27** (peloid packstone; fine to medium grained; PS; SAMPLE o37.25), **37.5-37.52** (intraclast/peloid packstone; medium grained), **37.6-37.65** (fossil/peloid/ intraclast packstone; actually 2 closely spaced layers; medium grained; trilobites and echinoderms present; PS), **38.35-38.37** (peloid/fossil packstone; fine grained; discontinuous), **38.7-38.72** (fossil/peloid packstone; fine to medium grained; PS; echinoderms and trilobites(?)), **39.1-39.15** (fossil/ peloid packstone; fine to medium grained; PS; echinoderms and trilobites (?); scalloped to irregular base), **39.6-39.61** (fossil/peloid packstone; fine grained; PS; very thin and discontinuous), **40.3-40.35** (intraclast/ fossil/peloid packstone; fine to coarse grained; abrupt, scalloped base, abrupt planar top; PS, but doesn't pinch out; echinoderms and trilobites; SAMPLE o40.3), **40.9-41.0** (fossil/pellet packstone; fine grained; irregular, scalloped base, gradational top), **42.8-42.9** (fossil/peloid/intraclast/ooid (?) packstone; medium grained; fairly regular thickeness, but local PS; abrupt scalloped base, irregular top; echinoderms; SAMPLE o42.8), **43.3-43.31** (fossil/peloid packstone; fine grained; PS; echinoderms), **44.1-44.3** (peloid/fossil/intraclast packstone; thin (<2 cm) burrowed mudstone layer at ~44.2; abrupt, scalloped base, abrupt, irregular to stylolitized top; echinoderms, trilobites; intraclasts up to ~1cm X 0.5cm), **45.4-45.45** (fossil/ intraclast/peloid packstone; medium to fine grained; small (<1cm), rounded intraclasts; abrupt, scalloped base), **45.5-45.6** fossil/intraclast/peloid packstone; fine to medium grained; abrupt irregular to planar base), **46.3-46.35** (fossil/peloid/intraclast packstone; fine to medium grained; abrupt planar lower contact, abrupt irregular to stylolitized upper; PS; SAMPLE o46.3), **47.1-47.15** (peloid/fossil packstone; fine grained; lower and upper contacts abrupt and planar; PS, but at ~5m lateral scale; cross-laminae; rare, small (<1cm) round intraclasts), **47.4-47.6** (peloid/fossil/ooid(?) packstone; fine grained; scattered burrowed

lenses; cross laminated; base abrupt stylolitized to scalloped, top gradational, irregular; SAMPLE o47.6), **48.3-48.31** (peloid/fossil packstone; medium grained; abrupt planar lower and upper contacts; PS), **48.6-48.7** (peloid/fossil packstone; medium grained; stylolitized lower contact, abrupt, planar upper; laterally continuous), **50.3-50.31** (fossil/peloid packstone; PS; fine grained), **50.4-50.43** (peloid/fossil packstone; PS (?); fine grained), **50.5-50.6** (peloid/fossil/ intraclast packstone; fine grained), **50.8-50.85** (intraclast/peloid packstone; intraclasts up to 3 cm, elongate; PS, with bottom undulatory), **50.9-51.0** (peloid/fossil/intraclast packstone; PS (?); medium grained; abrupt, irregular lower contact, abrupt, irregular upper), **51.1-51.12** (fossil/peloid packstone; irregular to scalloped base); **52.2-52.35** (peloid/fossil grainstone to packstone; medium to fine grained), **52.45-52.47** (peloid/fossil packstone; lower contact scalloped upper is prominent bedding plane), **52.6-52.65, 52.65-52.75** (two peloid/fossil/intraclast packstone layers, both PS; abrupt scalloped to stylolitized bases, abrupt irregular to planar tops), **53.25-53.45** (peloid/fossil /intraclast packstone; stylolitized base; gradational top; medium to fine grained), **53.9-53.95** (fossil/peloid packstone; fine grained; partly burowed; PS), **54.3-54.35** (intraclast/peloid packstone; gradational base and top; fine to coarse grained).

22 54.7-55.6 ooid grainstone/packstone; peloidal near base; massive; medium gray; lower contact scalloped (?); thin discontinuous mudstone lens at 55.4; cross-laminated; SAMPLE 55.4.

23 55.6-58.6 burrowed mottled mudstone; medium to dark gray; lower contact gradational; irregular "random" burrow pattern, burrows dolomitized; packstone/ grainstone layers at: **56.6-56.62** (fossil/peloid/intraclast packstone; fine grained; abrupt planar base, abrupt irregular top; PS), **57.2-57.3** (peloid/fossil packstone fine to medium grained; abrupt scalloped base, stylolitized top), **57.5-57.52** (peloid/intraclast/fossil peackstone; fine to medium grained; small (<5mm) intraclasts; abrupt, scalloped base, top undulatory, PS), **57.95-58.0** (peloid/fossil packstone; fine grained; PS (?); abrupt, scalloped base, irrgeular top), **58.4-58.45** (peloid/ooid packstone; medium to fine grained; PS (?); abrupt, scalloped base, stylolitized top); SAMPLES o56.1, o58.4.

24 58.6-58.95 peloid packstone/grainstone, coarsening up into peloid/oncoid (?) grainstone; medium gray; abrupt, scalloped base; fine to medium grained in lower part, coarse in upper part; cross-laminated; SAMPLES o58.7, o58.8.

25 58.95-59.3 mudstone to fossil wackestone; medium to dark gray; lower contact abrupt, irregular; sparse burrows mostly dolomitized; SAMPLE o59.3.

26 59.3-59.65 peloid/fossil/ooid(?) packstone to grainstone; medium gray; lower contact abrupt scalloped to stylolitized; medium to coarse grained; cross-laminated; dolomitic stringers; several thin, discontinuous burrow-mottled mudstone/wackestone layers.

27 59.65-60.0 mudstone to wackestone, sparse burrows, dolomitized where present; medium gray; abrupt, irregular base; very thin discontinuous packstone layers common in lowermost 15 cm, fine to medium grained.

28 60.0-60.6 burrow-mottled mudstone to wackestone; medium to dark gray; lower contact stylolitized; locally laminated; upper 10 cm extensively mottled.

29 60.6-61.4 ooid/fossil packstone to grainstone, intraclastic at base; medium gray; abrupt, planar base; fine to medium grained; dolomitic stringers; several thin (<4cm) discontinuous burrowed (wackestone?? mudstone??) layers from 61.2-61.4.

30 61.4-62.0 slightly mottled mudstone; dark gray; lower contact stylolitized; fetid odor; prominent bedding plane at 61.7; irregular mottle pattern; SAMPLE o60.5 (61.5).

31 62.0-63.3 ooid/fossil grainstone, with common intraclasts near base; light to medium gray; abrupt, scalloped base; medium grained; massive; discontinuous mudstone lenses at 61.75-61.78, 61.80-61.81, 61.9-61.95; some stylolites; "purest" oolite 0.55-0.9 m from base; SAMPLE o61.8 (62.8).

32 63.3-63.5 fossil wackestone abruptly grading up into fossil/intraclast/peloid packstone to grainstone; medium gray; lower contact stylolitized; echinoderms (?); intraclasts rounded, circular, less than 1 cm diameter.

33 63.5-64.6 mottled mudstone to wackestone; medium to dark gray; planar lower contact; poorly developed mottles; several thin (<1cm) grainy lenses in basal 0.2 m.

34 64.6-65.45 ooid grainstone; medium gray; base abrupt, scalloped; intraclastic near

base; cross-laminated (?); masive; medium grained; thin continuous mudstone layer at 64.35-64.40, with some burrows; SAMPLE o64.0 (65.0).

35 65.45-65.55 burrow-mottled mudstone/wackestone, interfingered (PS?) with ooid/fossil packstone/grainstone; medium gray; base gradational; fine to medium grained; burrows dolomitized, horizontal; small-scale cross-laminae; SAMPLE o64.55.

36 65.55-65.7 peloid/ooid/fossil packstone to grainstone; medium gray; base abrupt, scalloped, often follows burrows; fine to mediumm grained.

37 65.7-66.8 burrow-mottled mudstone to wackestone; medium to dark gray; base abrupt, irregular; burrows dolomitized, horizontal; intensely burrowed (<70%); locally laminated; several thin (<0.5cm) discontinuous packstone stringers throughout; SAMPLE o65.0 (66.0).

38 66.8-66.95 peloid/fossil packstone; medium gray; base abrupt, scalloped to irregular; fine to medium grained; echinoderms, trilobites; SAMPLE o65.8 (66.8).

39 66.95-67.05 burrow-mottled mudstone; dark gray; base sharp, planar to irregular; stylolites common near base and top, more prominent than burrows; burrow fills range from fine dolomite to white calcite spar to dark tan calcite (?) spar.

40 67.05-67.25 peloid/fossil/intraclast packstone to grainstone; medium gray; base abrupt, planar to scalloped to stylolitized; medium to coarse grained; cross-laminated; intraclasts rounded, circular, no more than 0.5 cm diameter; one thin (<1cm) discontinuous mudstone lens; SAMPLE o66.1 (67.1).

41 67.25-67.35 burrow-mottled mudstone; medium to dark gray; base sharp, planar; burrows dolomitized, horizontal; several thin (<1cm) packstone lenses.

42 67.35-67.6 peloid/intraclast/(oncoid??) packstone to grainstone; medium gray; base gradational; medium to coarse grained; intraclasts rounded, circular to elongate, <1 cm diameter; horizontal to cross-laminated; SAMPLE o66.5 (67.5).

--section transferred to upper ledge--

43 67.6-70.85 burrow-mottled mudstone; dark gray; lower contact gradational, non-planar; burrows dolomitized, horizontal; thick to massive bedded; prominent bedding plane at 67.8; locally laminated; packstone layers at: **69.05-69.15** (peloid/fossil packstone; sharp, planar to slightly undulatory base, abrupt planar top; medium grained), **69.75-69.8** (intraclast/peloid packstone; sharp, scalloped base, abrupt, planar top; PS; intraclasts elongate, rounded, up to 2 cm long), **69.85-69.9** (peloid/intraclast packstone; sharp, irregular to scalloped base, sharp irregular top; PS), **70.35-70.45** (peloid/fossil (?) packstone; sharp planar base and top; consistent thickness across outcrop).

44 70.85-71.6 ooid grainstone, peloidal near base; medium gray; base sharp, irregular, scalloped to stylolitized to irregular; medium grained; dolomitic stringers; SAMPLE o69.9 (70.9).

45 71.6-72.1 burrow-mottled mudstone; medium to dark gray; lower contact gradational, with some interfingering; more profusely burrowed above 71.8; local laminations; burrows dolomitized, horizontal.

46 72.1-72.2 peloid/oncoid(?) packstone to grainstone; medium gray; base abrupt, irregular; medium grained; well sorted; laminated (?); SAMPLE o71.1 (72.1).

47 72.2-72.4 burrow-mottled mudstone; medium to dark gray; planar base; locally laminated; common thin (<3mm) burrows.

48 72.4-72.9 ooid grainstone, peloidal (?) near base; medium gray; base sharp, scalloped to planar; fine to medium grained; cross-laminated; dolomitic stringers; SAMPLE o71.7 (72.7).

49 72.9-73.6 burrow-mottled mudstone.wackestone; dark gray; base sharp, undulatory; burrows dolomitized; stylolites; packstone layers at: 73.3-73.33 (peloidal packstone; medium grained; abrupt, irregular to stylolitized base), 73.45-73.55 (peloid/intraclast (?) packstone; medium to coarse grained; stylolitized base; abrupt, irregular top); SAMPLE o72.5 (73.5).

50 73.6-74.1 peloid/oid packstone to grainstone; medium gray; base sharp, iregular; fine to medium grained; common stylolites; laminated (?).

51 74.1-76.0 burrow-mottled mudstone to wackestone; base gradational; medium gray; burrows dolomitized, horizontal; SAMPLE o74.7 (75.7).

52 76.0-76.3 peloid/intraclast/(oncoid??) packstone to grainstone; medium gray; base

stylolitized; medium to coarse grained; intraclasts <2 cm, elongate; numerous thin, undulatory muddy lenses within unit; SAMPLE o75.2 (76.2).

53 76.3-76.4 burrow-mottled mudstone to wackestone; medium grained; gradational planar to undulatory base -- undulations thicken unit up to 0.2 m; rare thin (<2cm) packstone lenses.

54 76.4-76.5 peloid/intraclast/ooid?? packstone to grainstone; medium gray; base stylolitized; medium to coarse grained; intraclasts up to 2 cm long (most smaller), rounded, elongate.

55 76.5-76.8 burrow-mottled mudstone; medium to dark gray; base gradational; laminated; burrows dolomitized, horizontal; thin (<1cm) peloidal packstone layer at 76.2.

56 76.8-76.9 peloidal packstone to grainstone; medium gray; medium to coarse grained; sharp, scalloped base; SAMPLE o76.8 (77.8).

57 76.9-77.9 burrow-mottled mudstone; dark gray; base sharp planar to gradational planar; laminated; stylolites; packstone layers at: **77.1-77.12** (peloid/oncoid?? packstone; gradational base; medium to coarse grained; PS), **77.25-77.27** (fossil/peloid packstone; abrupt, planar base, abrupt undulatory top; medium grained; PS), **77.4-77.45** (peloid/fossil/ooid?? packstone; base stylolitized, top abrupt, planar; medium grained), **77.5-7.55** (peloid/fossil packstone; medium grained; abrupt, scalloped base, abrupt planar top), **77.75-77.8** (peloid/fossil packstone; abrupt planar base and top; PS, on meter scale); SAMPLE o76.1 (77.1).

--return to road level--

58 77.9-78.1 peloid/fossil packstone to grainstone; medium gray; base abrupt, scalloped; medium to coarse grained; cross (??) laminated; thin (<3 cm) discontinuous mudstone layer at 78.0.

59 78.1-78.4 intimately interstratified thin burrow-mottled mudstone and peloid/fossil packstone; irregular contacts; medium gray.

60 78.4-78.5 peloidal packstone; medium gray; abrupt stylolitized to scalloped base; medium grained; SAMPLE o78.4.

61 78.5-78.65 burrow-mottled mudstone; medium to dark gray; abrupt irregular to scalloped base; burrows dolomitized, horizontal.

62 78.65-78.8 peloid packstone to grainstone; medium gray; abrupt planar to irregular lower contact; medium to coarse grained; oncoids (??).

63 78.8-79.1 burrow-mottled mudstone; burrows dolomitized, some horizontal; dark gray; base gradational (?) to irregular; stylolites weather prominently; packstone layers: 78.9-78.93, 79.0-89.03 (fine to medium grained peloidal packstone; PS?).

64 79.1-79.5 ooid/peloid packstone to grainstone; fine to medium grained; base scalloped to stylolitized; SAMPLE o78.4 (79.4).

65 79.5-80.1 burrow-mottled mudstone; medium to dark gray; base gradational; burrows dolomitized, horizontal; stylolites; packstone layer at **79.6-79.67** (peloid/ooid packstone; fine to medium grained; scalloped base, abrupt, planar top).

66 80.1-81.0 ooid grainstone, peloidal near base and top; base abrupt, scalloped; medium gray; fine to medium grained; dolomitic stringers; cross laminated??; SAMPLE o79.5 (80.5).

67 81.0-81.2 burrow-mottled mudstone; medium to dark gray; abrupt, undulatory base; faint laminations.

68 81.2-81.3 peloid/ooid packstone to grainstone; medium gray; fine to medium grained; base stylolitized; SAMPLE o80.2 (81.2).

69 81.3-81.35 mudstone; medium to dark gray; base stylolitized; other stylolites also common; very localy burrowed, but burrows not extensive.

70 81.35-81.85 ooid/peloid grainstone; base abrupt, planar to irregular; medium gray; fine to medium grained; cross laminated; dolomitic stringers; stylolites common; several thin (<5cm) burrow-mottled mudstone lenses, discontinuous.

71 81.85-82.1 burrow-mottled mudstone/wackestone; medium gray; base abrupt, irregular to stylolitized; rare small echinoderm (?) grains; burrows dolomitized, horizontal.

72 82.1-86.5 ooid grainstone; light to medium gray; base abrupt, scalloped to stylolitized; fine to medium grained; massive; laminated to cross laminated; locally intraclastic (rounded, elongate, <1.5 cm) near base; dolomitic stringers; stylolites; some sparry vugs; mudstone layers: **82.35-82.37**, **82.6-82.7** (both burrowed, dolomitized; discontinuous,

abrupt, planar base), **85.8-85.87** (burrowed, dolomitized; abrupt irregular base, scalloped top), **86.2-86.3** (burrowed, dolomitized; discontinuous; abrupt, irregular base, some burrows extend down into oolite; abrupt, scalloped top); SAMPLES o81.2 (82.2), o84.1 (85.1), o85.4 (86.4).

73 86.5-86.65 burrow-mottled mudstone; medium to dark gray; scalloped to stylolitized base; laminated; prominent bedding plane at 86.55.

74 86.65-88.5 ooid grainstone; medium gray; base stylolitized; small (<1cm) rounded circular intraclasts in basal 3 cm; fine to medium grained; massive; mudstone at: 87.05-87.08, 87.1-87.15 (burrowed, dolomitized; planar base, scalloped top).

---FAULT---

Sockless Road Section

Exposed along road cuts on east side of Sockless Road, Jefferson Co., TN. Located approximately 1.3 miles west of junction with Deep Springs Road. At this location, the entire peritidal package is exposed, as well as much of the lower Nolichucky (which was not measured). Unfortunately, a driveway covers approximately 20 m of section. The exposed intervals are moderately well exposed.

bed number	cumulative thickness	description
		—— MARYVILLE LIMESTONE ------
		-- base not exposed --
1	0-2.9	ooid/fossil? packstone to grainstone; fine grained; base not exposed; medium gray; scattered thin mudstone lenses; massive; uppermost 0.2m fractured, light to medium gray; SAMPLE B1.2.
2	2.9-6.2	mudstone; base abrupt, undulatory on meter scale (erosional?); very fine grained; light gray, weathers buff; petroliferous odor; dolomitic; sparry vugs <1cm across; SAMPLE B3.5.
3	6.2-7.8	peloid/intraclast packstone; dolomitic; fine grained; porous; very light gray; cross-laminated?; intraclasts less than 1.0 X 0.5 cm; SAMPLE B6.7.
4	7.8-9.5	fenestral peloid packstone; fine grained; base forms bedding plane; thinly bedded; very light gray to buff; thin (<0.5cm) micritic layers; friable.
5	9.5-10.2	peloid packstone; light gray; base not exposed; fenestrae; fine to medium grained; rare laminations; medium bedded; SAMPLE B9.7.
6	10.2-12.5	laminated fenestral mudstone; flaggy, chippy, very thinly bedded; light gray to white; very fine grained; acicular and rosette crystals (replacement?) throughout unit; poorly exposed; SAMPLE B12.0.
7	12.5-13.5	peloid packstone; very fine grained; base not exposed; thinly bedded; light gray; very similar to bed 4; thin (<0.5cm) micritic layers; acicular anhydrite crystals (replaced by calcite?) in distinct horizons, especially just below partings; SAMPLES B12.8, B13.2.
8	13.5-14.4	laminated mudstone; flaggy, chippy, very thinly bedded; acicular crystals (replacement?); base apparently gradational; very light gray.

9 14.4-14.6 mudstone interlayered with breccias appx. 3 cm thick with angular clasts; fine grained; white; base poorly exposed; medium bedded; acicular crystals (replacement); intraclastic??; SAMPLES B14.5, B14.6.

10 14.6-29.2 covered (driveway)

11 29.2-30.9 cryptalgal laminite mudstone; thickly bedded; base not exposed; light gray; horizontal to LLH; base poorly exposed.

12 30.9-33.2 covered

13 33.2-33.6 mudstone to packstone; light gray; base not exposed; thick bedded; peloidal?; SAMPLE B33.3.

14 33.6-35.0 cryptalgal laminite mudstone; very fine grained; base abrupt, irregular (erosional?); light gray; locally intraclastic.

15 35.0-36.2 ooid/peloid/intraclast packstone/ grainstone; fine grained; base abrupt, irregular (erosional?); light gray to buff; massive; cross-laminated; SAMPLE B35.8.

16 36.2-36.8 ooid/intraclast packstone; fine to medium grained; gradational base; intraclasts all elongate (>4:1 H:W); planar to cross-laminated; SAMPLE B36.2.

17 36.8-38.6 ooid/peloid packstone/grainstone; thickly bedded; fine grained; base forms bedding plane; light gray; some areas with abundant blocky calcite; planar to cross-laminated; SAMPLE B37.5.

18 38.6-38.8 mudstone; light gray to white; very fine grained; lower half of unit laminated, "caps" oolite below, upper half is less resistant, forms recess.

19 38.8-40.05 mudstone; base abrupt bedding plane; very fine grained; light gray; laminated?; SAMPLE B38.9.

20a 40.05-40.5 mudstone; fenestral; light gray; base gradational; SAMPLES B40.2, B40.5.

20b 40.5-41.8 peloid/intraclast packstone to grainstone; base abrupt, erosional, up to 3 cm relief; medium to coarse grained; medium to light gray; horizontal- to cross-laminated; coarsening upward cycles??; common sparry vugs, subhorizontal; massive; dolomitic, porous; central

portion cryptalgal laminites; SAMPLES B40.2, B40.5, B41.7.

21 41.8-42.0 peloid/ooid? packstone; medium gray; base abrupt; horizontally laminated; very fine grained; SAMPLE B41.9.

22 42.0-42.3 cryptalgal laminite mudstone; very light gray to white; base abrupt; some small irregular fenestrae; less resistant; laminations planar; SAMPLE 42.2.

23 42.3-42.8 peloid/intraclast packstone to grainstone, dominantly intraclastic at base; cross-laminated; base abrupt, scalloped (erosional), up to 2 cm relief, truncating underlying laminae (in bed 22); light gray to buff; coarse to medium grained; shelter porosity; intraclasts up to 2 cm X 0.5 cm, elongate, many appear to be replaced by sparry calcite; intraclasts dominant in 0.2 m (intraclast grainstone); upper 2/3 mostly peloidal; SAMPLE B42.3.

24 42.8-42.9 cryptalgal laminite mudstone; base abrupt, bedding plane; weathered; mostly planar laminations; light gray.

25 42.9-43.0 intraclast/peloid packstone; medium to coarse grained; buff; fenestral; base erosional, up to 3cm local relief; intraclasts mostly bean shaped, bean sized; cross-laminae?.

26 43.0-43.3 cryptalgal laminite mudstone grading into fenestral laminated (algal??) peloid packstone; light gray; base abrupt? to planar; very fine grained.

27 43.3-43.4 intraclast/peloid packstone; buff; fine to coarse grained; base gradational; most intraclasts appear micritic, buff, bean shaped to slightly elongate; cross-to horizontally laminated; fenestrae; chert; SAMPLES B43.4 (3).

28 43.4-43.5 ooid/fossil grainstone; medium gray; base abrupt, scalloped; fine to coarse grained; abundant spar.

29 43.5-43.9 peloid/ooid packstone/grainstone; medium gray in lower half, light gray in upper half; fine to medium grained; thickly bedded; planar to cross laminated; erosional? base; SAMPLE B43.8.

30 43.9-44.2 mudstone; locally fenestral, especially in upper half; light gray to buff; thinly bedded; very fine grained; base gradational.

31 44.2-44.35 cryptalgal laminite mudstone; base abrupt, planar; light gray; laminations

LLH to planar; mound morphologies?, up to 0.5 m across and grossly undulatory.

32 44.35-46.0 peloid packstone, base intraclastic; locally laminate, fenestral; light gray to buff; base abrupt, erosional, irregular to scalloped; rare intraclast layers; sucrosic dolomite in upper 0.2 meters; SAMPLES B44.5, B44.35; B45.3.

33 46.0-47.1 cryptalgal laminite mudstone; buff to light gray; laminations planar to LLH; base abrupt, planar?; weak unit; thrombolitic??; fenestral?; SAMPLE B47.0.

34 47.1-48.8 covered, but float chips are cryptalgal laminite mudstone

35 48.8-49.8 cryptalgal laminite mudstone; base and top not exposed; buff; fine sucrosic texture; fenestral.

36 49.8-50.9 covered

37 50.9-51.8 peloid/ooid/intraclast grainstone; medium to coarse grained; base not exposed; thickly bedded; cross-laminated; intraclasts less than 1.5 x 0.25 cm, rounded; porous; very light gray; well sorted; sucrosic texture, more pronounced upwards; SAMPLE B51.5 (from 51.2), B51.3, B51.8.

38 51.8-53.0 cryptalgal laminte mudstone; base planar; light gray; massive; laminations planar 'crinkly'; possible teepee structures; SAMPLE B52.9.

39 53.0-53.8 ooid/peloid/intraclast packstone/ grainstone; medium grained; base abrupt, irregular; light gray to white; thick bedded; SAMPLE B53.2.

40 53.8-54.5 cryptalgal laminite mudstone; buff to light gray; base gradational?; SAMPLE B54.0.

41 54.5-55.8 cryptalgal laminite mudstone; light gray; laminations planar to LLH; base abrupt, planar.

42 55.8-56.1 mudstone; buff to light brown; sparry voids (dissolution?) encircled by reddish rims?; base stylolitized.

43 56.1-56.2 ooid grainstone; fine grained; base abrupt, irregular; buff.

44 56.2-58.4 fenestral mudstone; base forms bedding plane; buff to brown; sucrosic texture more pronounced upwards; very friable; petroliferous odor;

SAMPLE B56.3.

45 58.4-58.8 cryptalgal laminite mudstone; light gray; base abrupt, planar; laminations planar to LLH.

46 58.8-60.5 mudstone with very thin (<2cm) packstone layers/lenses; base abrupt; grayish brown; clotted texture; very fine grained; voids up to 1 cm partly filled with spar; mudcracks; SAMPLES B58.9, B59.7, B60.5. Interval from 60.3-60.4 contains discontinuous exposure-altered interval; not traceable laterally more than 5 m; light to medium gray; SAMPLE B60.31

48 60.5-60.9 cryptalgal laminite mudstone; base abrupt, locally bedding plane; light gray; SAMPLE 60.9

49 60.9-61.3 laminite; extensively altered; see SAMPLE 61.0

50a 61.3-61.8 cryptalgal laminite; light pinkish gray; planar laminations.

50b 61.8-63.0 peloid packstone/grainstone with rare intraclasts; base unclear (gradational?); cross-laminated; intraclasts elongate, rounded; many grains appear to have micritized rim; light pinkish gray; finer grained upwards; ; sparry voids (<1cm) common; SAMPLES B61.9

50c 63.0-63.4 cryptalgal laminte; planar laminations; base unclear.

50d 63.4-63.7 peloid/intraclast packstone to grainstone; medium to coarse grained; some grains dissolved?; some grains are dark reddish micrite. SAMPLE B63.5.

51 63.7-64.6 mudstone; medium to dark gray; fine grained; burrow-mottled??; base bedding plane; thick bedded; SAMPLE B63.9.

52 64.6-70.6 ooid/oncoid grainstone; medium to dark gray; fine to medium grained; some fossils.

53 70.6-76.8 other subtidal lithologies, especially burrow-mottled mudstone.

-------Nolichucky Formation-------

54 76.8 ---- paper-laminated shale

IS Section

Section is exposed in roadcuts on south side of Interstate 40, approximately 1.5 km east of Deep Springs Road. Lower 30 m of section is fairly well exposed; upper 34 m is extremely well exposed. Samples with an "n" suffix (ie. 28.9n) represent newer samples that were collected on a trip subsequent to the original section measuring. On this trip, many units were subdivided, and hence many of my original bed numbers were modified. Beds that were subdivided have suffixes, indicating relative order (ie. 1a, 1b, etc). This section is one of the two primary "tidal flat sections." The base of the peritidal package is not exposed, but a total of 36 m of it is present. Above this is the 28 m-thick backstepping shelf-platform package.

bed number	cumulative thickness	description
		--------- MARYVILLE LIMESTONE ----------
		-- base not exposed --
1a	0.0-0.9	breccia grading up into cryptalgal mudstone above 0.6m; base not exposed; very fine grained; light gray to buff; web-like fabric in breccia; breccia composed of angular to subrounded mudstone; planar laminations; teepee structures??;SAMPLES Hy0.2, Hy0.9.
1b	0.9-1.55	intraclast packstone; channel morphology, up to 0.65 m thick, but quickly thins laterally to 0.2 m; erosional base; from 0.85-1.05, numerous vugs (~2cm across) partly filled with calcite; intraclasts up to 5 cm, elongate to bean shaped, larger ones broken (ie. pre-lithified).
[2	1.4-1.55]	chert; cryptocrystalline; light to dark gray; roughly stratiform, but unit pinches out laterally; present only above thickest part of unit 1b; some irregular laminations; irregular, abrupt erosional (?) upper and lower contacts, undulose over meter scale; SAMPLE Hy1.54 (from where no chert, rather like unit 1).
3a	1.55-2.1	cryptalgal laminite mudstone; base abrupt, irregular, up to 0.2 m relief; buff; massive; laminites planar to LLH, paper thin to 1 cm thick; in general, more thick laminations upwards (up to 50%); mudcracks??; SAMPLE Hy1.8.
3b	2.1-2.6	peloid/intraclast packstone; medium to coarse grained; base erosional to stylolitized, up to 0.2 meters relief, unit thickens and thins laterally; unit also contains SH stromatolite, flanked by peloidal material; SH 0.1m across, up to 0.2m tall; SAMPLE Hy2.1n.

4 2.6-3.5 cryptalgal laminites interbedded with peloid/intraclast packstone to wackestone; fenestral; light orange to buff; base irregular; fine to medium grained; SAMPLE Hy2.9.

5 3.5-4.7 peloid packstone grading (?) up into fossil?? packstone; lower packstone buff, medium to coarse grained, with laminar fenestrae and rare intraclasts; upper very fine grained, medium gray, burrowed?; some laminations; base irregular bedding plane; SAMPLE Hy4.0, Hy4.1n, Hy4.5.

6a 4.7-5.1 cryptalgal laminite; planar laminations; base abrupt, planar?; light gray; upper 0.2 m thick laminite, buff to light gray; SAMPLE Hy4.9n.

6b 5.1-5.4 laminated mudstone to intraclast/peloid packstone; coarse grained; dolomitized; brecciated??; base abrupt, planar?; light buff; thick (<1cm) to paper-thin laminations; SAMPLE Hy5.2n.

6c 5.4-7.6 peloid packstone; intraclastic near base; light gray; base abrupt, irregular; some laminations; SAMPLE Hy5.4n.

7 7.6-8.5 cryptalgal laminite mudstone; very fine grained; base gradational?; light brown to buff; laminations from paper thin to 7mm thick, 'crinkly' dessication (??) features common; rare lenses (?) of intraclastic wackestone to packstone (fine to coarse grained, medium gray, peloidal, often overlain by micritic drape); SAMPLES Hy7.6, Hy8.1n, Hy8.4.

8a 8.5-8.9 intraclast/peloid packstone; medium to coarse grained; light gray; base abrupt, planar; intraclasts rounded, bean shaped, up to 1.5 X 0.8 cm large; distinct layers more intraclast-rich.

8b 8.9-9.1 cryptalgal laminite mudstone; base abrupt to stylolitized; light gray to buff; planar laminations.

8c 9.1-9.3 peloid/ooid packstone; medium to fine grained; base abrupt, planar; intraclastic near base, intraclasts made of laminite; cross-laminated.

8d 9.3-9.45 cryptalgal laminite mudstone; light gray to buff; base gradational to abrupt.

8e 9.45-9.6 intraclast/peloid/ooid packstone; intraclasts elongate, rounded, often imbricate, up to 2 X 0.25 cm large; cross-laminated; base abrupt, planar to stylolitized; SAMPLE Hy9.6.

8f 9.6-9.7 cryptalgal laminite mudstone; base unclear; light buff to light gray; poorly exposed.

9 9.7-11.7 ooid/intraclast/peloid packstone; light brown to light gray; base abrupt, erosionally scalloped and undulatory (0.3 m horizontal difference over 3 m lateral interval); graded beds; cross laminated locally; pseudo-laminated in lower part due to horizontally alligned intraclasts; intraclasts up to 2 cm long, most flat, rounded to subrounded, laminated; ooids concentrated in clusters (intraclasts?); above 11.0m, peloidal packstone with lesser ooids; SAMPLES Hy9.7, Hy10.5, Hy11.4.

10 11.7-14.1 peloid/intraclast packstone, locally oolitic; mostly intraclastic near base, peloidal above 12.5; light gray to buff; massive; poorly exposed; more dolomitic, orange near top; fine to coarse grained; thick laminations, locally cross-laminar; laminar fenestrae; intraclasts rounded, elongate to circular, from peloidal size to 3 cm X 1 cm; SAMPLES Hy12.2n, Hy12.5, Hy12.7, Hy13.5, Hy13.9n, Hy14.0.

11 14.1-14.4 peloid packstone; buff; fine grained; laminar fenestrae; base gradational; less resistant; SAMPLE Hy14.2n

12 14.4-16.4 peloid/intraclast/ooid packstone; light gray; base not exposed; fine to coarse grained; dolomitic; thick to thin bedded intraclasts elongate, rounded, no larger than 1 cm X 0.2 cm; from 15.2-15.4, ; pseudo-laminar due to parallel allignment of intraclasts; fenestrae (laminar to irregular) in scattered, discontinuous mudstone/wackestone layers weather out; local thin (<5mm) cryptalgal? laminite layers; herringbone cross-stratification??; SAMPLES Hy14.5, Hy15.2, Hy15.4, Hy16.1.

13 16.4-17.2 mudstone grading up to thick laminite; medium gray to buff; gradational base; mudcracks at 17.0 SAMPLES Hy16.4n, Hy16.5, Hy17.0.

14 17.2-17.9 mudstone, slightly silty near top; very fine grained; base gradational (?); light gray to light purplish gray; fenestrae abundant; thickly bedded; stylolites common; upper 0.2 m contains several thin (<1cm) peloidal/intraclast wackestone/packstone layers and some (algal??) laminations; SAMPLES Hy17.2, Hy17.7.

14b 17.9-18.1 cryptalgal laminite mudstone; buff.

15 18.1-18.9 mudstone; very fine grained; thickly bedded; light gray to light brown; completely dolomitized; base stylolitized to gradational (?); small

(<1cm) calcite-filled voids fairly common; SAMPLES Hy18.1, Hy18.2.

16 18.9-19.8 peloid/intraclast packstone to wackestone; rare ooids; base planar, abrupt; light brownish gray; intraclasts bean shaped to slightly elongate, all <1 cm; in general, more fenestral and coarsening upward (fine to medium grained near base, coarse near top); SAMPLES Hy19.0, Hy19.7.

17 19.8-20.2 mudstone to thick laminite; base apparently gradational; buff to light gray; fenestral; SAMPLE Hy20.0.

18 20.2-21.6 cryptalgal laminite mudstone; buff to light gray; stylolitized base; laminations planar to crinkly; fenestrae; rare mudstone lenses; SAMPLE Hy20.6.

19 21.6-22.5 ooid/peloid/intraclast packstone; light pinkish buff; medium to coarse grained; base erosional; intraclasts similar lithology to bed 18; irregular fenestrae; SAMPLES Hy22.0, Hy21.6an, Hy21.6bn, Hy22.4n.

19a 22.5-22.6 exposure altered interval; light red; dissolution voids? oolitic parent?.

20 22.6-23.8 mudstone; cryptalgally laminated upwards; locally intraclastic (<1cm, elongate) layers <2cm thick; light purplish gray; base forms bedding plane; irregular, contorted laminations present near top SAMPLES Hy22.6, Hy 23.0n, Hy23.5n.

21 23.8-24.1 cryptalgal laminite clasts?? overlain by peloid/ooid?? packstone/grainstone to intraclast/peloid packstone/grainstone; medium to coarse grained; buff to light pinkish gray; lower contact erosional; intraclasts rounded, elongate to bean shaped, show shelter porosity; SAMPLE Hy23.8n, Hy23.9, Hy24.0n.

22 24.1-25.3 cryptalgal laminite to thick laminite; locally intraclastic; poorly exposed.

23a 25.3-25.6 cryptalgal laminite; very fine grained; base forms bedding plane; planar to slightly undulatory laminations; light pinkish gray; SAMPLE Hy25.6bn.

23b 25.6-25.7 exposure altered interval; pinkish red; dissolution voids?.

23c 25.6-26.5 cryptalgal laminite mudstone; fine grained; irregular fenestrae; buff to light pinkish gray; base abrupt, irregular; teepee structures; SAMPLE

Hy25.7n.

24a 26.5-29.2 peloid/intraclast packstone to grainstone; base fine grained burrow homogenized mudstone; fine to medium to coarse grained; irregular fenestrae; buff to light pinkish gray; base not exposed; SAMPLES Hy26.5n, Hy27.5n, Hy27.6n.

24b 29.2-29.4 mudstone to thick laminite; very fine grained; base gradational?; buff to light gray.

24c 29.4-29.8 cryptalgal laminite coarsening up to thick laminite; buff; very fine grained; irregular fenestrae; SAMPLE Hy29.6n. Exposure-altered interval from 29.6-29.7.

24d 29.8-30.5 intraclast packstone; base sharp; light gray to buff; intraclasts up to 2 cm X 1 cm; SAMPLE 30.1n

24e 30.5-31.0 cryptalgal laminite mudstone; light gray to buff; base forms bedding plane; thin (<2 cm) peloidal/intraclastic lenses?; SAMPLE Hy 30.9n.

24f 31.0-31.3 intraclast/peloid packstone; light to medium gray; base obscured; coarse grained; intraclasts micritic, up to 3 cm long; SAMPLE Hy31.1n.

24g 31.3-31.4 mudstone; medium gray; very fine grained; poorly exposed.

24h 31.4-32.2 thick to thin laminite mudstone; light gray with touch of red; very fine grained; base obscured; SAMPLE Hy31.5n..

25a 32.2-33.0 peloidal packstone to mudstone with scattered intraclast/peloid packstone layers, quickly grading up into cryptalgal laminite mudstone with rare peloidal packstone layers; erosional base?; from 32.9-32.92 peloid/intraclast packstone; fine to coarse grained; poorly sorted; sharp planar to irregular (scoured??) base; Intraclasts up to 3 cm long, elongate to bean shaped; rounded; SAMPLE Hy 32.7.

25b 33.0-33.05 exposure latered interval; SAMPLE Hy 33.0.

25c 33.05-34.3 cryptalgal laminite mudstone with scattered peloidal/intraclast packstone layers; fine grained; SAMPLE Hy 33.8.

25d 34.3-34.7 exposure altered interval; blood red; extensive dissolution; erosional? base; SAMPLE Hy 34.3.

25e 34.7-36.0 cryptalgal laminite mudstone; uppermost 0.2 meters intraclast packstone

with darker brown/black mottles; SAMPLE Hy 36.0.

26 36.0-36.5 mudstone; base stylolitized; medium gray; very fine grained; quartz(?); stylolites; several centimeter-sized spar-filled voids; upper part laminated, undulatory, at times intraclastic; SAMPLE Hy36.5.

27 36.5-36.7 fossil (?) packstone; quartz-rich (??); fine to medium grained; well sorted; base undulatory, gradational; cross-bedded; locally oncoidal near top; SAMPLE Hy36.7.

28 36.7-36.9 oncoid/peloid packstone to grainstone with rare intraclasts; base abrupt, scalloped to irregular; medium gray; oncoids dolomitized, mostly ~3 cm, well sorted; discontinuous peloidal stringers; intraclasts elongate, rounded, up to 2cm by 0.5 cm in size; SAMPLE Hy36.8.

29 36.9-37.1 mudstone; base stylolitized; medium to dark gray; several oncoid to peloid packstone-grainstone lenses with scalloped bases and irrgeular, abrupt tops, fine to medium grained -- these lenses locally dominate the unit; locally laminated; SAMPLE Hy36.9.

30 37.1-39.3 ooid (??) grainstone; base planar, abrupt to stylolitized; fine grained; medium to dark gray; cross-laminated; intraclasts common in several zones: 37.1-37.25 (IC rounded, circular to (less commonly) elongate, made of oolitic lithology also; up to 3 cm long), 37.85-37.95 (most circular, rounded up to 2 cm long); mudstone layers at 37.45-37.55, (bounded by stylolites, fine grained, laminated, rare discontinuous intraclast/ooid grainstone lenses), 38.25-38.3 (locally laminated, unburrowed); discontinuous oncoidal layer at 37.6; small irregular voids in this unit upwards; prominent bedding planes at 37.7, 37.85; calcite filled burrow (??) rich interval from 38.1-38.25; 38.3-38.6, fining upward medium to coarse grained ooid/oncoid packstone/grainstone; SAMPLE Hy38.3.

31 39.3-39.8 oncoid/peloid/fossil/ooid grainstone; base stylolitized; fine to coarse grained; medium grained; bi-directional cross-laminations; rare intraclasts (up to 2 cm long); SAMPLE Hy39.7.

32 39.8-40.0 fossil/ooid grainstone; base stylolitized; medium gray; fine grained; cross-laminated; SAMPLE Hy40.0.

33 40.0-40.3 fossil/ooid wackestone to packstone; fine grained; medium gray; base stylolitized to abrupt;burrows filled with spar (?); local laminations, accentuated by grains; common cm-sized vugs, filled with spar; prominent stylolite at 40.2; SAMPLE Hy40.3.

34 40.3-40.6 ooid/fossil grainstone, grading(?) up into oncoid?/intraclast??/fossil grainstone; base gradational to styloitized; medium to coarse grained; muddy lenses fairly common; most oncoids fairly well sorted, replaced by dolomite and less commonly sparry calcite; sparry vugs up to 3 cm large common; SAMPLES Hy40.3, Hy40.5.

35 40.6-41.0 fossil/ooid grainstone; fine to medium grained; base forms prominent bedding plane; medium gray; several large (up to 4 cm) spar filled voids, most commonly elongate parallel to bedding; rare intraclasts (<1.5 cm long, elongate, lying parallel to bedding); cross-laminated??; this unit gradationally interfingers with unit 36 -- where it does, usually intraclastic/fossil grainstone (intraclasts up to 3 X 4 cm, rounded); SAMPLE Hy40.6.

36 41.0-41.25 mudstone to packstone; light reddish gray; base stylolitized to gradational to interfingering; fossils/ooids???; fine grained; numerous burrows from 41.0-41.2, most commonly spar filled; above 41.2, burrows weather out; numerous dissolution vugs, up to 0.1m across, commonly only partly filled with calcite; SAMPLE Hy41.2.

37 41.25-41.4 fossil/intraclast?? packstone; base stylolitized; medium to dark gray; medium to coarse grained; brecciated???; SAMPLES Hy41.4, Hy41.4HS

38 41.4-41.5 fossil/intraclast?/ooid grainstone; fine grained; base gradational; dark gray; stylolitized; fairly common small (<2mm) sparry vugs; SAMPLE Hy41.5.

39 41.5-41.75 oncoid/intraclast packstone; base forms bedding plane; medium gray; medium to coarse grained; 2 "cycles": the lower half of the unit is fining upward [very coarse oncoids to coarse oncoids and fossils] overlain by a more-muddy upward unit; contact between these is sharp, planar to scalloped; locally, uppermost 2 cm is finely laminated mudstone; rare mudstone lenses between "cycles"; SAMPLES Hy41.75, Hy41.6.

40 41.75-42.7 fossil/intraclast grainstone; base forms undulatory bedding plane; dark gray; medium to coarse grained; locally laminated to cross ?? laminated; intraclasts (rounded, elongate to bean shaped, imbricated; up to 4 cm long; appear to be made of skeletal packstone; often have shelter porosity beneath them) dominate lower half; stylolites; upper 0.2 m contains numerous partly filled vugs; appears to be two fining upwards cycles -- one from base to 42.4, other from 42.4 to top;

SAMPLE Hy42.4.

41 42.7-42.9 fossil packstone/grainstone (fine grained) grading up into oncoidal/intraclast packstone grainstone (coarse grained); base stylolitized; medium gray; numerous elongate, unoriented microspar filled voids (burrows??); SAMPLE Hy42.8.

42 42.9-43.2 mudstone; burrow-mottled; base stylolitized; medium gray with slight brownish tint; distinctive large (up to 0.1 m) dissolution? voids, partly filled with calcite; locally laminated.

43 43.2-43.9 ooid packstone/grainstone; fine to medium grained; base stylolitized; medium to dark gray; stylolites; rare small (<1cm) intraclasts; cross-laminated?; mudstone layers at: 43.4-43.42 (very fine grained; elongate spar filled 'burrows'), 43.5-43.53 (laminated, very fine grained), 43.8-43.82 ('burrows' and laminations); SAMPLE Hy43.6.

44 43.9-44.0 oncoid/intraclast/fossil packstone/ grainstone; medium gray; base stylolitized; coarse to medium grained; unit thickens laterally; oncoids - some dolomitized, others show laminations; intraclasts mostly elongate, rounded, up to 5 cm long, imbricated; echinoderm and trilobite fossils; SAMPLE Hy44.0.

45 44.0-44.3 fossil/ooid/peloid/intraclast/oncoid packstone to grainstone; fine to caorse grained; base gradational to stylolitized; moderately burrow-mottled; mega-ripple?? or fine grained material overlain by coarser material capped by laminations at 44.1; SAMPLE Hy44.2

46 44.3-45.1 mudstone; burrow-mottled; base gradational, drawn where grains become less common and burrows dominant; fine to coarse grained; massive; rare small (<2cm) dissolution voids; packstone/grainstone layers at: 44.72-44.74 (fossil/peloid/oncoid packstone; base stylolitized, top gradational; coarse to medium grained), 44.8-44.9 (fossil/oncoid/peloid packstone; base stylolitized, top abrupt, irregular; intrafingers with mudstone), 44.97-45.03 (oncoid/fossil packstone/grainstone; base and top stylolitized; coarse grained); basal part of unit quite grainy, but still burrowed.

47 45.1-47.5 ooid/fossil/oncoid/intraclast packstone to grainstone; medium to coarse grained; base irregular, scalloped; massive; basal 1.0 meters contains primarily ooids with fossils and some intraclasts (<3cm long, rounded, circular to elongate); from 46.1-46.8, dominantly ooid/fossil grainstone with rare oncoids, cross laminated, fine to medium grained, oncoids more common from 46.6-46.8, intraclasts

throughout; from 46.8-46.9, oncoid/fossil packstone, medium to coarse grained, seemingly more muddy than below; from 46.9-47.5, ooid/fossil/oncoid grainstone, grading up into oncoid/ooid/fossil grainstone in uppermost 0.1 meter. fine to coarse grained, intraclasts in basal 0.1 m (rounded, elongate, <1.5cm), ooids appear dolomitized, oncoids undolomitized, cross-laminated?; SAMPLES Hy45.2, Hy45.6, Hy 46.5, Hy47.4.

48 47.5-48.1 burrow-mottled mudstone to wackestone; intimately interlayered with oncoid/fossil packstone to grainstone; grainy layers have sharp, planar to scalloped bases, abrupt, but gradational tops; numerous open vugs (up to 3 X 3 cm) in muddy layers, other vugs appear to be filled with black?? material.

49 48.1-48.5 ooid/fossil/oncoid/intraclast grainstone; lower contact gradational to interfingering; fine to coarse grained; echinoderms and trilobites common; intraclasts mostly less than 1 cm, rounded, circular, reddish; numerous voids filled with black material??; ooids dolomitized; fairly small dissolution?? voids; iron oxide?? stains at top of unit; SAMPLES Hy45.5, Hy45.5HS.

50 48.5-49.1 calcareous siltstone; finely laminated; base abrupt, scalloped, up to 0.4 meters relief; medium gray to brown; rare pyrite; rare small (<1cm) open calcite-lined vugs; SAMPLE Hy49.0.

51 49.1-52.6 burrow-mottled mudstone/wackestone; base gradational over 0.2 meters; medium gray; irregular mottle pattern; very fine grained; thin (<5cm) continuous fossil to intraclast/fossil packstone/grainstone layers, more common upwards, towards the top, comprise 40% of unit, from 50.5 to top, often have channel morphology (up to 0.15m high by 3-5m wide) and imbricate intraclasts (up to 4 cm long); silty often in layers above thicker intraclast-rich zones; rare small (<1cm) calcite-lined vugs; SAMPLES Hy51.4, Hy51.6.

52 52.6-52.85 peloid/intraclast/fossil packstone; medium to coarse grained; medium gray; base abrupt, stylolitized; fairly well sorted; intraclasts mostly <1cm, rounded, bean shaped, some dolomitized; thin burrow mudstone lenses.

53 52.85-53.15 burrow-mottled mudstone; base abrupt, stylolitized; locally laminated; some pyrite.

54 53.15-53.35 ooid/peloid packstone/grainstone with rare intraclasts; base abrupt, stylolitized to scalloped; cross-laminated; fine to medium grained;

ooids appear dolomitized; intraclasts rounded, bean shaped, up to 1.5cm; some rather large (up to 1 cm) trilobite fragments near top; SAMPLE Hy53.3.

55 53.35-54.1 burrow-mottled mudstone to wackestone; thin lenses of very fine grained fossil packstone/grainstone throughout; laminated.

56 54.1-55.5 fossil/ooid packstone/grainstone rapidly grading up into ooid grainstone with rare fossils; base abrupt, irregular to stylolitized; medium gray; echinoderms; rare intraclasts near base; cross-laminated; fine grained; SAMPLE Hy54.9.

57 55.5-55.65 burrow-mottled wackestone; base abrupt, irregular; very fine grained; burrows dolomitized, horizontal; rare pyrite.

58 55.65-57.1 ooid grainstone, fossiliferous near base; base stylolitized; medium gray; fine grained; scattered intraclasts.

59 57.1-57.3 burrow-mottled mudstone; stylolitized base; medium to dark gray; burrows dolomitized, horizontal.

60 57.3-61.9 fossil/oncoid packstone/grainstone; medium to very coarse grained; trilobites and echinoderms common; pyrite; from 61.4-61.55, burrowed packstone; from 61.55-61.86, oncoid fossil grainstone, very coarse oncoids, up to 1 cm across; uppermost 3 cm laminated packstone?, very fine grained; SAMPLE Hy61.9.

61 61.9-63.2 burrow-mottled mudstone with distinct fossil/peloid packstone lenses (fine to medium grained, often overlain by mudstone layer); medium gray; some laminations.

62 63.2-64.6 fossil/oncoid/peloid packstone to grainstone; base abrupt, irregular; medium gray; medium to coarse grained; many allochems dolomitized and weather buff; laminated; oncoids dominate lower half; SAMPLES Hy63.2, 63.3, 64.6.

----------Nolichucky Shale----------

63 64.6----- paper laminated shale; SAMPLE Hy64.7

Sevierville Recycling Center

This section is located on TN139E, appx. 1.5 miles south of Kodak, TN, 0.2 miles north of West Mount Road. The uppermost Maryville and lowest Nolichucky are very well exposed in an old quarry, which now serves as the Sevierville Recycling Center. No peritidal facies are present at this location, even though 4 km in either direction, peritidal facies are present.

bed number	cumulative thickness	description
		----------Maryville Limestone----------
1	0.0-0.7	peloid/ooid packstone; massive; base not exposed; very fine-grained; trilobites?; medium to dark gray.
2	0.7-2.2	peloid-ooid grainstone; thickly bedded; base abrupt; fine grained; above 1.1 m, grades upward into oncoid/fossil packstone to grainstone; medium to coarse grained; medium to dark gray; uppermost 0.2 m is peloid packstone.
3	2.2-3.9	interlayered burrow-mottled mudstone and oncoid/peloid/ooid packstone grainstone layers/lenses; medium to dark gray; base gradational; grainy layers have abrupt base (up to 3 cm relief), some are cross-laminated, all are less than 5 cm thick.
4	3.9-4.2	ooid/trilobite packstone; medium to dark gray; medium grained; base gradational to irregular.
5	4.2-4.9	burrow-mottled wackestone to packstone with grainy (ooid/oncoid) lenses/layers (<5 cm thick); medium to dark gray.
6	4.9-5.5	oncoid/ooid grainstone; medium to coarse grained; base abrupt bedding plane; medium to dark gray.
7	5.5-5.8	ooid/oncoid grainstone; fine to medium grained; base gradational?; medium to dark gray.
8	5.8-7.6	basal ooid grainstone overlain by oncoid/fossil/ooid packstone to grainstone; overall coarsening-up, from fine to medium-coarse grained; SAMPLE SQ 7.0.
9	7.6-8.1	burrow-mottled mudstone; base gradational; dark gray; pyrite?; SAMPLES SQ 8.1, SQ 8.0.

10 8.1-14.1 burrow-mottled mudstone, grading up into finely laminated ribbon-rock; burrow-mottled layers are thickly bedded with dolomitized burrows; ribbon-rock is finely laminated, with regular dolomitized layers, and ripple forms and ripple cross-laminae; rare pyrite; rare thin (< 5cm) lenses of oncoid/intraclast packstone.

11 14.1-18.2 burrow-mottled mudstone; base gradational; medium to dark gray; burrows dolomitized; thin grainy lenses; rare trilobites.

12 18.2-19.4 ooid/fossil/oncoid? packstone/grainstone; fine to medium grained; medium gray.

13 19.4-19.6 burrow-mottled mudstone; base stylolitized.

14 19.6-21.4 ooid grainstone; fine to medium grained; intraclastic near base; medium gray; SAMPLE SQ 19.6.

15 21.4-23.4 peloid/oncoid/ooid? packstone to grainstone; medium gray; medium grained; base is prominent bedding plane.

16 23.4-30.4 peloid/oncoid/fossil/ooid packstone; base forms bedding plane; ,assive bedded; medium gray; SAMPLE SQ 28.3.

17 30.4-30.8 burrow-mottled mudstone; nase unclear (gradational?); dark gray; prominent bedding plane runs through middle of unit.

18 30.8-34.6 oncoid/fossil/ooid grainstone; fine to coarse grained; base unclear; massive.

19 34.6-34.7 quartz silt peloid packstone; thickly bedded; medium gray.

20 34.7-36.2 oncoid/ooid/fossil grainstone; medium to coarse grained; coarsening-upward; abundant trilobites in upper part; SAMPLE SQ 34.8.

21 36.2-36.4 burrow-mottled mudstone/wackestone with oncoid/peloid packstone grainstone layers; quartz silt.

22 36.4-38.1 interbedded oncoid/trilobite grainstone and quartz silty peloid packstone; grainy layers have erosional base; medium to coarse grained.

----------Nolichucky Shale---------

23 38.1 + shale to quartz silty packstone

IS Section cycle num.	range*	DFT**	cycle thick***	intra/supra thick***	subtidal thick***	% IS
22	35.8-36.0	0.2	0.2	0	0.2	0%
21	34.3-35.8	1.7	1.5	1.5	0	100%
20	33.1-34.3	2.9	1.2	1.2	0	100%
19	32.2-33.1	3.8	0.9	0.6	0.3	67%
18	31.0-32.2	5	1.2	0.8	0.4	67%
17	29.8-31.0	6.2	1.2	0.5	0.7	42%
16	29.6-29.8	6.4	0.2	0.2	0	100%
15	26.5-29.6	9.5	3.1	1.5	1.6	48%
14	23.8-26.5	12.2	2.7	2.4	0.2	89%
13	22.6-23.8	13.4	1.2	1	0.2	83%
12	21.6-22.6	14.4	1	0.2	0.8	20%
11	18.9-21.6	17.1	2.7	2.3	0.4	85%
10	14.4-18.9	21.6	4.5	3.8	0.7	84%
9	9.7-14.4	26.3	4.7	1.4	3.3	30%
8	9.5-9.7	26.5	0.2	0.1	0.1	50%
7	9.1-9.5	26.9	0.4	0.2	0.2	50%
6	8.5-9.1	27.5	0.6	0.2	0.4	33%
5	5.1-8.5	30.9	3.4	0.9	2.5	26%
4	3.5-5.1	32.5	1.6	1.2	0.4	75%
3	2.1-3.5	33.9	1.4	0.9	0.5	64%
2	0.9-2.1	35.1	1.2	0.5	0.7	42%
1	0.0-0.9	36	0.9	0.9	0	100%
	IS averages (n=22):		1.71	0.62	1.03	

SR Section cycle num.	range*	DFT**	cycle thick***	intra/supra thick***	subtidal thick***	% IS
22	63.4-63.7	0.3	0.4	0	0.4	0%
21	61.8-64.3	1.9	1.6	0.4	1.2	25%
20	61.3-61.8	2.4	0.5	0.5	0	100%
19	60.4-61.3	3.3	0.9	0.9	0	100%
18	56.1-60.4	7.6	4.4	2.4	2	55%
17	53.0-56.1	10.7	3.1	2.3	0.8	74%
16	50.9-53.0	12.8	1.1	0.2	0.9	18%
15	covered interval					
14	44.3-47.1	19.4	2.8	1.8	1	64%
13	43.3-44.3	20.4	1	0.5	0.5	50%
12	42.3-43.3	21.4	1	0.5	0.5	50%
11	40.5-42.3	23.2	1.8	1	0.8	56%
10	35.0-40.5	28.7	5.5	2.5	3	45%
9	33.5-35.0	30.1	1.4	1.4	0	100%
	SR average (n=13):		1.96	0.85	1.11	

* range = stratigraphic interval, measured from base of measured section; in meters

DFT = distance from base of cycle to top of peritidal package; * = in meters

Cycles in SR section are numbered 9-22 to facilitate direct comparison with IS section cycles; note that cycle 22 = top

APPENDIX C - Lithologic Transition Table: Peritidal Package, Maryville Limestone

IS section

		overlying lithology							
		exp alt	cryptal	ooid w/	IC p/g	peloid p	mudsto	thick la	*total across*
	Exp-alt		4	0	0	1	0	0	*5*
	cryptalgal	3		2	7	4	1	0	*16*
underly.	ooid w/p	1	0		0	1	0	0	*2*
lithology	IC p/g	0	5	0		3	2	0	*10*
	pel. p/g	0	4	0	1		2	2	*9*
	mudstone	1	3	0	1	1		0	*7*
	thick lam	0	1	0	0	0	1		*2*
	total down	*5*	*17*	*2*	*9*	*10*	*6*	*2*	

SR Section

		overlying lithology							
		exp-alt	cryptal	ooid w/	IC p/g	peloid p	mudsto	thick la	*total across*
	exp-alt		4	2	0	0	0	0	*6*
	cryptalgal	3		2	1	4	2	0	*12*
underly.	ooid w/p	0	1		0	1	2	0	*4*
lithology	IC p/g	0	1	1		0	0	0	*2*
	pel. p/g	0	4	0	1		3	0	*8*
	mudstone	1	3	1	0	2		0	*7*
	thick lam	0	0	0	0	0	0		*0*
	total down	*4*	*13*	*6*	*2*	*7*	*7*	*0*	

Note: vertical and horizontal totals dissimilar because of covered intervals

APPENDIX D - Carbon, Oxygen, and Strontium Isotope Data

Calcite spar from inter- and intragranular porosity from girvanella oncoids and Renalcis (Maryville) and wholesale and fabric-selctive dissolution voids (Craig)

Maryville data is taken DIRECTLY from Srinivasan (1993); the Craig Ratios and Strontium ratios presented here represent new data

The following are isotope ratios from the Maryville:

Sample No:	d 18O	d 13C	Petrographic features
W.G. 31.8mab	-8.9	0.16	Clear coarse calc.spar , intergranular pore space
28.8 mab	-9.1	0.27	Clear coarse calc.spars in oncoids
12.1 mab	-9.2	0.15	Clear calc.spar, intergranular pore space
14.1 mab	-9.5	-0.1	Clear calc spar, intergranular porosity
17.8mab	-8.6	0.36	Clear spar, pore central
25 mab	-9.2	0.38	Clear spar from girvanella oncoids
W.G. 19.6m	-8.6	0.01	Clear , coarse calcite spar, intergranular porosity
	-9.5	-1.4	Intergranular, clear calc.spar
W.G. 33.8m	-9.5	0.1	Intragranular, clear calc.spar, coarse
W.G 30.2m	-9.7	-0.39	do
W.G 21.1m	-9.1	-0.92	
W.G. 8.0m	-9.4	0.72	Intergranular, clear calc.spar
Date: 06/04/91			
W.G. 34.6m	-9.6	-0.03	Intragranular, clear, blocky calcite spar
W.G. 26.2m	-9.4	0.24	do
W.G. 27.6m	-9.3	0.1	Intragranular clear blocky calcite spar
W.G. 24.1m	-9.6	0.15	Intergranular, clear blocky calcite spar
W.G. 45.8m	-9.7	0.06	do
Date: 06-06-91			
GS 30.8m	-9.24	-0.04	Intragranular, clear, blocky calcite spar
W.G. 20.4m	-8.95	0.3	Intragranular, clear, blocky calcite
W.G. 15.2m	-9.9	-0.04	?

The following are isotope ratios from the Craig

Gr 29.1	-11.3	-0.18	clear, blocky calcite in large dissolution voids
Gr 29.1	-10.8	-0.51	clear, blocky calcite in large dissolution voids
Gr 29.3	-11.4	0.39	clear, blocky calcite in large dissolution voids
26.2 (C8)	-11.3	-0.46	clear, blocky calcite in large dissolution voids
26.2 (C3)	-10.4	-0.31	clear, blocky calcite in large dissolution voids
26.2 (C7)	-10.7	0.9	clear, blocky calcite in large dissolution voids
26.2 (C6)	-11.1	-0.43	clear, blocky calcite in large dissolution voids
o29.3b (C10)	-12.3	-0.74	clear, blocky calcite in large dissolution voids
o29.3b (C5)	-11.7	-0.42	clear, blocky calcite in large dissolution voids
o29.3b (C4)	-11.1	-0.54	clear, blocky calcite in large dissolution voids

Internal standards for the entire analysis

Date: 01-20-91			
Chcc			
Chcc			
Chcc	-10.882	-10.885	Standard
Chcc	-10.832	-10.934	do
Date: 05-25-91			
Chcc			
Date: 05-26-91	-11.09	-10.6	Standard
Chcc	-11.01	-10.42	Std
Chcc			
Chcc	-11.01	-10.9	Standard
Chcc	-11.1	-10.6	Standard
Chcc			
Chcc	-10.78	-10.78	Standard
Chcc	-10.75	-10.83	Standard
Date: 06-06-91	-10.2	-10.79	Standard
Chcc	-10.3	-10.72	Standard
Chcc			
Chcc	-10.837	-10.824	Std at 55c
Chcc	-10.748	-10.78	
	-10.776	-10.568	
	-10.669	-10.176	

Strontium ratios are as follows (samples analyzed by S. Goldberg, UNC)

Sample	87Sr/86S	error	
122.1	0.709133	0.000004	Bladed to fibrous calcite in shelter void of Maryville
o29.4A	0.709562	0.000006	Clear, equant calcite in dissolution voids, Craig
o29.4B	0.709448	0.000004	Clear, equant calcite in dissolution voids, Craig
o29.4C	0.7103	0.000005	Clear, equant calcite in dissolution voids, Craig, cross-cut by fracture

Vita

Eugene Carlton Rankey was born in St. Louis, Missouri on November 27, 1968 and grew up in Kirkwood, Missouri. He attended high school at St. John Vianney High School, where he played baseball and raquetball, was elected to the National Honor Society, and graduated with honors. He graduated from Augustana College, Rock Island, Illinois, in May 1991. While at Augustana, he was elected to Aristea, the Freshman Honor Society, was awarded a 4-year Presidential Scholarship, won the Hill-Erikson Award for undergraduate research, was vice-president and president of *Sigma Gamma Epsilon*, won the W.A. Tarr award from *SGE*, and was elected a *Phi Beta Kappa* scholar. He graduated *Magna Cum Laude* from Augustana with a B.A. in Geology. Immediately after graduation, he came to the University of Tennessee to begin work on this M.S. thesis. At Tennessee, he was elected vice-president of *Sigma Gamma Epsilon*, served on the Graduate Program Committe of the Department of Geological Sciences, and taught undergraduate historical geology labs, field camp, and graduate carbonate sedimentology lab. He has been a member of the Geological Society of America since 1990.

Mr. Rankey has accepted a Department of Energy EPSCoR fellowship at the University of Kansas, Lawrence, and will begin study on a doctoral degree in the Fall of 1993.